CHAPTER 1

INTRODUCTION

1.1 Biological Significance of *S*-Nitrosothiols and Nitric Oxide

In the late 1980s it was first reported that nitric oxide (NO) has numerous physiological functions including acting as a neurotransmitter, an anticoagulant and a smooth muscle relaxation mediator.[1, 2] Since then, great effort has been made to detect NO in biological samples to determine the concentrations required to perform the listed functions of this simple gas species. Numerous techniques have been employed in order to gain a better understanding of NO's chemistry and the associated reactions that take place *in vivo*. Nitric oxide has a short half-life under physiological conditions, seconds, thus there is a challenge for NO detection methods.[3]

S-Nitrosothiols (RSNOs) are proteins or peptides that are nitrosated at a cysteine residue. They are believed to act as NO reservoirs and are formed upon the reaction of NO with a free thiol. These molecules are labile and are easily decomposed by metal ions, light, or heat.[4] Once decomposed, NO is released and can be used by the body. There are high molecular weight RSNO species, including *S*-nitrosoalbumin (AlbSNO) and *S*-nitrosohemoglobin (HbSNO). Low molecular weight species include *S*-nitrosoglutathione (GSNO), *S*-nitrosocysteine (CysNO) and *S*-nitroso-N-acetyl-L-

cysteine (SNAC) (Figure 1.1). *S*-nitrosothiols are characterized by UV-Vis absorbance bands from 330-350 nm and from 550-600 nm.[5] The NO can be released if the RSNO is irraditated at either 340 or 545 nm with the process following approximately first-order reaction kinetics, and yields a radical thiol species, which dimerizes to form a disulfide.[5] The characteristic absorbance bands allow for the decomposition of RSNOs to be followed using optical detection methods.

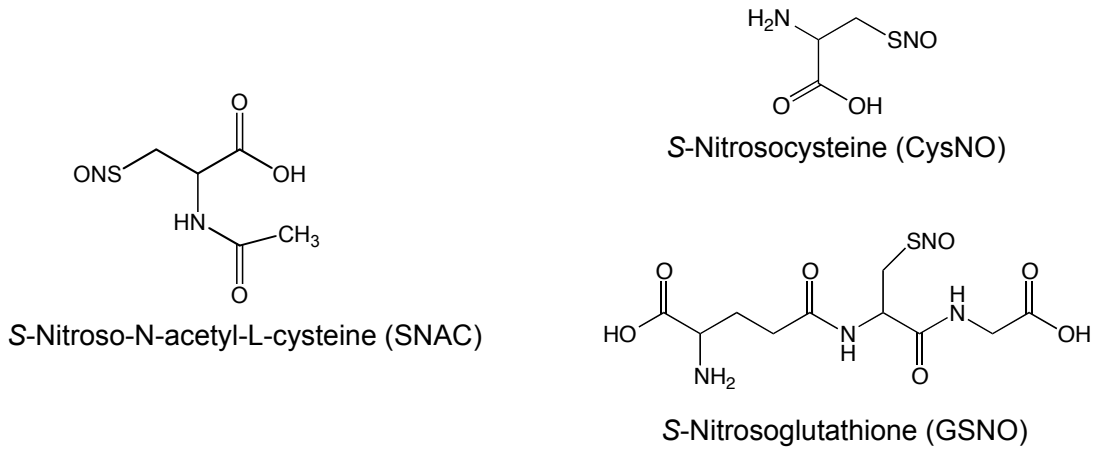

Figure 1.1 Structures of the three low molecular weight RSNOs used in this study.

Most of the RSNO detection methods reported to date are indirect methods and detect the NO released. In some cases, the NO is further reacted with oxygen or other species prior to detection. Measurement of RSNO levels in blood, plasma, and other biological fluids is of interest because they may help to predict disease states. Increases in RSNO concentration are seen in diseases such as preeclampsia and sepsis, while decreases are seen in diabetes, endothelial dysfunction and stroke.[6-9] The concentrations reported in the literature for these molecules of interest vary widely depending on the specific methods used, thus there is a need for more research to develop more reliable analytical methods.

1.1.2 Formation of Nitric Oxide

In the body, NO is formed enzymatically from nitric oxide synthase (NOS). There are three isoforms of the enzyme, endothelial-NOS (eNOS), neuronal-NOS (nNOS) and inducible-NOS (iNOS), all of which use L-arginine as a substrate, and NADPH and O_2 are cosubstrates.[10] In addition to NO, L-citrulline is a product (Figure 1.2). Two of the isoforms, eNOS and nNOS, are calcium dependent and will generate NO when there is an increase in Ca^{2+}. The third isoform, iNOS, is calcium independent and is present in only specific tissues.[10] Most commonly, the production of iNOS is upregulated in response to inflammation.[10]

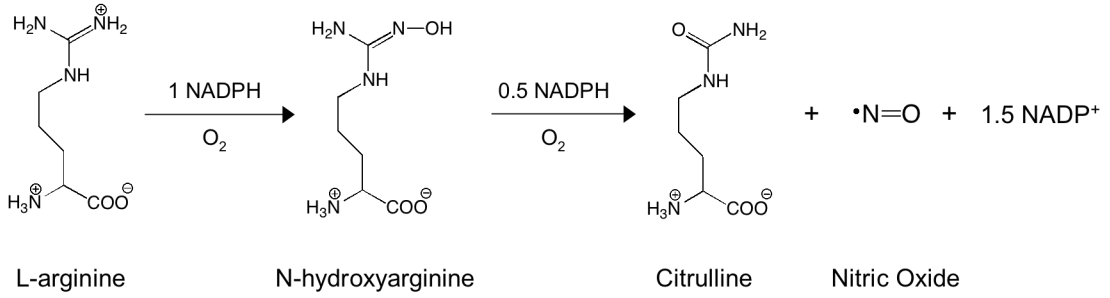

Figure 1.2 Synthesis of NO and citrulline from L-arginine.

1.1.3 Reactions with Nitric Oxide

Nitric oxide will quickly react with oxygen following third order kinetics with a *k* value of 2.1 x 10^6 $M^{-2}s^{-1}$ at 25°C.[11] The overall reaction follows the steps shown below with the end product being nitrite.

$$2NO + O_2 \rightarrow 2NO_2 \quad (1.1)$$

$$NO_2 + NO \rightarrow N_2O_3 \quad (1.2)$$

$$N_2O_3 + H_2O \rightarrow 2NO_2^- + 2H^+ \quad (1.3)$$

The speed of this reaction can make it difficult for NO to be detected in biological systems where oxygen is present. Nitric oxide will also react with superoxide to form peroxynitrite, which is cytotoxic at high concentrations.[12] Oxyhemoglobin is also a rapid scavenger of NO, with concentrations as high as 10 mM in blood and with a reaction rate of 3×10^7 $M^{-1}s^{-1}$.[13]

Another type of reaction that is commonly observed in biological systems is transnitrosation. In this reaction, the NO^+ from a RSNO species is transferred to a nearby free thiol (see Equation 1.4), following reversible second-order kinetics.[14]

$$RSNO + R'SH \rightarrow R'SNO + RSH \qquad (1.4)$$

The reaction occurs spontaneously at pH 7.4 and at 37°C and can be controlled by the pK_a of the thiol. Transnitrosation is believed to occur as the result of nucleophilic attack by the RS^- on the nitrogen of the RSNO and may be involved in signaling.[14] With millimolar concentrations of glutathione in the intracellular environment, transnitrosation reactions are likely to occur and may be a way for NO on protein RSNOs to move across cell membranes.[15]

1.2. Current NO and RSNO Detection Methods

1.2.1 Fluorescence

In 1998, Kojima et al. first reported the use of a fluorescent dye for the detection of NO.[16] The dye, 4,5-diaminofluorescein (DAF-2), forms a triazole compound, DAF-2T, when it reacts with N_2O_3, formed in the reaction of NO with ambient oxygen (Figure 1.3). The limit of detection at physiological pH is 5 nM.[16] Diaminofluoresceins can be functionalized with a diacetate group to allow for the transport of such species through

cell membranes. Once inside the cell, an esterase hydrolyzes the dye to DAF-2, which cannot diffuse out of the cell and reacts with NO produced within the cell to form DAF-2T.[16] It should be noted that DAF-2 concentrations higher than 10 μM may be toxic to some cells.[17] Kojima et al. successfully used DAF-2 to detect NO produced from macrophages and were able to use the dye to image NO within cultured rat aortic smooth muscle cells. They also report that DAF-2 is selective to NO over NO_2^-, NO_3^-, $O_2^{\bullet-}$, H_2O_2, and $ONOO^-$.

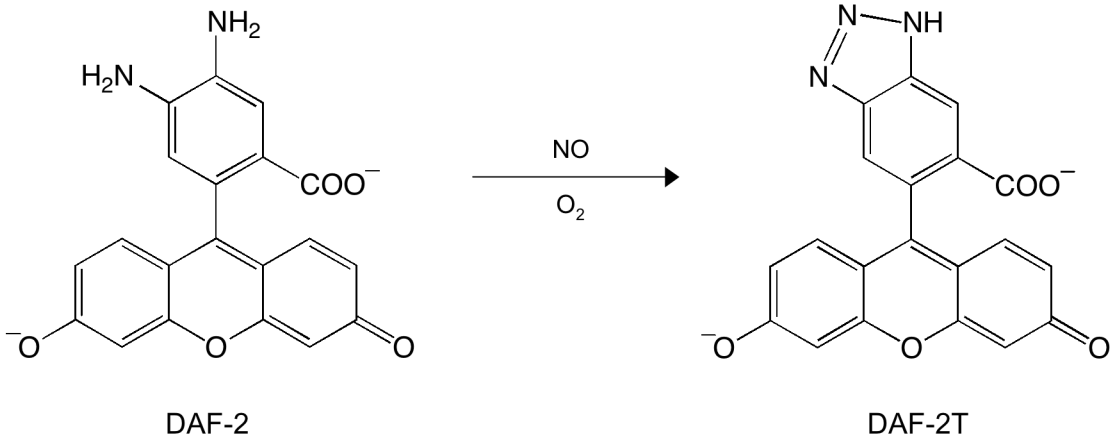

DAF-2 DAF-2T

Figure 1.3 Reaction of DAF-2 with NO and oxygen to form the fluorescent triazole compound, DAF-2T.

Separation methods such as capillary electrophoresis and HPLC can be coupled with using fluorescent dyes as the detection method. In order to use HPLC, the NO is first reacted with a dye and then separated on the column from the unreacted dye. The use of the dye 1,3,5,7-tetramethyl-8-(3',4'-diaminophenyl)difluoroboradiaza-*s*-indacene (TMDABODIPY) was employed by Huang et al. to determine NO concentrations in serum with an LOD of 20 pM.[18] Ascorbic acid and its oxidized form, dehydroascorbic acid, are known interferences to DAF-2 with the reaction product DAF-dehydroascorbic acid having a similar fluorescent signal to DAF-2T.[16] In order to remove this product

from a biological sample mixture, CE was used by Kim et al. to measure NO produced from *Aplysia californica* metacerebral cells.[19]

Fiber optic NO sensors coupled with fluorescent dyes have also been developed.[20, 21] These sensors incorporate either a fluorescein derivative adsorbed to colloidal gold or a heme domain labeled with a fluorescent reporter dye. Using the colloidal gold setup, a limit of detection of 20 μM was determined with no interference from nitrite or nitrate, but there was a slight interference from superoxide and hydrogen peroxide. While the heme based sensors had a better LOD of 1 μM, there was a response to glutathione. A correction could be made to account for the response, but would require additional time and reagents.

Fluorescent detection of RSNOs is indirect, with the dyes reacting with the decomposition products of the RSNOs. In one case, 2,3-diaminonaphthalene (DAN) was used to react with nitrite to form 2,3-naphthotriazole (NAT).[22] This study suffered from a lack of reproducibility as well as poor selectivity, that may be due to the addition of sulfamate to bind background nitrite. There is a wide range of plasma RSNO concentrations reported in the literature, from undetectable up to 9.2 μM, and while this DAN-based method offers a good LOD, the selectivity issues and the wide range of plasma values make fluorescence techniques less desirable for RSNO detection.[23]

1.2.2 Absorbance

The Griess assay was first developed in 1864 for the detection of nitrite.[24] Nitric oxide will react with oxygen in solution to produce nitrite (see reactions 1.1-1.3, above). Acidified sulfanilamide then interacts with the nitrite, and reacts further with *N*-(1-

naphthyl)ethylenediamine to form a water-soluble diazo compound with a maximum absorbance at 540 nm (Figure 1.4). The limit of detection is reported to be around 0.5 μM.[25] The assay has good selectivity over nitrate, but can be modified using nitrate reductase or copper coated cadmium to reduce nitrate to nitrite, and thereby quantify nitrate as well.[26] The Griess assay has been successfully applied for determination of NO/nitrite levels in plasma, serum, blood, and urine.[27-30]

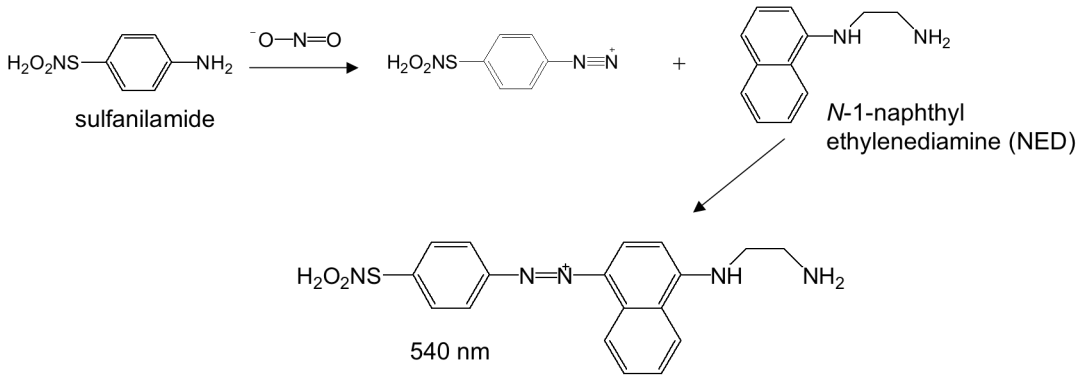

Figure 1.4 Schematic representation of the Griess Assay with acidified sulfanilamide reacting with nitrite to form an intermediate, which reacts with NED. The final diazo product is easily detected using UV-Vis with a maximum absorbance at 540 nm.

While the Griess assay was first used to detect nitrite, it can also be used in conjunction with the Saville assay to detect RSNOs.[31] Mercury(II) chloride is added to solutions containing RSNOs and this reagent breaks the S – NO bond. Nitrite is naturally present in biological samples, so the Griess assay must also be run in order to determine background nitrite level. Alternatively, the pre-existing nitrite may be removed via gel-filtration or ultrafiltration or reduced to N_2 using sulfamate, but this may not completely rid the samples of nitrite and may cause some breakdown of the RSNOs.[23] The limit of detection for the technique is around 0.2 μM, making it not sensitive enough for the potentially low concentrations of RSNOs in biological samples.[23]

1.2.3 Mass Spectrometry

Mass spectrometry has been used for NO detection, but is not commonly reported on in the literature. Conrath et al. used membrane inlet mass spectrometry (MIMS) and restriction capillary inlet mass spectrometry (RIMS) to examine the use of a fungicide to increase NO production in plants.[32] A thin semipermeable membrane separates a sample chamber and the inlet to the ionization source. These techniques allow for non-invasive online detection and are able to measure other gases, i.e. O_2 and CO_2, at the same time. While they were able to report on the effect of the fungicide, they also mention the main limitation of MS to detect small changes in the intracellular NO concentration, suggesting that the fluorescent dye DAF-2 might need to be used instead to obtain better NO quantitation.[32]

Coupled with either gas chromatography or liquid chromatography, mass spectrometry has also been used for RSNO detection. High accuracy and selectivity make MS an attractive option, but the main issue is the required separation technique. Gas chromatography is not ideal because the RSNOs are thermally labile and require derivatization in order to become volatile.[23] This method is also hampered by the complexity of the protein rich samples, which also cause a problem in LC methods. Typically, only LMW RSNOs are detected with LC-MS, but even this is difficult due to the low concentrations of these species present in biological samples.[23]

1.2.4 Chemiluminescence

Considered to be the "gold standard" of NO detection, chemiluminescence is a sensitive and selective technique. The Nitric Oxide Analyzer (NOA) is a commercially

available instrument that reacts ozone with NO to produce a photon following the reaction scheme in Equations 1.5 and 1.6:

$$NO + O_3 \rightarrow NO_2^* + O_2, \quad (1.5)$$

$$NO_2^* \rightarrow NO_2 + h\nu \quad (1.6)$$

The photons generated are detected using a PMT and the signal can be quantified. For detecting NO in gas samples, the LOD is 0.5 ppb, while for solution phase, the LOD varies depending on sample volume, but ranges from picomolar to nanomolar.[33] Using this method, NO has been detected in the circulatory systems of humans, in exhaled breath, and in food products.[34-36]

For RSNO determinations, there are two commonly used assay systems that catalyze the release of NO from the RSNO species. The first is called the tri-iodide assay. This assay uses potassium iodide and iodine dissolved in glacial acetic acid to reduce the S – NO bond.[37] While this assay is efficient in breaking the bond, it will also reduce nitrite to NO, thus a correction must be made. The sample must first be divided into aliquots, with one aliquot treated with acidified sulfanilamide. Like in the Griess assay, this will selectively bind nitrite, preventing its reduction to NO. Some biological samples may also contain compounds with nitrosated NH_2 residues.[37] As a result, an additional aliquot is pretreated with $HgCl_2$ and acidified sulfanilamide to liberate the NO from the RSNOs, which then reacts with oxygen to form nitrite that is bound by the sulfanilamide. While this assay is well understood, the need for significant sample separation and pretreatment is not ideal.

Copper(I) ions are well known catalysts for the breakdown of RSNOs.[5] Typically, copper(II) chloride is used in the assay system with cysteine as the reducing

agent. This method also provides good sensitivity for RSNOs, but suffers from the nitrite interference at higher nitrite concentrations. Additionally, CuCl has low solubility at neutral pH, so the possibility of losing some of the catalytic function exists.[23]

Another method to generate a chemiluminescence signal involves use of hydrogen peroxide and luminol. Nitric oxide reacts with the peroxide to produce peroxynitrite, $ONOO^-$, which then reacts with luminol to generate chemiluminescence.[38] Kikuchi et al. first described using this system and were able to monitor NO from a perfused rat kidney. They determined there is no interference from NO_2^- or NO_3^-, but there is a slight interference from NO_2. Subsequent studies have looked at using this chemistry with porous hollow fiber membranes and fiber optic probes to detect NO in the gas phase and solution phase, respectively.[39, 40] The LOD varies depending on the system, but have been reported to be as low as 0.3 ppb in gas phase and 1.3 μM in solution phase. Due to the rapid reaction of NO with oxygen, the signals can be increased in the absence of oxygen.

1.2.5 Electron Paramagnetic Resonance Spectroscopy

Electron paramagnetic resonance (EPR) spectroscopy is widely used for NO detection due to NO having 11 valence electrons.[41] Since the unpaired electron makes NO a free radical, it can readily be detected using EPR. However, a trapping agent must be used because NO is highly reactive and will quickly form a nonparamagnetic species.[3] The trapping agent will enable the radical species to be much more stable. Trapping agents may be endogeneous, such as hemoglobin or other metalloproteins, or may be

exogeneous like iron-dithiocarbamates.[42] Common interferences such as NO_2^- and NO_3^- will not give a response in EPR, making it a good detection platform for monitoring NO.

Endogeneous hemoglobin is able to bind NO in either the oxy- or deoxy- forms. A mixture of Hb/NO paramagnetic derivatives are formed and can be detected in the EPR spectrum. Depending on which subunit the NO is bound to, α or β, will determine if the NO is bound via penta- or hexa-coordination.[42] Both coordinations are EPR active and are indicative of NO binding. Use of hemoglobin as the trapping agent was demonstrated by Dikalov and Fink in their work to detect NO in whole blood and erythrocytes to determine NOS activity.[43] Additionally, CO- and O_2-heme complexes will not yield an EPR signal because they are diamagnetic, adding to the selectivity for the technique.[44]

Iron-dithiocarbamates have also been used as spin traps for looking at NO in various cell and tissue types. Nitric oxide has a high affinity for Fe centers and the general structure of the dithiocarbamate can be modified to become more or less lipophilic, depending on the location of desired NO detection.[3] This allows for NO detection to occur in numerous locations within live animals.[45, 46]

For RSNO detection, Rocks et al. homolytically cleaved the S – NO bond with *N*-methyl-D-glucamine (MGD) under basic conditions.[47] The NO that is released is then trapped by Fe^{2+} complexed MGD and detected with EPR. A LOD of 50 nM was reported, however, this assay examined only standards of GSNO, while blood or serum samples will likely have large concentrations of HMW RSNOs.

1.2.6 Oxyhemoglobin Assay

Nitric oxide reacts with oxyhemoglobin in a nearly diffusion limited reaction with a rate constant of 3.7 x 10^7 $M^{-1}s^{-1}$.[13] The NO binds to the oxygen on the heme, isomerizes and is then released as nitrate. At the same time, the oxyhemoglobin is oxidized from Fe^{2+} to Fe^{3+} and forms methemoglobin, and the Soret band shifts from 415 nm to 406 nm.[13] This assay has been used to detect NO released from platelets, tissues, as well as cultured endothelial cells.[48-50] These reports utilize the change in the absorbance for detection and few papers report monitoring the generation of nitrate as the detection method.[13, 51] Temperature fluctutations, changes in pH and the presence of other heme containing proteins can cause interferences by impacting the absorbance spectrum of methemoglobin.[3] Heme containing proteins, like myoglobin, can also be used for NO detection.[13] The use of the oxyhemoglobin assay will be discussed in greater detail in Chapter 4 of this thesis.

1.2.7 Electrochemical

Electrochemistry has been widely used for the detection of NO, with the first amperometric sensor reported in 1990.[52] Due to the ability to miniaturize electrodes, detect NO in real-time, and the variety of modifiers available to augment the selectivity and and sensitivity, amperometry is now often used.[3] Most of the sensors described oxidize NO at potentials of + 0.7 to + 0.9 V vs. Ag/AgCl in either a 2 or 3 electron process.[3] Common interferences include NO_2^-, CO, H_2S, ammonia, ascorbic acid and uric acid; thus the need for outer membranes and other modifiers to enhance selectivity.[3, 53] Membranes consisting of Nafion, electropolymerized porphyrins, sol-gels,

polycarbazole cellulose acetate, polytetrafluoroethylene (PTFE) or multiple layers of different membrane types have been employed to block some of these species.[54-59] Other electrode materials have been used to alter the response, including Au, carbon fiber, Ru, and multi-walled carbon nanotubes.[60-63] There are commercially available NO sensors, with the lowest limit of detection reported to be 0.2 nM;[64] however, these sensors are delicate and can easily be broken during use.

For electrochemical RSNO detection, a catalyst is typically used to break the S – NO bond with the liberated NO then diffusing to the electrode surface. In 2004, Rafikova et al. reported using $CuCl_2$ in solution with an NO electrode to detect RSNOs in rat plasma.[65] Concentrations as low as 10 nM were detected; however, the system was not well characterized and displayed different detection limits for HMW and LMW RSNOs.

Previous work in this lab performed by Dr. Wansik Cha and Dr. Mustafa Musameh utilized a platinized platinum working electrode with a PTFE-gas permeable membrane modified with Teflon AF to create a sensitive and selective NO sensor, that was then used with an immobilized catalyst to detect RSNOs.[53] Cha et al. used a copper catalyst, but immobilized it in a polymeric film that was attached at the distal end of the NO sensor.[66] The sensors were able to detect ≤ 1μM of both HMW and LMW RSNO species and had a lifetime of at least 10 days. Another type of RSNO sensor was developed by immobilizing glutathione peroxidase (GPx) behind a dialysis membrane on the NO sensor.[67] Glutathione peroxidase is a seleno-enzyme naturally present in the body that prevents lipid peroxidation and catalyzes the breakdown of RSNOs to NO.[68] The immobilized enzyme breaks down the RSNOs, liberating NO that diffuses through the

gas permeable membrane of the sensor and is oxidized at the platinum electrode surface. With the immobilized enzyme present, the LOD was 0.2 μM for CysNO with a response time of less than 5 min. The lifetime of the sensor was limited, with a 50% decrease in sensitivity after two days. A new sensor was designed using an immobilized organoselenium catalyst in place of the enzyme. Several iterations of this sensor were produced with the catalyst immobilized in various ways.[69, 70] The most recent design utilized selenocystamine (SeCA) covalently attached to a dialysis membrane (Figure 1.5). The lifetime of the sensor was improved to 2 weeks with the LOD improving to 20 nM for CysNO and GSNO.

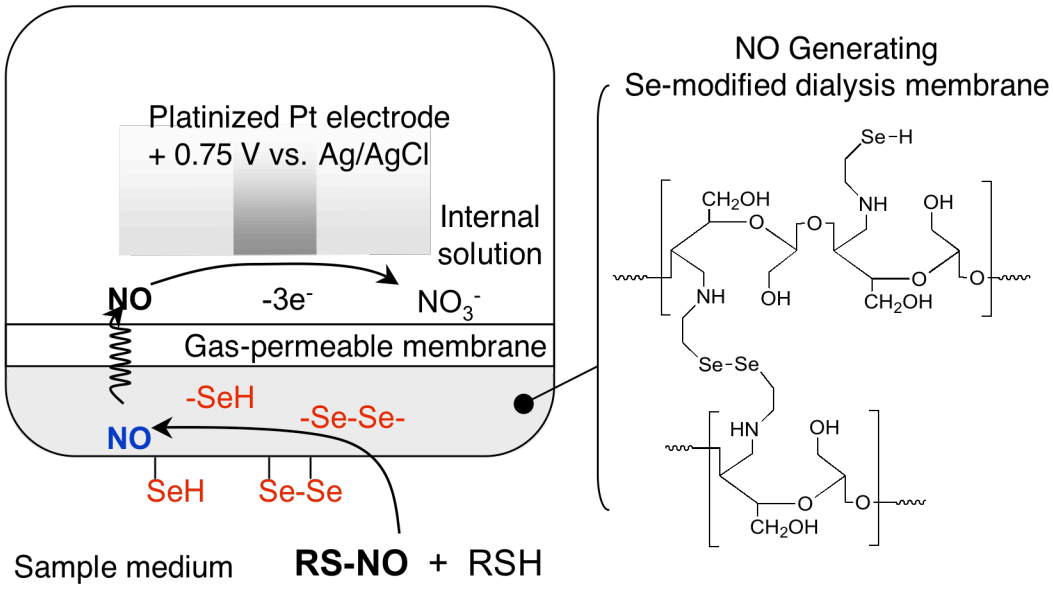

Figure 1.5 Amperometric RSNO sensor consisting of a platinized platinum electrode behind a gas permeable membrane and an outer dialysis membrane with a selenium catalyst covalently attached.

1.3 Nasal Nitric Oxide Detection

1.3.1 Origin and Function of Nasal NO

Many studies have been published reporting the presence of NO in exhaled nasal air. It is not known exactly where the NO originates, but it is believed that the majority is generated in the paranasal sinuses, specifically in the mucosa, with contributions from the lower respiratory tract.[71, 72] There has been some debate over whether or not bacteria contribute to the NO production, but most studies have shown no difference in NO levels, with and without antibiotics present.[73] Figure 1.6 shows the approximate NO concentrations found in different parts of the respiratory tract, with the majority being produced in the sinuses.[74]

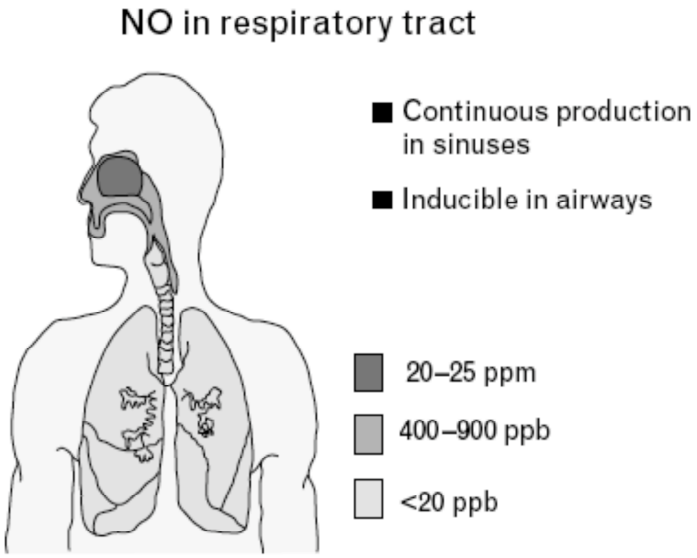

Figure 1.6 Diagram showing NO concentrations detected in different regions of the airways using a chemiluminescence analyzer.

Within the airways, NO has multiple functions including host defense, stimulating ciliary motility, acting as a antibacterial and antiviral agent and may serve as an aerocrine

messenger molecule.[75] Nitric oxide has also been shown to improve arterial oxygenation and reduce pulmonary vascular resistance. Indeed, a study by Lundberg et al. found that inhaling through the nose, thereby moving the nasal NO into the lungs, improves oxygen uptake. They also found that patients who were intubated or mechanically ventilated benefited from having air supplemented with NO.[76] Nitric oxide may also play a role in nasal temperature and humidity control. Holden et al. found that by inhibiting NO release within the nasal passages, the nasal air was cooler. This is likely due to NO controlling the dilation and constriction of nasal capacitance vessels, that control nasal temperature.[77]

1.3.2 Detection of Nasal NO

Chemiluminescence is the most commonly used detection method for nasal NO, and while it is a sensitive and selective technique, there are some pitfalls in its use. The instrumentation is bulky and not easily operated in a clinical setting. As a result, a hand-held chemiluminescence analyzer has been developed by Aerocrine; however, the system is costly.[78] A less expensive hand-held device has been developed utilizing an amperometric sensor.[79] The sensor has a LOD of 5 ppb and a dynamic range of 5-300 ppb, which is somewhat limiting in terms of diagnostics. Both of these devices have been compared against the traditional chemiluminescence analyzers with good correlation.[78, 80] While the electrochemical device is less expensive than the chemiluminescence device, it still costs an estimated $4000.[79]

1.3.3 Nasal NO in Disease

Nasal NO may be useful in aiding diagnosis and in monitoring the effectiveness of treatments. Diseases such as primary ciliary dyskinesias, cystic fibrosis, chronic sinusitis, and sinonasal polyposis are associated with low levels of nasal NO.[81-85] This is likely due to lower diffusion of the NO through the mucosa in the sinuses because of the excess mucous generated in these disease states. Higher NO concentrations have been observed in patients with asthma; however, these patients also had allergic rhinitis.[86] There have been few studies with patients suffering from just asthma, but there have been multiple reports that asthma causes an increase in orally exhaled NO.[87] With a noninvasive, inexpensive, easy-to-use NO detection method, nasal NO measurements could be used as a means to better determine the presence of one of these diseases.[88] Additionally, if high concentrations of nasal NO are detected, certain diseases can be ruled out. Currently, nasal NO is not commonly monitored due to expensive equipment and limited availability.[88]

1.4 Statement of Research

In this dissertation, new methods for the detection of nitric oxide and *S*-nitrosothiols in blood and breath are examined. Chapter 2 describes the development of a chemiluminescence assay system using a soluble organoselenium catalyst with a free thiol reducing agent for the potential detection of RSNOs in plasma and the detection of HbSNO in red blood cells. Optimal concentrations of the selenocystamine (SeCA) catalyst and glutathione (GSH) reducing agent are determined, along with the sensitivity of the new assay for three LMW RSNOs, GSNO, CysNO and SNAC, and one HMW

RSNO, AlbSNO. Selectivity over nitrite is established with the results compared to the well known copper/cysteine assay. To ensure the catalyst remains active in a biological matrix, plasma samples spiked with RSNOs are tested. Attempts to detect *S*-nitrosohemoglobin from sheep blood is also reported in this chapter.

In Chapter 3, the new SeCA/GSH assay system is used to detect whether there are RSNOs present in exhaled breath condensate (EBC). Exhaled breath condensate is collected in a homemade glass device over a period of 15 min with a volunteer breathing normally. The EBC is then assayed for RSNOs using the new SeGA/GSH homogeneous RSNO assay system and the $CuCl_2$/Cys system for comparison. The Saville/Griess assays are also used for RSNO and nitrite detection to further verify the results.

Chapter 4 focuses on the use of the oxyhemoglobin assay to detect NO in exhaled nasal air. The oxyhemoglobin reaction generates both methemoglobin, which is detected via UV-Vis spectroscopy, and nitrate, which is detected with an ion-selective electrode (ISE). The composition of the ISE membrane is optimized, examining at the possible use of a vanadyl salen compound acting as a nitrate ionophore. The response of the membrane to hemoglobin is investigated, using an asymmetric cellulose triacetate membrane to fabricate the ISEs. This approach is shown to overcome a background potentiometric response to the oxyhemoglobin. Calibration curves for both the UV-Vis and ISE systems are generated using a stock NO solution, along with proof-of-principle experiments using gas permeable tubing containing oxyhemoglobin for detecting NO(g). Finally, nasal air samples from volunteers are collected and analyzed for NO using this new, inexpensive approach.

In Chapter 5, conclusions will be presented along with a plan for future work. Ways to improve the nitrate ISE as well as a new application of the oxyHb assay with nitrate detection will be discussed.

1.5 References

(1) Ignarro, L. J.; Buga, G. M.; Wood, K. S.; Byrns, R. E.; Chaudhuri, G. *Proceedings of the National Academy of Sciences* **1987**, *84*, 9265-9269.

(2) Bredt, D. S.; Hwang, P. M.; Snyder, S. H. *Nature* **1990**, *347*, 768-770.

(3) Hetrick, E. M.; Schoenfisch, M. H. *Annual Review of Analytical Chemistry* **2009**, *2*, 409-433.

(4) Butler, A. R.; Rhodes, P. *Analytical Biochemistry* **1997**, *249*, 1-9.

(5) Williams, D. L. H. *Accounts of Chemical Research* **1999**, *32*, 869-876.

(6) Tyurin, V. A.; Liu, S.-X.; Tyurina, Y. Y.; Sussman, N. B.; Hubel, C. A.; Roberts, J. M.; Taylor, R. N.; Kagan, V. E. *Circulation Research* **2001**, *88*, 1210-1215.

(7) Liu, L.; Yan, Y.; Zeng, M.; Zhang, J.; Hanes, M. A.; Ahearn, G.; McMahon, T. J.; Dickfeld, T.; Marshall, H. E.; Que, L. G.; Stamler, J. S. *Cell* **2004**, *116*, 617-628.

(8) James, P. E.; Lang, D.; Tufnell-Barret, T.; Milsom, A. B.; Frenneaux, M. *Circulation Research* **2004**, *94*, 976-983.

(9) Feletou, M.; Vanhoutte, P. M. *Americal Journal of Physiology Heart and Circulatory Physiology* **2006**, *291*, H985-H1002.

(10) Stuehr, D. J. *Biochimica et Biophysica Acta* **1999**, *1411*, 217-230.

(11) Lewis, R. S.; Deen, W. M. *Chemical Research in Toxicology* **1994**, *7*, 568-574.

(12) Stamler, J. S.; Feelisch, M. In *Methods in Nitric Oxide Research*; Feelisch, M., Stamler, J. S., Eds.; John Wiley & Sons, Ltd: New York, NY, 1996, pp 19-27.

(13) Feelisch, M.; Kubitzek, D.; Werringloer, J. In *Methods in Nitric Oxide Research*; Feelisch, M., Stamler, J. S., Eds.; John Wiley & Sons, Ltd.: New York, NY, 1996, pp 455-478.

(14) Hogg, N. *Analytical Biochemistry* **1999**, *272*, 257-262.

(15) Zhang, Y.; Hogg, N. *Proceedings of the National Academy of Sciences* **2004**, *101*, 7891-7896.

(16) Kojima, H.; Nakatsubo, N.; Kikuchi, K.; Kawahara, S.; Kirino, Y.; Nagoshi, H.; Hirata, Y.; Nagano, T. *Analytical Chemistry* **1998**, *70*, 2446-2453.

(17) Havenga, M. J. E.; van Dam, V.; Groot, B. S.; Grimbergen, J. M.; Valerio, D.; Bout, A.; Quax, P. H. A. *Analytical Biochemistry* **2001**, *290*, 283-291.

(18) Huang, K.-J.; Wang, H.; Zhang, Q.-Y.; Ma, M.; Hu, J.-F.; Zhang, H.-S. *Analytical and Bioanalytical Chemistry* **2006**, *384*, 1284-1290.

(19) Kim, W.-S.; Ye, X.; Rubakhin, S. S.; Sweedler, J. V. *Analytical Chemistry* **2006**, *78*, 1859-1865.

(20) Barker, S. L. R.; Kopelman, R. *Analytical Chemistry* **1998**, *70*, 4902-4906.

(21) Barker, S. L. R.; Zhao, Y.; Marletta, M. A.; Kopelman, R. *Analytical Chemistry* **1999**, *71*, 2071-2075.

(22) Marzinzig, M.; Nussler, A. K.; Stadler, J.; Marzinzig, E.; Barthlen, W.; Nussler, N. C.; Beger, H. G.; Morris Jr, S. M.; Bruckner, U. B. *Nitric Oxide* **1997**, *1*, 177-189.

(23) Giustarini, D.; Milzani, A.; Dalle-Donne, I.; Rossi, R. *Journal of Chromatography B* **2007**, *851*, 124-139.

(24) Griess, J. P. *Philosophilcal Transactions of the Royal Society (London)* **1864**, *154*, 667-731.

(25) Sun, J.; Zhang, X.; Broderick, M.; Fein, H. *Sensors* **2003**, *3*, 276-284.

(26) Higuchi, K.; Motomizu, S. *Analytical Sciences* **1999**, *15*, 129-134.

(27) Giustarini, D.; Dalle-Donne, I.; Colombo, R.; Milzani, A.; Rossi, R. *Free Radical Research* **2004**, *38*, 1235-1240.

(28) Ozkan, Y.; Yardim-Akaydin, S.; Sepici, A.; Engin, B.; Sepici, V.; Simsek, B. *Clinical Chemistry and Laboratory Medicine* **2007**, *45*, 73-77.

(29) Schulz, K.; Kerber, S.; Kelm, M. *Nitric Oxide* **1999**, *3*, 225-234.

(30) Joharchi, K.; Jorjano, M. *European Journal of Pharmacology* **2007**, *570*, 66-71.

(31) Saville, B. *Analyst* **1958**, *83*, 670-672.

(32) Conrath, U.; Amoroso, G.; Kohle, H.; Sultemeyer, D. F. *The Plant Journal* **2004**, *38*, 1015-1022.

(33) Instruments, G. A. *Sievers* Nitric Oxide Analyzer NOA 280i Operation and Maintenance Manual* **2006**, 2-1.

(34) Zweier, J. L.; Li, H.; Samouilov, A.; Liu, X. *Nitric Oxide* **2010**, *22*, 83-90.

(35) Abba, A. A. *Annals of Thoracic Medicine* **2009**, *4*, 173-181.

(36) Liu, M.; Lin, Z.; Lin, J.-M. *Analytica Chimica Acta* **2010**, *670*, 1-10.

(37) Feelisch, M.; Rassaf, T.; Mnaimneh, S.; Singh, N.; Bryan, N. S.; Jourd'heuil, D.; Kelm, M. *The Journal of the Federation of American Societies for Experimental Biology* **2002**, *16*, 1775-1785.

(38) Kikucki, K.; Nagano, T.; Hayakawa, H.; Hirata, Y.; Hirobe, M. *Analytical Chemistry* **1993**, *65*, 1794-1799.

(39) Robinson, J. K.; Bollinger, M. J.; Birks, J. W. *Analytical Chemistry* **1999**, *71*, 5131-5136.

(40) Zhou, X.; Arnold, M. A. *Analytical Chemistry* **1996**, *68*, 1748-1754.

(41) Singel, D., J.; Lancaster Jr., J. R. In *Methods in Nitric Oxide Research*; Feelisch, M., Stamler, J. S., Eds.; John Wiley & Sons, Ltd.: New York, NY, 1996, pp 341-356.

(42) Kleschyov, A. L.; Wenzel, P.; Munzel, T. *Journal of Chromatography B* **2007**, *851*, 12-20.

(43) Dikalov, S.; Fink, B. *Methods in Enzymology* **2005**, *396*, 597-610.

(44) Van Doorslaer, S.; Desmet, F. *Methods in Enzymology* **2008**, *437*, 287-310.

(45) Hirayama, A.; Nagase, S.; Ueda, A.; Yoh, K.; Oteki, T.; Obara, M.; Takada, K.; Shimozawa, Y.; Aoyagi, K.; Koyama, A. *Molecular and Cellular Biochemistry* **2003**, *244*, 63-67.

(46) Vanin, A. F.; Poltorakov, A. P.; Mikoyan, V. D.; Kubrina, L. N.; van Faassen, E. *Nitric Oxide* **2006**, *15*, 295-311.

(47) Rocks, S. A.; Davies, C. A.; Hicks, S. L.; Webb, A. J.; Klocke, R.; Timmins, G. S.; Johnson, A.; Jawad, A. S. M.; Blake, D. R.; Benjamin, N.; Winyard, P. G. *Free Radical Biology & Medicine* **2005**, *39*, 937-948.

(48) Zhou, Q.; Hellermann, G. R.; Solomonson, L. P. *Thrombosis Research* **1995**, *77*, 87-96.

(49) Kelm, M.; Schrader, J. *European Journal of Pharmacology* **1988**, *155*, 17-21.

(50) Kelm, M.; Feelisch, M.; Spahr, R.; Piper, H.-M.; Noack, E.; Schrader, J. *Biochemical and Biophysical Research Communications* **1988**, *154*, 236-244.

(51) Feelisch, M.; Noack, E. *European Journal of Pharmacology* **1987**, *139*, 19-30.

(52) Shibuki, K. *Neuroscience Research* **1990**, *9*, 69-76.

(53) Cha, W.; Meyerhoff, M. E. *Chem. Anal. (Warsaw)* **2006**, *51*, 949-961.

(54) Villeneuve, N.; Bedioui, F.; Voituriez, K.; Avaro, S.; Vilane, J. P. *Journal of Pharmacological and Toxicological Methods* **1998**, *40*, 95-100.

(55) Cserey, A.; Gratzl, M. *Analytical Chemistry* **2001**, *73*, 3965-3974.

(56) Joshi, M. S.; Lancaster Jr., J. R.; Liu, X.; Ferguson Jr., T. B. *Nitric Oxide* **2001**, *5*, 561-565.

(57) Prahash, R.; Srivastava, R. C.; Seth, P. K. *Polymer Bulletin* **2001**, *46*, 487-490.

(58) Malinski, T.; Taha, Z.; Burewicz, A.; Tomboulian, P. *Analytica Chimica Acta* **1993**, *279*, 135-140.

(59) Shin, J. H.; Privett, B. J.; Kita, J. M.; Wightman, R. M.; Schoenfisch, M. H. *Analytical Chemistry* **2008**, *80*, 6850-6859.

(60) Ye, S.; Zhou, W.; Abe, M.; Nishida, T.; Cui, L.; Uosaki, K.; Osawa, M.; Sasaki, Y. *Journal of the American Chemical Society* **2004**, *126*, 7434-7435.

(61) Allen, B. W.; Piantadosi, C. A.; Coury Jr., L. A. *Nitric Oxide* **2000**, *4*, 75-84.

(62) Yao, S.; Xu, W.; Wolfson Jr, S. K. *ASAIO Journal* **1995**, *41*, M404-M409.

(63) Wu, F.-H.; Zhao, G.-C.; Wei, X.-W. *Electrochemistry Communications* **2002**, *4*, 690-694.

(64) Lob, H.; Rosenkranz, A. C.; Breitenbach, T.; Berkels, R.; Drummond, G.; Roesen, R. *Pharmacology* **2006**, *76*, 8-18.

(65) Rafikova, O.; Sokolova, E.; Rafikov, R.; Nudler, E. *Circulation* **2004**, *110*, 3573-3580.

(66) Cha, W.; Lee, Y.; Oh, B. K.; Meyerhoff, M. E. *Analytical Chemistry* **2005**, *77*, 3516-3524.

(67) Musameh, M.; Moezzi, N.; Schauman, L. M.; Meyerhoff, M. E. *Electroanalysis* **2006**, *18*, 2043-2048.

(68) Hou, Y.; Guo, Z.; Li, J.; Wang, P. G. *Biochemical and Biophysical Research Communications* **1996**, *88*, 88-93.

(69) Cha, W.; Meyerhoff, M. E. *Biomaterials* **2007**, *28*, 19-27.

(70) Cha, W.; Anderson, M. R.; Zhang, F.; Meyerhoff, M. E. *Biosensors and Bioelectronics* **2009**, *24*, 2441-2446.

(71) Lundberg, J. O.; Farkas-Szallasi, T.; Weitzberg, E.; Rinder, J.; Lidholm, J.; Anggaard, A.; Hokfelt, T.; Lundberg, J. M.; Alving, K. *Nature Medicine* **1995**, *1*, 370-373.

(72) Maniscalco, M.; Lundberg, J. O. *European Respiratory Monograph* **2010**, *49*, 71-81.

(73) Al-Ali, M. K.; Howarth, P. H. *Respiratory Medicine* **1998**, *92*, 701-715.

(74) Scadding, G. *Current Opinin in Otolaryngology & Head and Neck Surgery* **2007**, *15*, 258-263.

(75) Jorissen, M.; Lefevere, L.; Willems, T. *Allergy* **2001**, *56*, 1026-1033.

(76) Lundberg, J. O.; Lundberg, J. M.; Settergren, G.; Alving, K.; Weitzberg, E. *Acta Physiologica Scandinavica* **1995**, *155*, 467-468.

(77) Holden, W. E.; Wilkins, J. P.; Harris, M.; Milczuk, H. A.; Giraud, G. D. *Journal of Applied Physiology* **1999**, *87*, 1260-1265.

(78) Alving, K.; Janson, C.; Nordvall, L. *Respiratory Research* **2006**, *7*, 67-73.

(79) Hemmingsson, T.; Linnarsson, D.; Gambert, R. *Journal of Clinical Monitoring and Computing* **2004**, *18*, 379-387.

(80) Maniscalco, M.; de Laurentiis, D.; Weitzberg, E.; Lundberg, J. O.; Sofia, M. *European Journal of Clinical Investigation* **2008**, *38*, 197-200.

(81) Lundberg, J. O.; Weitzberg, E.; Nordvall, S. L.; Kuylenstierna, R.; Lundberg, J. M.; Alving, K. *European Respiratory Journal* **1994**, *7*, 1501-1504.

(82) Arnal, J. F.; Flores, P.; Rami, J.; Murris-Espin, M.; Bremont, F.; Pasto Aguilla, I.; Serrano, E.; Didier, A. *European Respiratory Journal* **1999**, *13*, 307-312.

(83) Wodehouse, T.; Kharitonov, S. A.; Mackay, I. S.; Barnes, P. J.; Wilson, R.; Cole, P. J. *European Respiratory Journal* **2003**, *21*, 43-47.

(84) Thomas, S.; Kharitonov, S. A.; Scott, S.; Hodson, M.; Barnes, P. J. *Chest* **2000**, *117*, 1085-1089.

(85) Lindberg, S.; Cervin, A.; Runer, T. *Acta Otolaryngologica* **1997**, *117*, 113-117.

(86) Kharitonov, S. A.; Rajaulasingam, K.; O'Conner, B.; Durham, S. R.; Barnes, P. J. *Journal of Allergy and Clinical Immunology* **1997**, *99*, 58-64.

(87) Alving, K.; Weitzberg, E.; Lundberg, J. M. *European Respiratory Journal* **1993**, *6*, 1368-1370.

(88) Serrano, C.; Valero, A.; Picado, C. *Archivos de Bronconeumologia* **2004**, *40*, 222-230.

CHAPTER 2

CHEMILUMINESCENT DETECTION OF *S*-NITROSOTHIOLS USING A SENSITIVE AND SELECTIVE ORGANOSELENIUM CATALYST

2.1 Introduction

S-Nitrosothiols are important biological molecules responsible for the transport of nitric oxide throughout the body. Acting as vasodilators and signaling molecules, RSNOs are also markers for health conditions like heart attack, stroke, sepsis and diabetes, with concentrations present deviating from normal in patients that have had or are at risk of having such conditions.[1-4] *S*-Nitrosothiols are small molecules, peptides, and proteins which are nitrosated at a thiol group and can easily be degraded upon exposure to heat, light or metal ions.[5] As mentioned in Chapter 1, there are two main classes of RSNOs, low molecular weight, including *S*-nitrosoglutathione (GSNO), *S*-nitrosocysteine (CysNO) and *S*-nitroso-N-acetyl-L-cysteine (SNAC) (see Figure 1.1), and high molecular weight or protein RSNOs, including *S*-nitrosoalbumin (AlbSNO) and *S*-nitrosohemoglobin (HbSNO).

As summarized in Chapter 1, previous work in this lab led to the development of an amperometric RSNO sensor using an immobilized selenium catalyst.[6, 7] Selenocystamine (SeCA) was used, with the catalytic cycle of this glutathione peroxidase mimic deciphered (Figure 2.1). The diselenide is reduced using glutathione to produce a selenosulfide, which is further reduced to a selenol/selenolate. This final species reacts with the RSNO, liberating the NO, which can then be detected. The diselenide may also react with RSNOs, but at a slower rate.

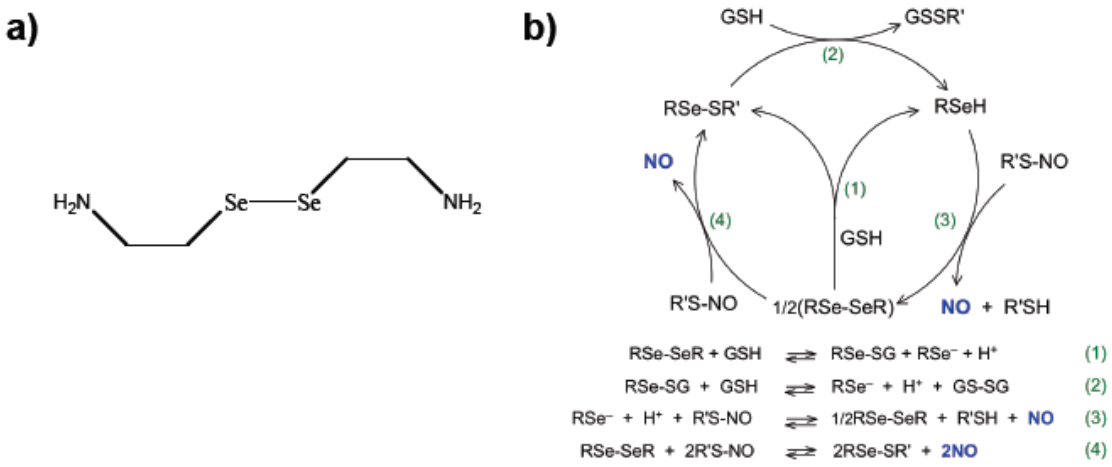

Figure 2.1 a) Structure of selenocystamine. **b)** Catalytic cycle for the selenocystamine. The diselenide (RSe-SeR) is reduced to either the selenosulfide (RSe-SR') or the selenol (RSeH), and the latter reacts with the RSNO to release NO.

Aside from the electrochemical approach, chemiluminescence is commonly used for RSNO detection, with two assay systems mainly used; copper(II) with cysteine and the tri-iodide assay.[8-10] These assays are indirect detection methods, with the observed signal coming from the NO released from the RSNOs by the catalyst/reducing agent system. The assays are sensitive for RSNOs, but may also respond to interferences such as nitrite and N-nitrosamines. As a result, samples must be pretreated with additional reagents to account for these species, adding time and cost to the analysis. Protein

RSNOs can be detected with these methods, but there has been some debated over how effective the assays really are.[10]

To detect protein RSNOs, the biotin-switch technique (BST) is often used. First introduced in 2001, this method utilizes biotin and removes the NO^+ from the RSNO and replaces it with biotin in a three step reaction sequence (Figure 2.2).[11] First, methylmethane thiosulfonate is used to block free cysteine thiols, followed by the addition of ascorbate to allow for transnitrosation to occur, leaving free thiol groups. Biotin-HPDP is then added, binding to the thiol group on the protein. In order to detect the biotin labeled protein, immunoblotting is used. The BST will provide qualitative information, but can provide only relative quantitative information. The method is able to detect the protein RSNOs in complex mixtures, however, more reagents and time are required for such samples.

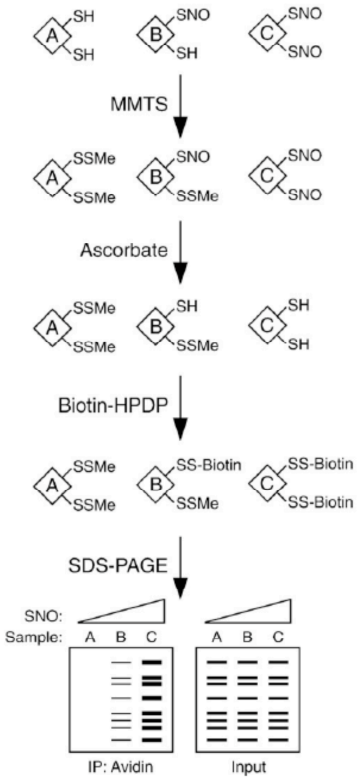

Figure 2.2 Schematic of the biotin-switch method for protein RSNO detection.

Believed to be a method of NO transport, transnitrosation can also be used to detect protein RSNOs.[12] The NO^+ from a RSNO can be transferred to a nearby free thiol (Equation 2.1) following reversible second-order kinetics.[13]

$$RSNO + R'SH \rightarrow R'SNO + RSH \quad (2.1)$$

Through a series of transnitrosation reactions, NO^+ can move across cell membranes, thus enabling the detection on intracellular RSNOs without the need of lysing the cells.[12] As previously mentioned in Chapter 1, these reactions occur spontaneously at pH 7.4 and at 37°C and can be controlled by the pK_a of the thiol.[13]

S-Nitrosohemoglobin is another protein RSNO naturally occurring in the body. Like other RSNOs, it is believed to be involved with vasodilation and is thought to be a marker for sepsis. Further, low concentrations may be linked to older banked blood clotting after transfusion.[14, 15] The NO^+ is located on the β monomer at cysteine 93 (Figure 2.3) and at high oxygen concentrations it is oriented toward the interior of the protein. When the hemoglobin shifts conformations at low oxygen levels, the NO^+ is then exposed to the solvent and can more easily undergo transnitrosation. Currently, HbSNO has been detected via EPR, the two chemiluminescence assay systems mentioned above, and HPLC, with each of these techniques having the drawbacks mentioned in Chapter 1.[14, 16, 17]

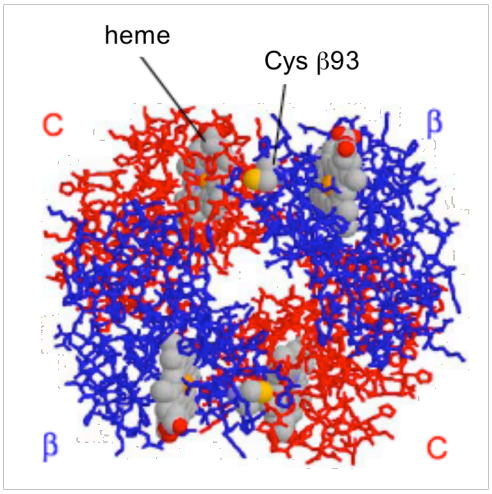

Figure 2.3 Model structure of *S*-nitrosohemoglobin showing the NO located on the cysteine β93 residue, with β and C representing the different subunits of the hemoglobin..

In this chapter, a new chemiluminescence assay system for RSNOs is developed using a homogeneous organoselenium catalyst with glutathione as the reducing agent. Assay conditions are optimized and sensitivities for LMW and HMW RSNOs are determined, along with selectivity over nitrite. Results are compared with the Cu(II)/Cys assay system. Transnitrosation is examined using AlbSNO as a model protein with different concentrations of GSH, Cys and NAC and varying incubation times. To ensure the assay remains functional in a biological matrix, plasma samples from pig, sheep and rabbit were spiked with GSNO and AlbSNO and tested. Finally, efforts to use the new assay to detect *S*-nitrosohemoglobin in blood samples from sheep and pigs using transnitrosation to move the NO^+ from the HbSNO across the membrane of intact red blood cells are summarized (Figure 2.4).

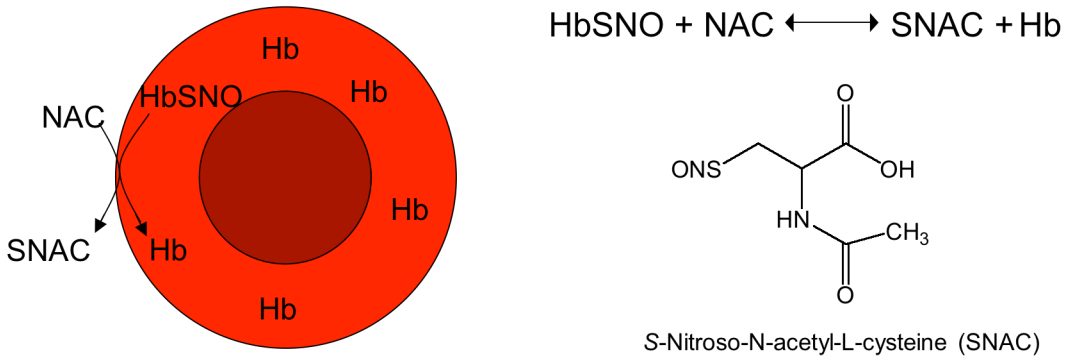

Figure 2.4 Schematic for HbSNO detection with the NO^+ moving across the cell membrane to the free NAC to form SNAC. The equation for the reaction, as well as the structure of SNAC, are also shown.

2.2 Experimental

2.2.1 Materials and Instruments

Glutathione (GSH), L-cysteine (Cys), N-acetyl-L-cysteine (NAC), bovine serum albumin (BSA), sodium nitrite, sulfuric acid, sodium hydroxide, ethylenediaminetetraacetic acid (EDTA), copper(II) chloride, sodium phosphate monobasic, and sodium phosphate dibasic were purchased from Sigma-Aldrich (St. Louis, MO). D,L-dithiothreitol was obtained from Fluka (St. Louis, MO). Anti-foaming agent was purchased from GE Analytical (Boulder, CO). All buffers and solutions were prepared using Milli-Q grade deionized water (18.2 MΩ, Millipore Corp., Billerica, MA). Sheep, pig, and rabbit whole blood and plasma were obtained from the Medical School at the University of Michigan. Additional sheep plasma was purchased from Lampire Biological Laboratories (Pipersville, PA).

A Nitric Oxide Analyzer (NOA), model 280i from GE Analytical (Boulder, CO), was used for all experiments. Gas-tight syringes used were from Hamilton (Reno, NV). Millipore centrifuge tubes with 30,000 molecular weight cutoff filters and sodium chloride were purchased from Fisher (Pittsburgh, PA).

2.2.2 Synthesis of RSNOs

S-Nitrosoglutathione (GSNO), *S*-nitrosocysteine (CysNO) and *S*-nitroso-N-acetyl-L-cysteine (SNAC) were made by dissolving 15 mmols of the corresponding thiol in 9.75 mL of 20 μM EDTA. Fifteen microliters of concentrated sulfuric acid were then added along with 0.25 mL of 200 mM $NaNO_2$. *S*-nitrosoalbumin (AlbSNO) was made by dissolving 200 mg of BSA in 15 mL of 10 μM EDTA. To reduce the disulfide bonds, 150 μL of a 25 mM solution of DTT was added, and the combined solution was incubated in a 37°C oven for 1 h. After the incubation period the solution was transferred to a centrifuge tube with a 30,000 molecular weight cut-off filter inside and the solution was spun down at 4000 rpm for 30 min. The protein was resuspended in 15 mL of nitrogen-purged, 10 μM EDTA solution and spun down again. This was repeated two more times. The solution of reduced BSA was transferred to a 20 mL vial where 32 μL of concentrated sulfuric acid and 0.25 mL of 20 mM $NaNO_2$ were added and incubated at room temperature for 30 min. To neutralize the acid, 1 M NaOH was added drop-wise until the pH was 7.4. The nitrosated BSA was concentrated and diluted three times using the centrifuge filter tube with PBS with 10 μM EDTA as the solvent. The concentration of AlbSNO was determined using the chemiluminescent assay.

2.2.3 Synthesis of Selenocystamine

Selenocystamine (SeCA) was synthesized following the procedures in the literature.[18-20] Briefly, 0.1 mole potassium sulfite was dissolved in water with 0.1 mole finely powdered selenium and allowed to stir for 30-60 min at 80-90°C. The solution was then filtered with coarse filter paper. A solution with 0.1 mole 2-aminoethylchloride

hydrochloride was made in ethanol and added drop-wise into the stirred solution of the selenium compound over the course of 1 h. This solution was also filtered with the coarse filter paper and chilled overnight. Crystals were collected and extracted with 100 mL aliquots of hot 80% ethanol using 0.45 μM cellulose acetate filters and water aspiration. Filtrates were combined and dried under vacuum before being recrystallized in methanol or dilute ethanol. The dried residue was dissolved in 200 mL of 1N HCl, with about two-thirds of the solution allowed to evaporate. The pH was adjusted to around 4 using HCl or KOH, with the mixture then dried. Using boiling absolute ethanol the residue was extracted until it was colorless, then crystallized in ice overnight. The product was filtered and washed with excess chloroform and then vacuum dried. The synthesis and characterization were performed by Dr. Kun Liu.

2.2.4 Nitric Oxide Analyzer (NOA) Assays

Figure 2.5 shows the setup of the NOA cell with N_2 used as the purge gas, as well as the carrier gas. As NO is released in the solution it is bubbled out and pulled into the analyzer via vacuum. Once inside the reaction chamber, the NO will react with ozone, to generate nitrogen dioxide in the excited state, which when relaxes back to ground state, releases a photon (Equations 2.2, 2.3).

$$NO + O_3 \rightarrow NO_2^* + O_2 \quad (2.2)$$

$$NO_2^* \rightarrow NO_2 + h\nu \quad (2.3)$$

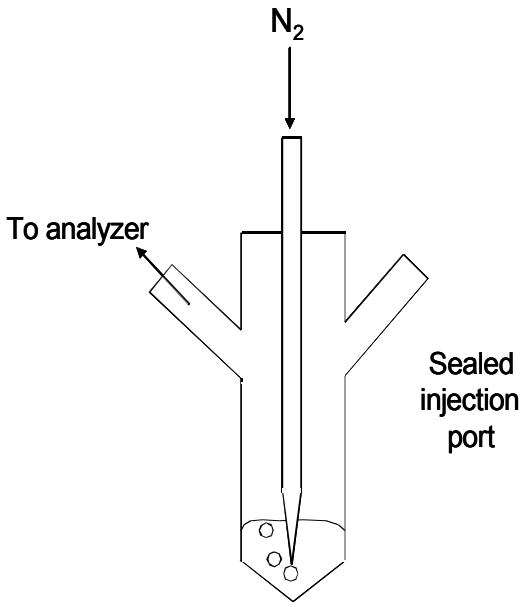

Figure 2.5 The cell used for the NOA assays with the assay reagents in the bottom being purged with N_2(g). A sealed injection port on the side allows for samples to be injected without opening the chamber to ambient air. The gas is then pulled in to the NO analyzer via vacuum.

A 50 mM stock solution of SeCA was prepared in water and used for all assays. The stock solution was stored in a 2°C refrigerator in a foil-covered vial. To the NOA cell, PBS with 100 μM EDTA, 0.5 mM SeCA and 5 μM GSH were added. Other concentrations of the SeCA and GSH were tried in order to optimize the assay system. For the calibration data reported there was a 1:1 dilution for all samples, for both the 2 mL total volume and the 3 mL total volume experiments. Each RSNO concentration was analyzed in separate experiments. Calibration was performed for GSNO, CysNO, SNAC and AlbSNO.

For the copper(II) chloride/cysteine based assay, 5 mM $CuCl_2$ and 3 mM Cys were added to the NOA cell using PBS as the solvent. The copper reacts with RSNOs according to the equations below.

$$2Cu^{2+} + 2RS^{-} \rightarrow 2Cu^{+} + RSSR \quad (2.4)$$

$$Cu^{+} + RSNO \rightarrow Cu^{2+} + RS^{-} + NO \quad (2.5)$$

The same procedure described above was used for the calibration using GSNO, CysNO, and SNAC.

2.2.5 Testing Transnitrosation

To test the concept of transnitrosation, AlbSNO was added to nitrogen purged PBS to achieve a final concentration of 25 μM, with the PBS also containing either 25 μM, 100 μM or 250 μM of a LMW thiol; GSH, Cys or NAC, in a foil wrapped centrifuge tube with a 30,000 molecular weight cutoff filter (Figure 2.6). The mixture was incubated in a water bath at 37°C with a blanket of nitrogen for either 15 or 30 min. At the end of the incubation period, the mixture was spun down at 4000 rpm for 10 min. One milliliter of the resulting filtrate was injected into the NOA for analysis.

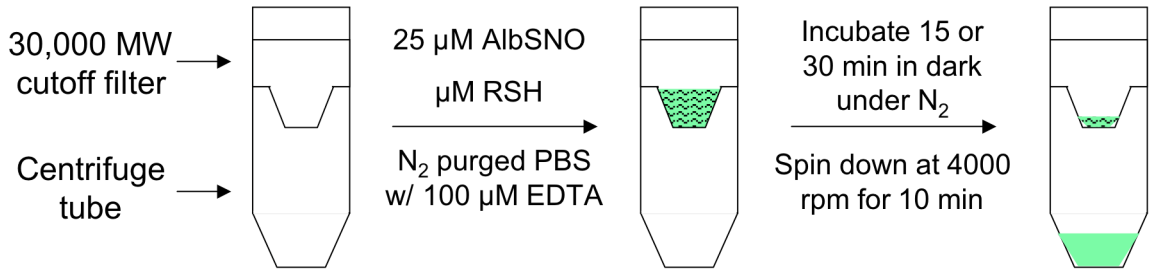

Figure 2.6 Samples containing 25 μM AlbSNO with either 25, 100 or 250 μM of one of the LMW thiols were loaded into a centrifuge tube containing a 30,000 MW cutoff filter. After incubating in the dark under N_2 for either 15 or 30 min, the tube was spun down, leaving the protein in the filter and the filtrate containing the transnitrosated LMW RSNO.

2.2.6 Plasma RSNO Testing

Fresh blood from a sheep, pig, or rabbit was drawn into a foil-covered vacutainer coated with heparin. The blood was removed and spun down at 4000 rpm for 10 min. One milliliter of plasma was drawn into a syringe and injected into the NOA cell

containing 1 mL of PBS with 100 μM, 0.5 mM SeCA, and 5 μM GSH and the anti-foaming agent. After the initial signal was collected, 10 μM AlbSNO or GSNO was spiked into the sample. Percent recovery was then calculated.

For the time trials, 4 mL plasma was placed into a foil-covered vial and then spiked with 10 μM GSNO. Initially, 1 mL of the spiked plasma was injected into the NOA and analyzed with the remaining plasma stored either at room temperature, 37°C, or 4°C, and tested after 1 h, 2 h and 5.5 h. Control experiments were performed using PBS as the background solution.

2.2.7 Detection of HbSNO

Fresh pig blood was drawn into a foil-covered heparinized syringe. The blood was transferred to a small centrifuge tube and spun down to separate the red cells from the plasma. The plasma was removed and enough isotonic buffer containing 50 mM phosphate, 85 mM NaCl, 4.5 mM KCl and 100 μM DTPA at pH 7.0 was added to equal the original volume of the blood. The red cells were placed into the spin tonometer with 50 μM NAC and deoxygenated with 95% N_2/5% CO_2 for 10 min, allowing for transnitrosation to occur between the HbSNO and the NAC. After tonometering, the suspended red cells were placed in a centrifuge tube with a 30,000 molecular weight cutoff filter and spun down at 3,200 rpm for 10 min. One milliliter of the resulting filtrate was injected into the NOA for analysis of SNAC concentration. Figure 2.7 summarizes the process.

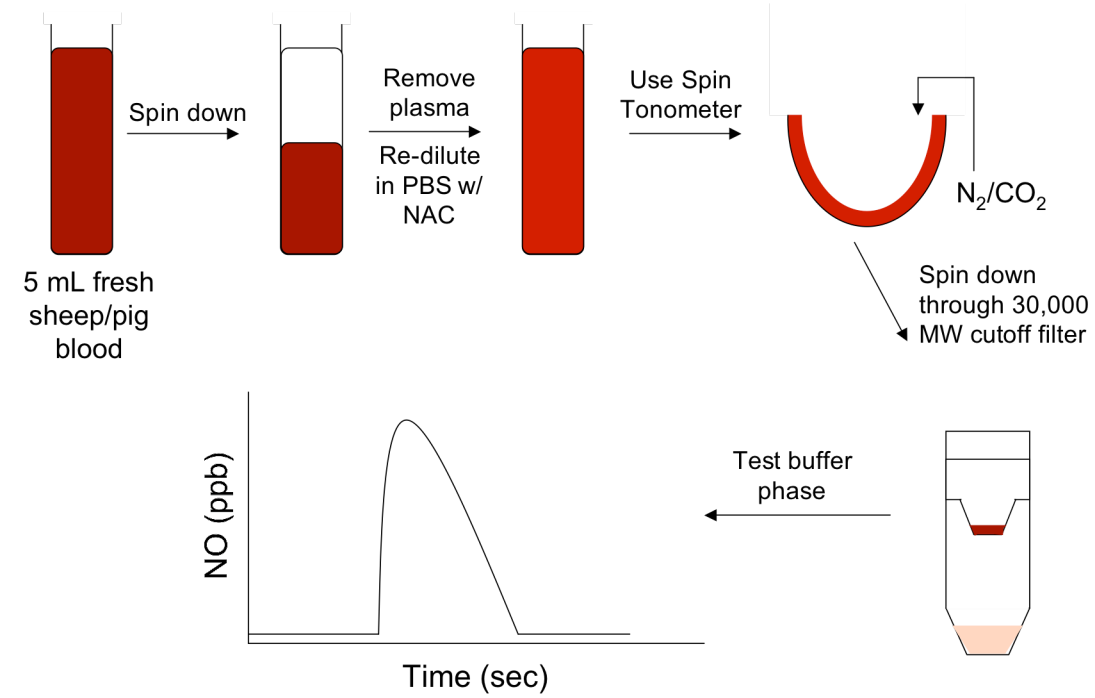

Figure 2.7 To detect HbSNO, fresh sheep or pig blood was obtained and spun down to remove the plasma. Buffer was added, along with NAC, and the sample was deoxygenated in the spin tonometer for 10 min. After, the solution was spun down through a 30,000 MW cutoff filter and 1 mL of the buffer phase was analyzed in the NOA.

Sheep and rabbit blood were obtained and the same procedure described above was followed, with the exception of the red cells being lysed with 50 mM phosphate buffer containing 100 μM EDTA, pH 7.4, prior to tonometering. The solution was spun down through the 30,000 MW cutoff filter for 10 min with 1 mL of the filtrate then injected into the NOA cell.

2.3 Results and Discussion

2.3.1 Optimization of Selenocystamine/Glutathione Assay

Four different concentrations of SeCA, 5 mM, 1 mM, 0.5 mM and 0.05 mM, were examined along with 3 concentrations of GSH, 0.5 mM, 0.05 mM and 5 μM. Higher concentrations of the SeCA did not change the rate of the catalysis and did not

decrease the time required for analysis. This is likely due to the low concentrations of RSNO analyzed, as well as limitations as to how quickly the NO can be purged from the reaction solution. The rate was slower at 0.05 mM, indicating some dependence of rate versus concentration, so 0.5 mM was chosen for all future work in order to minimize the use of the reagent, while maximizing the speed of analysis. There was a small difference in signal depending on the GSH concentration, but 5 μM was chosen for future experiments due to the report from Hogg et al. stating that excess GSH may scavenge NO under anaerobic conditions (Equation 2.6).[21]

$$2GSH + 2NO \rightarrow GSSG + N_2O + H_2O \qquad (2.6)$$

Additionally, the stability of the catalyst solution was monitored using UV-Vis over the course of 2 years. Figure 2.8 shows the maximum absorbance band remains constant at 298 nm, with the difference in absorbance coming from the stock solution becoming more concentrated as the water slowly evaporated over the 2 year period.

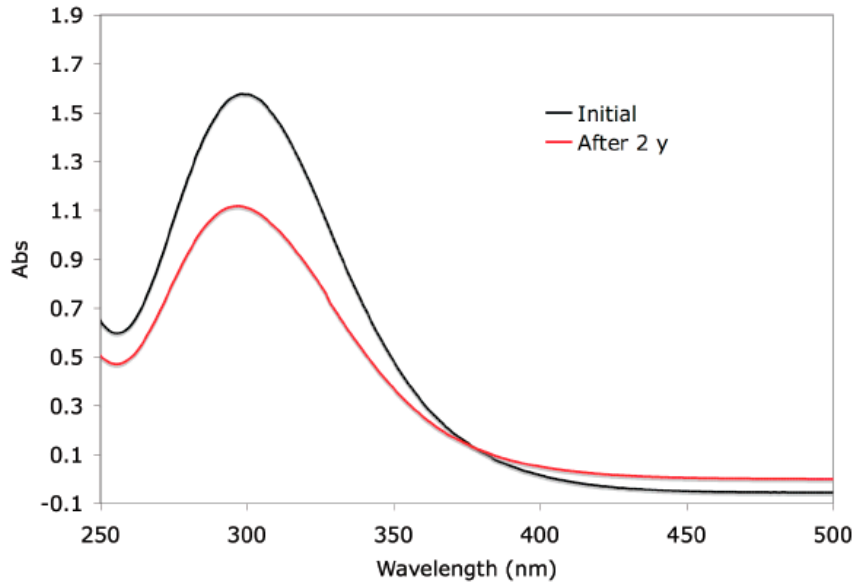

Figure 2.8 UV-Vis spectra of SeCA over time.

2.3.2 Characterization of Selenocystamine/Glutathione Assay

The sensitivity for each of the three LMW RSNOs, GSNO, CysNO and SNAC, was examined in two different total assay volumes, 2 mL and 3 mL. For each concentration, the area under the curve was integrated with a calibration curve generated, plotting area versus concentration. The lowest concentration tested was 20 nM and this level was easily detected (Figure 2.9). Overall, the sensitivities at each volume were similar among the three RSNOs, shown in Figure 2.10a, with good reproducibility (Figure 2.10b). The sensitivities at 3 mL were higher due to there being a greater number of moles present in each sample. Comparing these values to the same calibrations using the Cu(II)/Cys assay (Figure 2.11) shows comparable results, with the SeCA/GSH assay being slightly more sensitive. The solubility of Cu^{+} ions at a neutral pH is low, which may account for the decrease in sensitivity since some of the catalyst may not be active.

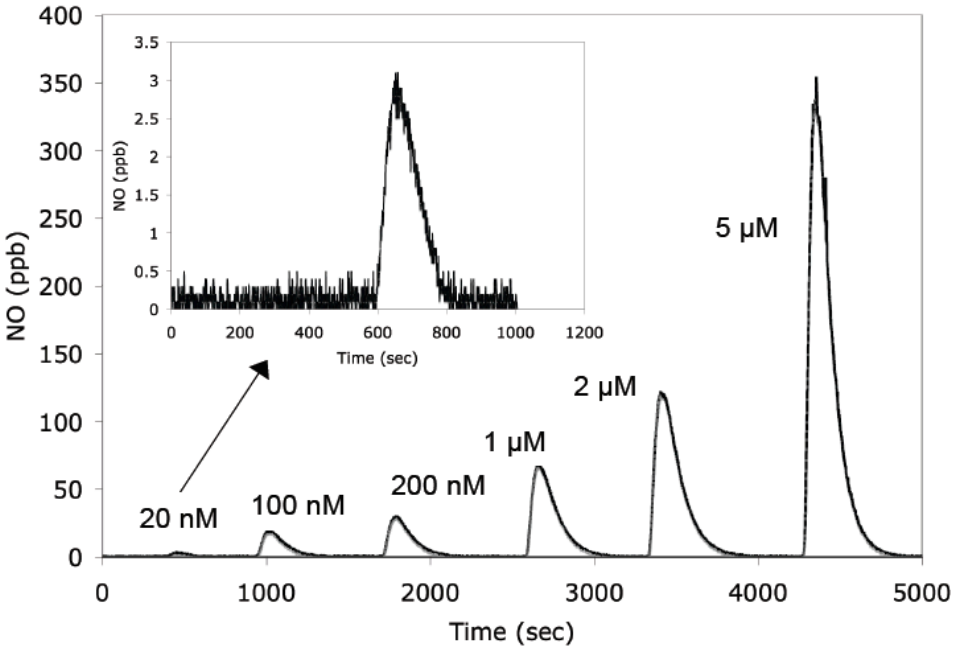

Figure 2.9 *S*-Nitrosoglutathione calibration in 2 mL with 0.5 mM SeCA and 5 µM GSH. **Inset**. The lowest concentration tested, 20 nM, is clearly observed.

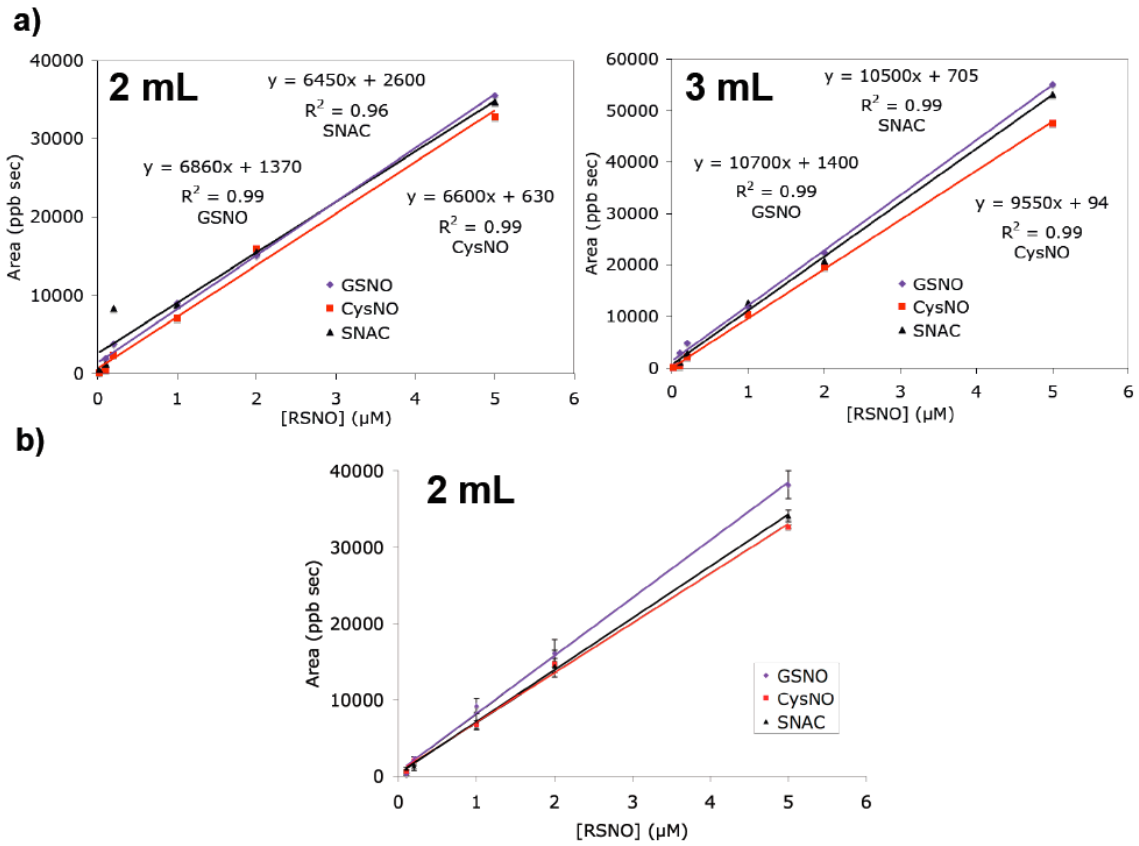

Figure 2.10 a) Typical calibration curves at 2 mL and 3 mL total volume for GSNO, CysNO, and SNAC. **b)** Reproducibility of the SeCA.GSH assay in 2 mL, for n = 3 measurements.

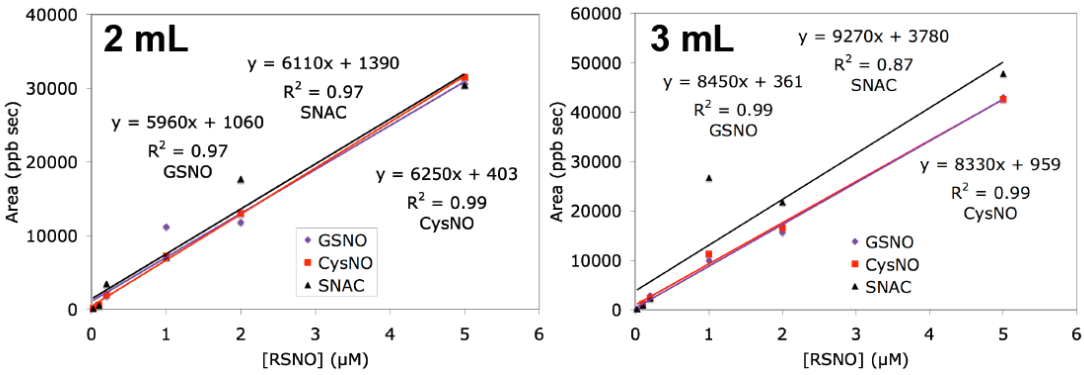

Figure 2.11 Calibration curves for GSNO, CysNO, and SNAC using the Cu(II)/Cys assay system at both 2 mL and 3 mL total volume.

Response to nitrite was determined for each assay system. With the addition of 10 μM NO_2^- to the Cu(II)/Cys assay there is a very slight change in the baseline (Figure 2.12a). A change of about 2 ppb NO was observed with the addition of 100 μM NO_2^-,

which remained constant for ca. 1.4 h. At this point another injection of NO_2^- was made, bringing the final concentration in the cell to 1 mM. This resulted in a slow release of NO with a gradual decay toward the baseline. The same injections into the SeCA/GSH (Figure 2.12b) assay were made with no change in the baseline, even up to 2 mM NO_2^-, indicating excellent selectivity of the new assay over nitrite.

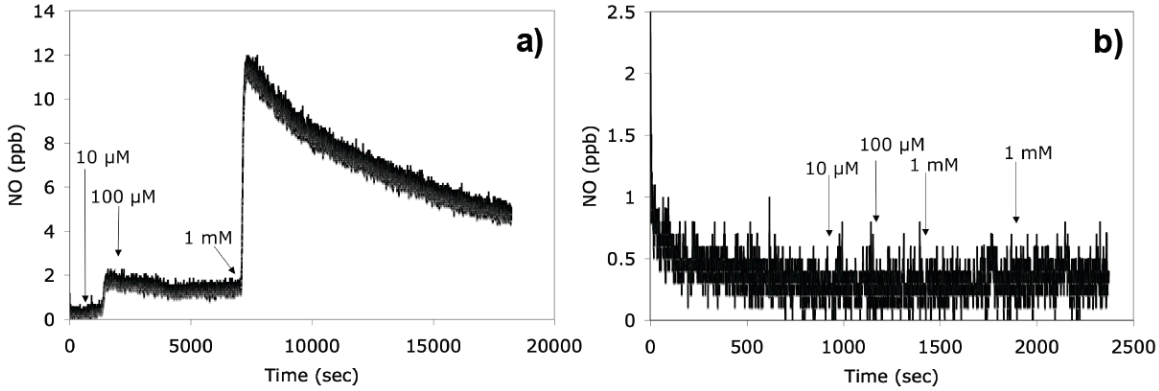

Figure 2.12 Response to nitrite for the **a)** Cu(II)/Cys assay and for the **b)** SeCA/GSH assay.

Calibration with AlbSNO was also performed with the SeCA/GSH assay in 2 mL total volume (Figure 2.13). The sensitivity is higher than for the LMW RSNOs and there is more error associated with these measurements, likely because of the foaming generated when protein solutions are bubbled with N_2. Trials without GSH present were also run and generated a curve similar to trials with the reducing agent (Figure 2.14). The analysis time increased almost four-fold, but still a signal linearly proportional to concentration was observed. This is not the case with the LMW RSNOs, leading to the conclusion that free thiols within the protein RSNO are able to act as the reducing agent for the SeCA. However, in biological samples free thiols will always be present so it will not be possible to distinguish between the LMW and HMW species using the new homogeneous SeCA-based assay method.

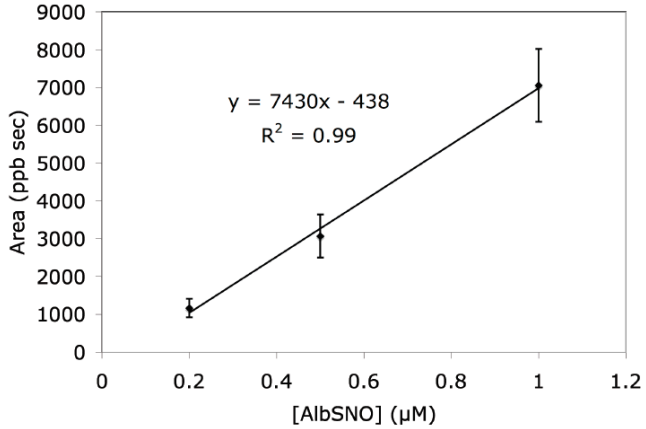

Figure 2.13 Calibration curve for AlbSNO in 2 mL total volume using the SeCA/GSH assay (n = 3 for each calibration point). Error bars are ± s.d.

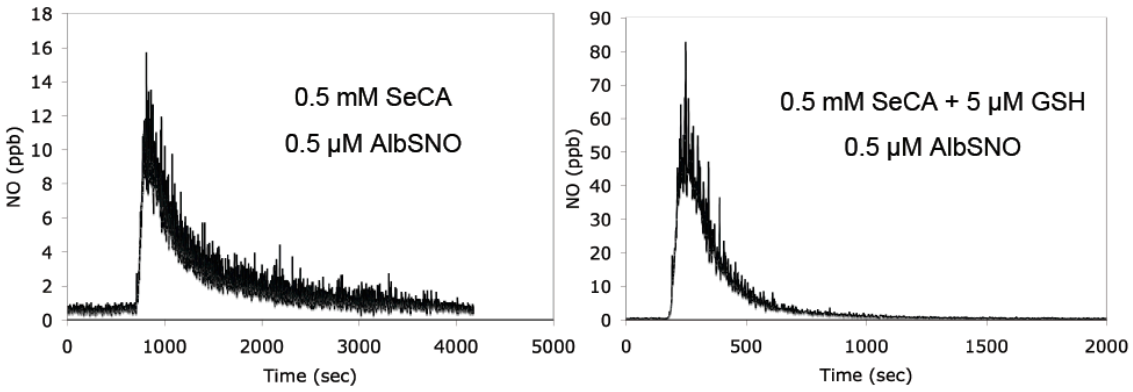

Figure 2.14 Injections of AlbSNO with and without GSH present. The thiols on the proteins act as the reducing agent for the SeCA catalyst, but the reaction is much slower.

2.3.3 Transnitrosation Analysis

Percent transnitrosation was calculated for each trial for all incubations times and concentrations (Figure 2.15). The three LMW thiols tested displayed interesting trends. For NAC and GSH, the percent transnitrosation increased with both concentration and time. There was a difference in Cys between 25 μM and 100 μM, but there was no difference between 100 μM and 250 μM. There was also no change if the incubation

time was extended from 15 min to 30 min. One possible explanation is that CysNO is known to be less stable than SNAC or GSNO.[22]

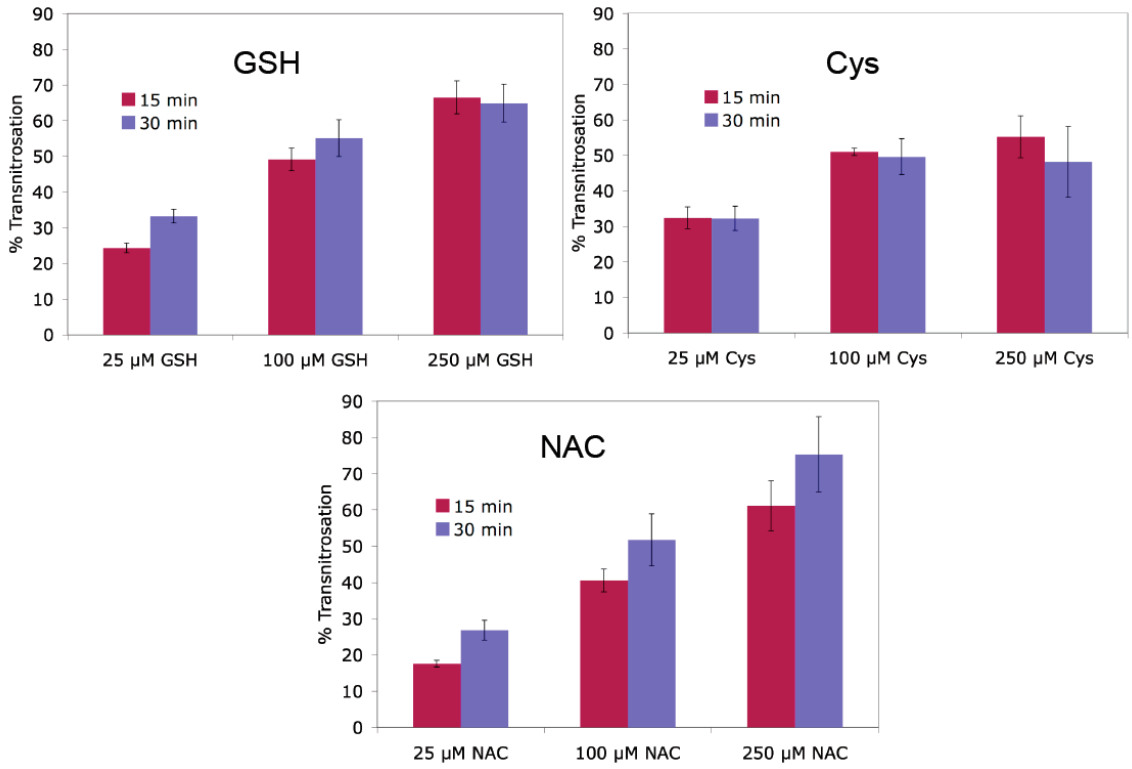

Figure 2.15 Percent transnitrosation for GSH, Cys, and NAC at the three concentrations of thiols tested and the two incubation times, with n = 3 for each set. Error bars are ± s.d.

Equilibrium values, *K*, were calculated for the different trials according to Equation 2.7, and compared with published values from Hogg.[13]

$$K = \frac{[RSNO][Alb]}{[AlbSNO][RSH]} \tag{2.7}$$

The values, shown in Table 2.1, are comparable among the thiols and are slightly higher than the published values (Table 2.2). The difference is likely caused by the Hogg report using HPLC as the detection method, which is not as sensitive as chemiluminescence. Overall, these results indicate that NAC or GSH are better thiols to use if trying to

transnitrosate from a protein RSNO. Furthermore, use of the SeCA/GSH assay could be extended to look at other transnitrosation reactions.

Table 2.1 *K* values for three LMW thiols used in the transnitrosation studies.

[AlbSNO] (μM)	[RSH] (μM)	K_{GSH}	K_{Cys}	K_{NAC}
25	25	0.178	0.232	0.107
25	100	0.170	0.147	0.149
25	250	0.135	0.064	0.194
Average		0.16 ± 0.02	0.15 ± 0.08	0.15 ± 0.04

Table 2.2 *K* values for AlbSNO incubated with GSH at varying concentrations, as reported by Hogg et al.[13]

[AlbSNO] (μM)	[GSH] (μM)	K_{Hogg}
33.80	50	0.201
33.80	100	0.098
33.80	200	0.131
33.80	300	0.088
Average		0.13 ± 0.05

2.3.4 Spiked Plasma Testing

In order to inject plasma into the NOA, an anti-foaming agent (AF) must be added to the assay to prevent the proteins from foaming and fouling the instrument. The AF is a silicone dispersion that lowers the surface tension of a solution, thereby inhibiting the formation of bubbles.[23] To ensure the AF does not alter the SeCA/GSH assay, injections of 1 μM GSNO were made in the presence and absence of the additive, and the area

under each NO release curve was integrated (Figure 2.16). There is no significant difference in the area, indicating the assay remains functional with the AF present.

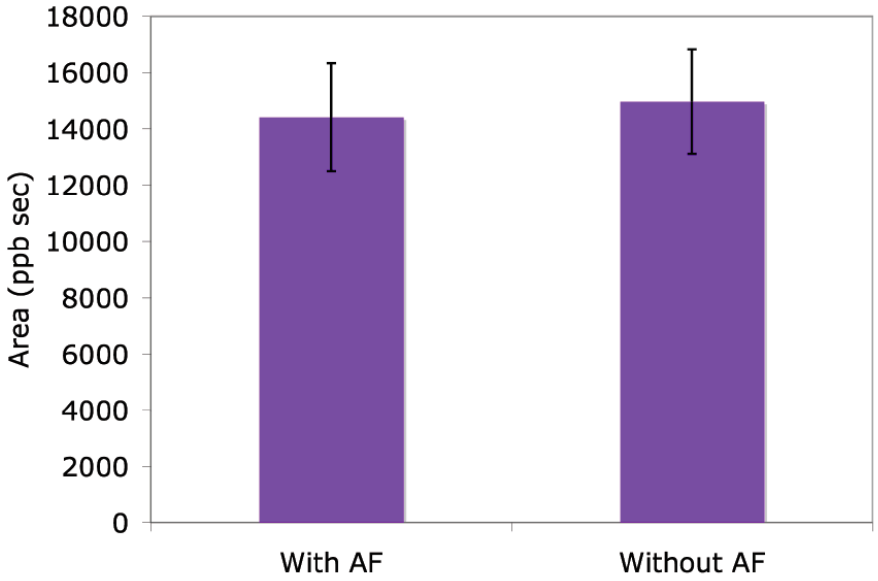

Figure 2.16 Samples of 1 μM GSNO analyzed with and without AF present. There is no significant change if the AF is in the assay mixture. Error bars represent ± s.d. for n = 3 measurements.

Samples of sheep and pig plasma were spiked with 10 μM AlbSNO and analyzed for percent recovery, with only 61.3% and 70.0% seen, respectively. Rabbit plasma spiked with 2 μM and 10 μM GSNO was also analyzed, with higher recoveries seen. Over 80% was recovered from the rabbit plasma, but it was unclear if the increase was due to the type of RSNO, the source of the plasma, or species in the plasma degrading the RSNOs. The results are summarized in Table 2.3.

Table 2.3 Summary of spiked plasma results.

	AlbSNO		GSNO	
	Pig (10 µM)	**Sheep (10 µM)**	**Rabbit (2 µM)**	**Rabbit (10 µM)**
Trial 1	74.4%	68.2%	75.8%	94.7%
Trial 2	69.4%	48.2%	81.5%	92.0%
Trial 3	66.1%	67.6%	85.1%	89.8%
Average	70.% ± 4	61% ± 11	81% ± 5	92% ± 3

One reason for the low recovery is the presence of trace amounts of hemoglobin. Oxyhemoglobin is a known scavenger of NO and will quickly react with the gas, preventing it from being detected by the NOA.[24] Additionally, there are many enzymes in plasma, which are known to breakdown GSNO and may breakdown other RSNOs.[25] These enzymes and their reaction products are shown in Table 2.4. Many of these products will not be detect by the NOA, supporting the conclusion that these enzymes are decomposing GSNO within the plasma. Ceruloplasmin, a copper containing enzyme, is also present and may act as an NO oxidase, further limiting the amount of NO that will be detected.[26]

Table 2.4 Enzymes present in plasma that are known to breakdown GSNO. Reproduced from reference 23.

Enzyme	Nitrogen oxide product	Size (kDa)
(Thioredoxin) thioredoxin reductase	Nitric oxide	55
Glutathione peroxidase	Nitric oxide	84.5
γ-Glutamyl transpeptidase	S-Nitroso-cysteinyl glycine	80
(Xanthine) Xanthine oxidase	Peroxynitrite	270
Glutathione-dependent formaldehyde dehydrogenase	Hydroxylamine[a]	40

[a] Under conditions of excess reduced thiol.

To gain a better understanding of this loss of RSNO species as a function of time, additional sheep plasma samples spiked with 10 μM GSNO and incubated at 23 °C were then tested over the course of 5.5 h, with data points take at t=0 h, 1 h, 2 h, and 5.5 h, to determine if there was a decrease in the GSNO level (Figure 2.17a). These experiments were repeated with incubation temperatures of 4 °C and 37 °C (Figure 2.17b and 2.17c). Additionally, the plasma was also filtered using a MW cutoff of 30,000 and incubated at 23 °C as well (Figure 2.17a). Controls at each temperature of 10 μM GSNO in buffer were also run in order to establish degradation caused by temperature alone. In all trials there was little to no change in the buffer samples, indicating that temperature was not a direct cause of the GSNO loss. For the unfiltered trials at all incubation temperatures, the initial percent GSNO recovery was between 50 and 60 percent because of hemoglobin contamination. When the plasma was filtered, this initial point was ca. 100 percent, similar to the controls, but a significant decline was still observed. While the enzymes listed in Table 2.4 should have been removed, it is possible that the filtration was

incomplete or that some of these HMW species came through the filter, as was reported by Georgiou et al.[27]

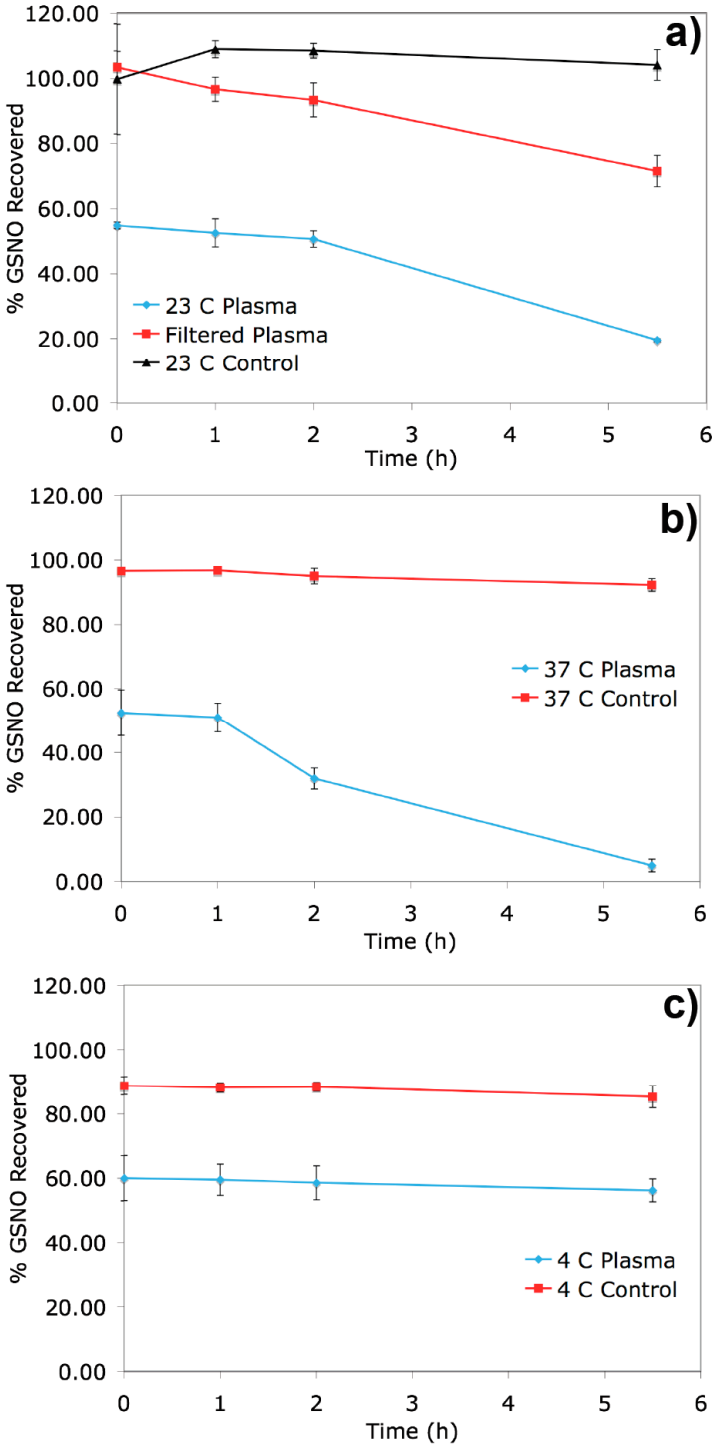

Figure 2.17 Time trials of sheep plasma spiked with 10 μM GSNO at **a)** 23 °C, **b)** 37 °C, and **c)** 4 °C. Control trials run with buffer as the bulk solution.

If the decline was due to enzymatic activity, the rate of GSNO decline should correlate to changes in incubation temperature. Indeed, this was observed, with the rate increasing at 37 °C, and with almost no change at 4 °C. It can be concluded that RSNO degradation in plasma will occur unless the samples are stored at 4 °C.

2.3.5 S-Nitrosohemoglobin Detection

After 10 min in the spin tonometer in the presence of 50 μM NAC, 140 nM of HbSNO was detected in a pig blood sample (Figure 2.18). To ensure the catalyst was still functional after the addition of the sample, 2.5 μM SNAC was injected, with 100% of the moles recovered. Additional trials were run using sheep blood and there was no change in signal after injection into the NOA. In subsequent trials, the red cells were lysed giving the NAC direct access to the HbSNO. Despite this modification to the assay method, still no HbSNO was detected. In surveying the literature, there are no reports on detecting HbSNO in sheep, which may be because there is no measurable level of HbSNO in this animal. Rabbit blood was also tested, but again no HbSNO was detected. At least 10-15 mL of blood is required for testing, a volume that cannot be drawn from a rabbit unless it is the terminal draw. As a result, the blood was obtained as the terminal draw from a rabbit that had undergone 7 h of insulin and glucose infusions, as part of a different experiment. There are several studies reporting that insulin secretion and glucose uptake are NO dependent, so it is likely that the NO/RSNO equilibrium was shifted to allow for more NO to be available for the glucose/insulin chemistry, leaving a lower RSNO concentration.[28-30] Currently, the volume of blood needed to perform the experiments is not conducive to testing blood from a rabbit model.

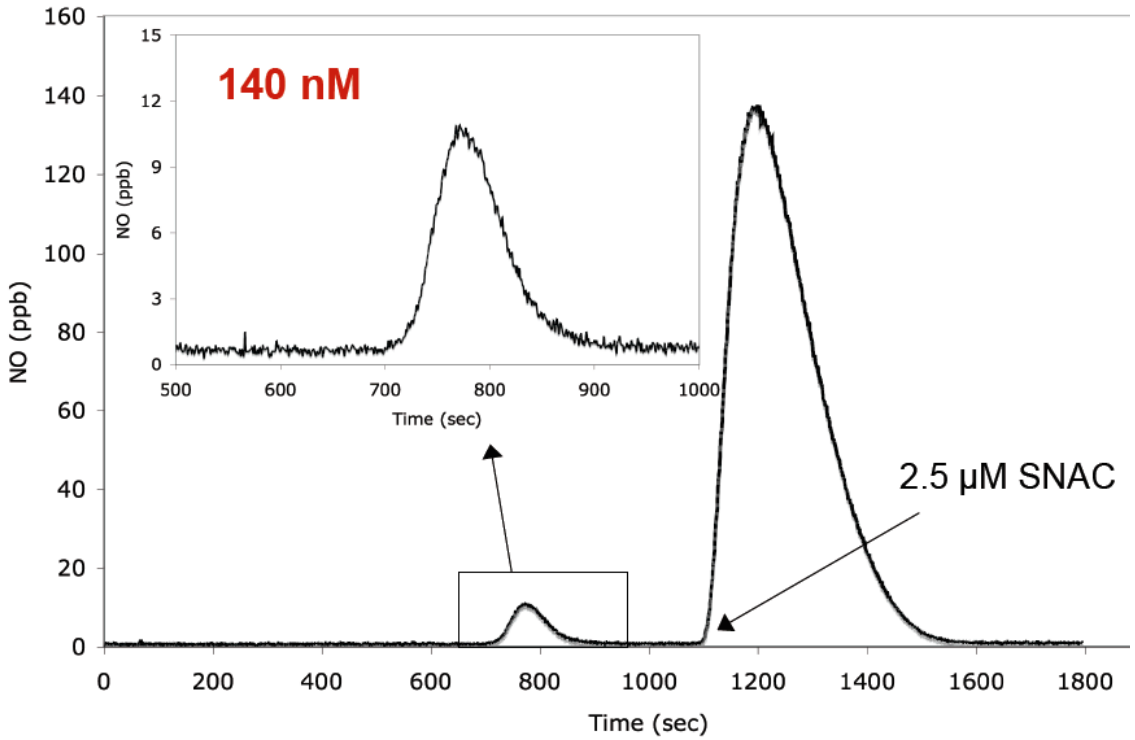

Figure 2.18 Detection of HbSNO from pig blood using NAC for transnitrosation. Injection of 2.5 µM SNAC made to ensure the assay system was still functional after HbSNO addition.

2.4 Conclusion

A homogeneous NOA assay using an organoselenium catalyst, SeCA, has been developed and optimized for RSNO detection. There is good sensitivity and detection limits for GSNO, CysNO and SNAC that are comparable to the Cu(II)/Cys assay. Detection of AlbSNO was also observed, with a calibration curve easily generated. It has been demonstrated that the assay system is functional in a biological matrix, and can be used for examining transnitrosation reactions. Additionally, plasma samples spiked with GSNO were analyzed over time at different incubation temperatures for GSNO degradation. Significant GSNO decomposition was observed at 37 °C, with less at 23 °C, and almost no change at 4 °C, indicating breakdown caused by enzymatic activities. Lastly, this assay was used to demonstrate the detection of HbSNO in pig blood samples,

but surprisingly, no HbSNO was observed in sheep blood. Rabbit blood also did not contain any detectable HbSNO, but this may be due to the animal having received insulin and glucose infusions prior to HbSNO analysis.

2.5 References

(1) Feletou, M.; Vanhoutte, P. M. *Americal Journal of Physiology Heart and Circulatory Physiology* **2006**, *291*, H985-H1002.

(2) James, P. E.; Lang, D.; Tufnell-Barret, T.; Milsom, A. B.; Frenneaux, M. *Circulation Research* **2004**, *94*.

(3) Liu, L.; Yan, Y.; Zeng, M.; Zhang, J.; Hanes, M. A.; Ahearn, G.; McMahon, T. J.; Dickfeld, T.; Marshall, H. E.; Que, L. G.; Stamler, J. S. *Cell* **2004**, *116*, 617-628.

(4) Tyurin, V. A.; Liu, S.-X.; Tyurina, Y. Y.; Sussman, N. B.; Hubel, C. A.; Roberts, J. M.; Taylor, R. N.; Kagan, V. E. *Circulation Research* **2001**, *88*, 1210-1215.

(5) Butler, A. R.; Rhodes, P. *Analytical Biochemistry* **1997**, *249*, 1-9.

(6) Cha, W.; Meyerhoff, M. E. *Biomaterials* **2007**, *28*, 19-27.

(7) Cha, W.; Anderson, M. R.; Zhang, F.; Meyerhoff, M. E. *Biosensors and Bioelectronics* **2009**, *24*, 2441-2446.

(8) Williams, D. L. H. *Accounts of Chemical Research* **1999**, *32*, 869-876.

(9) Feelisch, M.; Rassaf, T.; Mnaimneh, S.; Singh, N.; Bryan, N. S.; Jourd'heuil, D.; Kelm, M. *The Journal of the Federation of American Societies for Experimental Biology* **2002**, *16*, 1775-1785.

(10) Giustarini, D.; Milzani, A.; Dalle-Donne, I.; Rossi, R. *Journal of Chromatography B* **2007**, *851*, 124-139.

(11) Forrester, M. T.; Foster, M. W.; Benhar, M.; Stamler, J. S. *Free Radical Biology & Medicine* **2009**, *46*, 119-126.

(12) Zhang, Y.; Hogg, N. *Proceedings of the National Academy of Sciences* **2004**, *101*, 7891-7896.

(13) Hogg, N. *Analytical Biochemistry* **1999**, *272*, 257-262.

(14) Doctor, A.; Platt, R.; Sheram, M. L.; Eischeid, A.; McMahon, T. J.; Maxey, T.; Doherty, J.; Axelrod, M.; Kline, J.; Gurka, M.; Gow, A.; Gaston, B. *Proceedings of the National Academy of Sciences* **2005**, *102*, 5709-5714.

(15) Reynolds, J. D.; Ahearn, G.; Angelo, M.; Zhang, J.; Cobb, F.; Stamler, J. S. *Proceedings of the National Academy of Sciences* **2007**, *104*, 17058-17062.

(16) Gladwin, M. T.; Ognibene, F. P.; Pannell, L. K.; Nichols, J. S.; Pease-Fye, M. E.; Shelhamer, J. H.; Schechter, A. N. *Proceedings of the National Academy of Sciences* **2000**, *97*, 9943-9948.

(17) Patel, R. P.; Hogg, N.; Spencer, N. Y.; Kalyanaraman, B.; Matalon, S.; Darley-Usmar, V. M. *The Journal of Biological Chemistry* **1999**, *274*, 15487-15492.

(18) Gunther, W. H. H.; Mautner, H. G. *Journal of Medicinal Chemistry* **1964**, *7*, 229-232.

(19) Kalyman, D. *Journal of Organic Chemistry* **1965**, *30*, 2454-2456.

(20) Koch, T.; Suenson, E.; Henriksen, U.; Buchardt, O. *Bioconjugate Chemistry* **1990**, *1*, 296-304.

(21) Hogg, N.; Singh, R. J.; Kalyanaraman, B. *FEBS Letters* **1996**, *382*, 223-228.

(22) de Oliveira, M. G.; Shishido, S. M.; Seabra, A. B.; Morgon, N. H. *Journal of Physical Chemistry A* **2002**, *106*, 8963-8970.

(23) Kulkarni, R. D.; Goddard, E. D.; Kanner, B. *Journal of Colloid and Interface Science* **1977**, *59*, 468-476.

(24) Feelisch, M.; Kubitzek, D.; Werringloer, J. In *Methods in Nitric Oxide Research*; Feelisch, M., Stamler, J. S., Eds.; John Wiley & Sons, Ltd.: New York, NY, 1996, pp 455-478.

(25) Gaston, B. *Biochimica et Biophysica Acta* **1999**, *1411*, 323-333.

(26) Shiva, S.; Wang, X.; Ringwood, L. A.; Xu, X.; Yuditskaya, S.; Annavajjhala, V.; Miyajima, H.; Hogg, N.; Harris, Z. L.; Gladwin, M. T. *Nature Chemical Biology* **2006**, *2*, 486-493.

(27) Georgious, H. M.; Rice, G. E.; Baker, M. S. *Proteomics* **2001**, *1*, 1503-1506.

(28) Roy, D.; Perreault, M.; Marette, A. *Americal Journal of Physiology* **1998**, *274*, E692-E699.

(29) Shankar, R.; Zhu, J.-S.; Ladd, B.; Henry, D.; Shen, H.-Q.; Baron, A. D. *Journal of Clinical Investigation* **1998**, *102*, 1403-1412.

(30) Cabou, C.; Cani, P. D.; Campistron, G.; Knauf, C.; Mathieu, C.; Sartori, C.; Amar, J.; Scherrer, U.; Burcelin, R. *Diabetes* **2007**, *56*, 2872-2877.

CHAPTER 3

CHEMILUMINESCENT AND OPTICAL DETECTION OF *S*-NITROSOTHIOLS IN EXHALED BREATH CONDENSATE

3.1 Introduction

Exhaled breath is composed mostly of water vapor droplets containing nonvolatile components, such as proteins and DNA, and the gaseous portion containing volatile components, such as nitric oxide (NO), carbon monoxide and various hydrocarbons. Exhaled breath condensate (EBC) was first measured in the 1980s in Russia.[1] Since then it has proven to be an excellent noninvasive method for quantifying compounds in the breath and for discovering more about the composition of the bronchoalveolar extracellular lining fluid.[1] The source of breath condensate within the lungs is not well defined. There are many possible sources including the oral and nasal cavities, both lower and upper airways, and the alveoli.[2]

Current methods for examining airway conditions are invasive such as bronchoalveolar lavage, bronchial biopsy or induced sputum by inhalation of hypertonic salt solution.[3] Blood and urine analysis has also been attempted, but with little reproducibility and the results do not always correlate with disease state.[2] Sampling exhaled breath directly from the lung is advantageous over sampling from blood or urine

because there is little dilution and any critical biomarkers have not been metabolized.[1] Additionally, the method of collecting the condensate is simple and can be performed by anyone, including young children.[2] Collection can be performed multiple times within a short period without fear of side effects or any negative consequences.[2] Presently, contamination of samples is a major limitation to the collection process. Ambient conditions, delay in analysis after collection, and saliva contamination can alter the measurements and cause a lack of long-term reproducibility.[4]

Analysis of EBC has been used to determine concentrations of hydrogen peroxide, nitrite, nitrate and other markers of oxidative stress such as 8-isoprostane, leukotrienes, and prostaglandins.[5] Researchers have been able to correlate the concentrations of these biomarkers with disease states such as asthma, chronic obstructive pulmonary disease (COPD), and cystic fibrosis (CF).[6, 7] It is also well documented that asthmatic patients have higher concentrations of these oxidative markers due to the increase in inflammatory cell response associated with this disorder.[8, 9]

Several studies have already been performed to examine *S*-nitrosothiol (RSNO) levels in breath condensate. The reported values vary greatly, ranging from 0.03-0.94 μM in healthy patients, and from 0.05-1.73 μM in patients with asthma.[10-14] There are two conflicting reports regarding the RSNO concentrations in asthmatic patients. The first from Corradi et al. suggests an increase in RSNO levels in patients with severe asthma.[13] The second, a study from Gaston et al., found a decrease in the concentration of RSNOs in samples taken from asthmatic children.[14] There are a few differences between the studies, one being different sampling locations. Gaston and coworkers sampled directly from the lining of the trachea, while Corradi looked at EBC. The other

main difference is the detection methods used. Gaston used chemiluminescence with a copper catalyst and Gaston used the Saville-Griess assay; both of these methods will be examined in this chapter. The reproducibility of these previous RSNO measurements has not been reported and the concentrations found include a very wide range of values, likely due to the known lability of RSNOs. Further, in the previous reports from Gaston and Corradi there is no mention of the time gap after collection until analysis, or if the samples were protected from light. These conditions may account for some of the discrepancy in the results. Indeed, with an improved method of testing, EBC RSNOs could become a more useful marker for disease diagnostics.[4]

In this chapter, chemiluminescent and optical detection methods are used to assess the true detectable concentrations of RSNOs in the EBC of 5 healthy subjects. The homogeneous selenocystamine assay, described in Chapter 2, is used along with the well known copper(II) chloride assay. To further verify the results, the Saville-Griess assay, also used by the Corradi group, is employed to determine both nitrite and RSNO concentrations in EBC samples.

3.2 Experimental

3.2.1 Materials and Instruments

Glutathione, copper(II) chloride, cysteine, mercury(II) chloride, *N*-(1-naphthyl)ethylenediamine (NED), hydrochloric acid, sulfuric acid, ethylenediaminetetraacetic acid and sodium nitrite were obtained from Sigma-Aldrich (St. Louis, MO). Sulfanilamide was from Acros (New Jersey). All buffers and solutions used were prepared using Milli-Q grade deionized water (18.2 MΩ, Millipore Corp.,

Billerica, MA). The collection device and collection vial were custom made in house. The two-way non-rebreathing valve, one-way valve, mouthpiece and nose clip were purchased from Hans Rudolph, Inc. (Shawnee, KS).

A Nitric Oxide Analyzer (NOA), model 280i from GE Analytical (Boulder, CO) was used for all chemiluminescence measurements. Optical measurements for the Saville-Griess assay were performed on a PerkinElmer Lambda 35 UV-Vis spectrophotometer (Waltham, MA).

3.2.2 Collection of Breath Condensate

Using a newly designed collection apparatus (Figure 3.1), breath condensate was collected from five healthy volunteers. To prevent photodecomposition of the RSNOs, the glassware was either wrapped in black electrical tape or made with amber glass. Prior to collection, the device was rinsed three times with 100 μM EDTA, and the subject rinsed their mouth with water. A two-way non-rebreathing valve allowed for breath to enter the chamber upon exhaling and allowed for the subject to inhale, but separated the inhaled and exhaled air. The breath then entered a chamber cooled to 0°C using an ice bath and condenses, with the solution falling into a small amber glass container specially designed for this apparatus (Figure 3.1), containing a 200 μL of 100 μM EDTA. It should be noted that this added solution volume was taken into account when concentrations were calculated. The breath was allowed to leave the device through a one-way valve, which prevented ambient air from entering. After 15 min of collection, a 1 mL foil covered disposable syringe was inserted into the side port of the collection vial,

removing 1 mL of the condensate, which was then injected into the NOA cell with the reagents present.

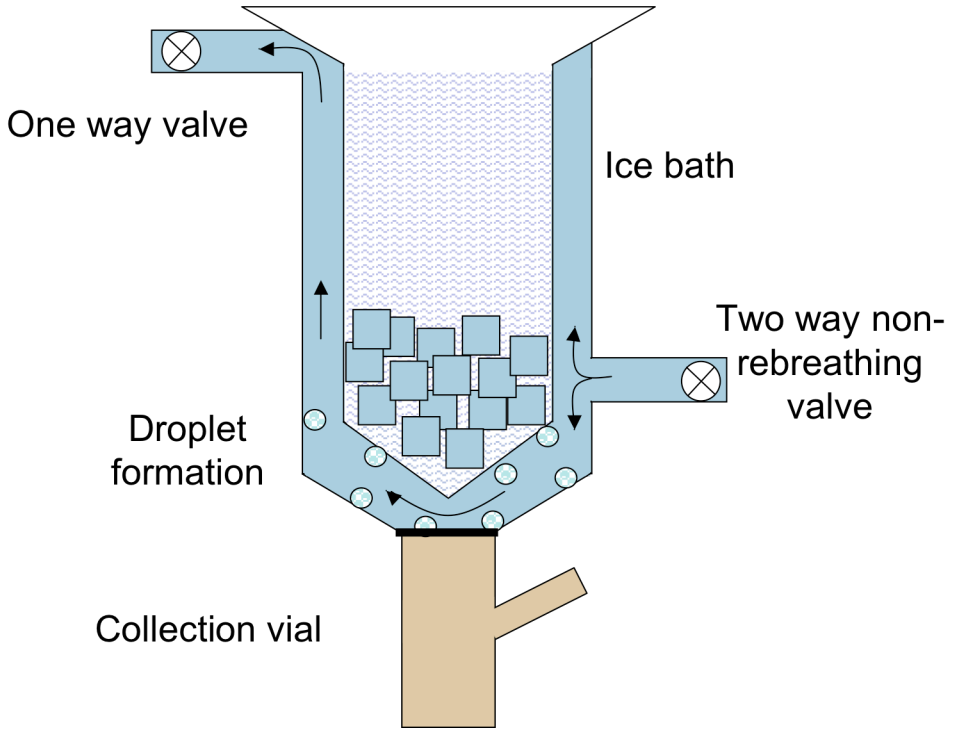

Figure 3.1 Schematic of exhaled breath condensate collection device fabricated and used in this research.

To ensure the collection process was not decomposing RSNOs prior to analysis, a small spray bottle was filled with 5 mL of 10 μM GSNO. The solution was sprayed into the condenser under the same conditions as the EBC is obtained, with 1 mL of the collected solution injected into the NOA cell containing 5 mM SeCA and 5 μM GSH in 1 mL of PBS with 100 μM EDTA. For controls, 1 mL of the 10 μM GSNO solution was directly injected into the NOA and 5 mL of the GSNO solution was sprayed into a foil-covered vial, with 1 mL then analyzed.

3.2.3 Nitric Oxide Analyzer Analysis

Copper/Cysteine Assay System

A solution of 5 mM copper(II) chloride and 3 mM cysteine as the reducing agent was placed into the NOA cell. Cysteine reduces the Cu(II) to Cu(I) ions that then interact with RSNOs to liberate the NO, in accordance with the following reactions:

$$2Cu^{2+} + 2RS^{-} \rightarrow 2Cu^{+} + RSSR \quad (3.1)$$

$$Cu^{+} + RSNO \rightarrow Cu^{2+} + RS^{-} + NO \quad (3.2)$$

However, the Cu(I) ions can also reduce nitrite to NO.[15]

$$Cu(I) + NO_2^{-} + H_2O \rightarrow NO + 2OH^{-} + Cu(II) \quad (3.3)$$

Selenocystamine/Glutathione Assay System

Selenocystamine was synthesized in house (see Chapter 2). A 50 mM stock solution of SeCA was made in water and characterized using UV-Vis. The assay utilized 5 mM SeCA with 0.5 mM GSH as the reducing agent in PBS buffer (10 mM, 140 mM NaCl, pH 7.4). Ethylenediaminetetraacetic acid was also added at 100 μM to chelate any trace metal ions. It should be noted that the concentrations used differ from those determined to be optimal in Chapter 2 due to the fact that this work was completed prior to finalizing the research described Chapter 2.

3.2.4. Optical Detection Using the Saville-Griess Assay

To detect nitrite, the Griess assay is commonly used. The Griess reagent was prepared by dissolving 0.25 g of sulfanilamide into 75 mL of 1 M HCl. A 2% solution of N-napthylethylnediamine was made in Milli-Q water and was then added to the

sulfanilamide solution. Water was added to make 100 mL total volume. Nitrite standards were made using $NaNO_2$. A 1:1 ratio of sample:Griess reagent was mixed and allowed to react for 10 min, during which time a colored azo complex is formed (Figure 3.2). After the incubation period, a UV-Vis spectrum was taken from 300-800 nm, with maximum absorbance at 542 nm.

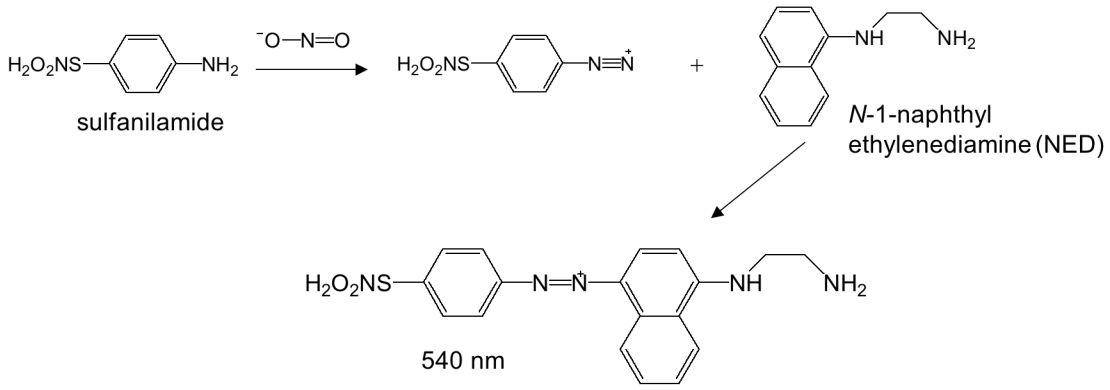

Figure 3.2 The chemistry of the Griess Assay showing the final azo product with a maximum absorbance at 540 nm.

The Saville assay uses mercury compounds to cleave the S-NO bond (Figure 3.3). The NO then reacts with oxygen to produce nitrite, which can be detected via the Griess assay. To prepare the Saville reagent, 0.01086 g of mercury(II) chloride was added to 10 mL of the Griess reagent to yield a final concentration of 4.0 mM $HgCl_2$. Again, a 1:1 sample:Saville reagent ratio was used with a 10 min incubation time. The spectrum was collected between 400 nm and 800 nm with a maximum absorbance at 542 nm. *S*-nitrosoglutathione standards were made from 16 mg of GSH dissolved in 9.75 mL of 20 μM EDTA with 15 μL concentrated sulfuric acid and 250 μL of 200 mM $NaNO_2$.

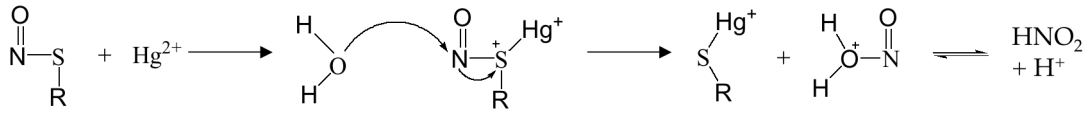

Figure 3.3 The chemistry of the Saville Assay. Once the nitrite is formed it reacts with the Griess reagent to form the final azo product.

3.3 Results and Discussion

3.3.1 Nitric Oxide Analyzer Analysis

Using the Cu(II)/Cys assay system, EBC samples from 3 participants were analyzed for RSNOs. A signal was observed for all samples from the test subjects with the calculated values ranging from 0.110 μM to 0.240 μM, giving an average of 0.19 μM (Table 1). It is known that the Cu(I) ions generated in this assay will reduce nitrite to NO, and there are literature reports that nitrite is present in EBC at concentrations similar to those found here.[16] In order to determine if this signal was from nitrite or RSNOs, a fresh EBC sample was collected and two – 1 mL aliquots were injected (Figure 3.4a) into the NOA. A concentration of 0.130 μM was determined with the sample then stored overnight in the 2°C refrigerator and analyzed again with the same assay conditions. The calculated concentration unexpectedly increased to 0.240 μM (Figure 3.4b). With the sample stored in the refrigerator it is likely that the majority of the RSNOs were preserved overnight since the pH of the EBC is between 5 and 6, depending on the sample, and RSNOs are more stable in a cool, acidic environment. However, it is unlikely that the concentration would almost double. This increase is more likely to be nitrite, given previous literature reporting an increase in the nitrite concentration in an EBC sample over time.[17]

Table 3.1 Nitrite concentrations detected from 3 subjects using the Cu/Cys chemiluminescent assay.

	Cu/Cys NOA Assay
A	0.200 μM
B	0.110 μM
C	0.240 μM
Avg	0.19 μM ± 0.08

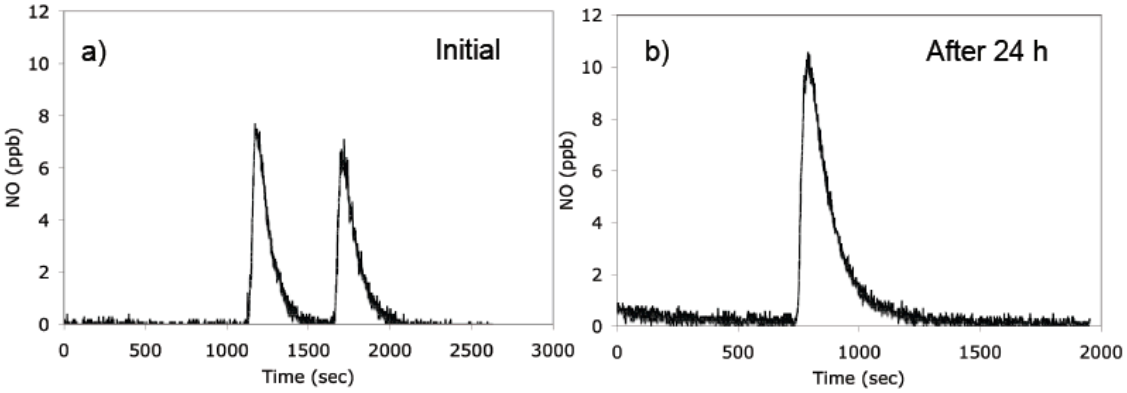

Figure 3.4 Analysis of the same EBC sample using the Cu/Cys assay showing initial results of two – 1 mL aliquots (a) and analysis after 24 h (b).

Another example to indicate the presence of nitrite in the EBC is a sample that was kept on the benchtop for 3 d and tested again. This sample increased from 0.280 μM to 0.450 μM. It is also possible that some NO from the ambient air was trapped by the condensate and when reacted with oxygen produced more nitrite, but again, it is unlikely that the RSNO concentration increased during this time period. The presence of nitrite was further confirmed with the Griess Assay, as discussed below.

All of the Cu(II)/Cys assays were run with water as the bulk solution in the NOA cell. As a result, the pH of the assay was not controlled and was in fact slightly acidic. It

is known that when nitrite is acidified, NO will be generated,[18] which is also why a signal was observed in all cases. Another EBC sample was collected and tested with the Cu(II)/Cys assay, but with PBS (pH 7.4) as the bulk solution and no signal was seen (Figure 3.5), further supporting the conclusion that there are no RSNOs detected in the EBC, but there is nitrite.

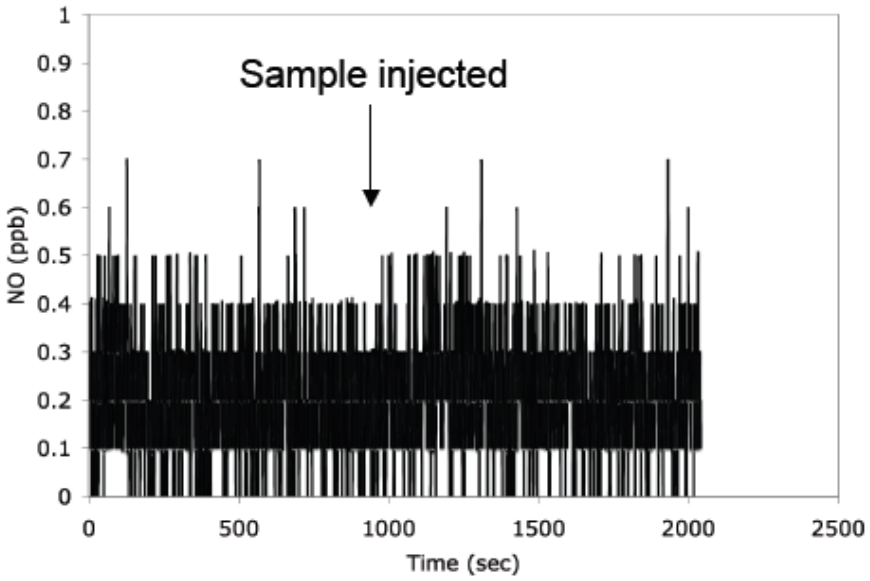

Figure 3.5 Analysis of 1 mL of EBC using 5 mM $CuCl_2$ and 3 mM Cys in PBS (pH 7.4).

When a fresh EBC sample was collected, the SeCA/GSH assay was used and there was no change in the baseline (Figure 3.6). This was consistent for all 5 participants. As previously discussed in Chapter 2, this assay system does not respond to nitrite, but has excellent sensitivity toward both low molecular weight and high molecular weight RSNOs. Even with the increased dilution factor due to the majority of EBC being water vapor, the RSNO concentration is expected to be ca. 0.030 μM, based on literature reports. As shown in Chapter 2, this concentration can be readily detected with this assay system. A comparison of the results from the same subject with both the Cu assay and

the Se assay are shown in Figure 3.7. Based on these observations, the conclusion is that there are no detectable RSNOs present in the EBC, but there is nitrite.

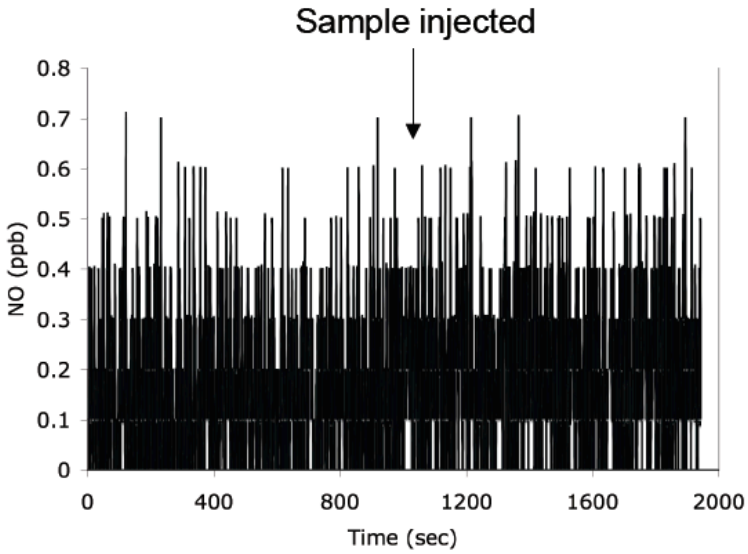

Figure 3.6 Analysis of 1 mL of EBC using 5 mM SeCA with 0.5 mM GSH.

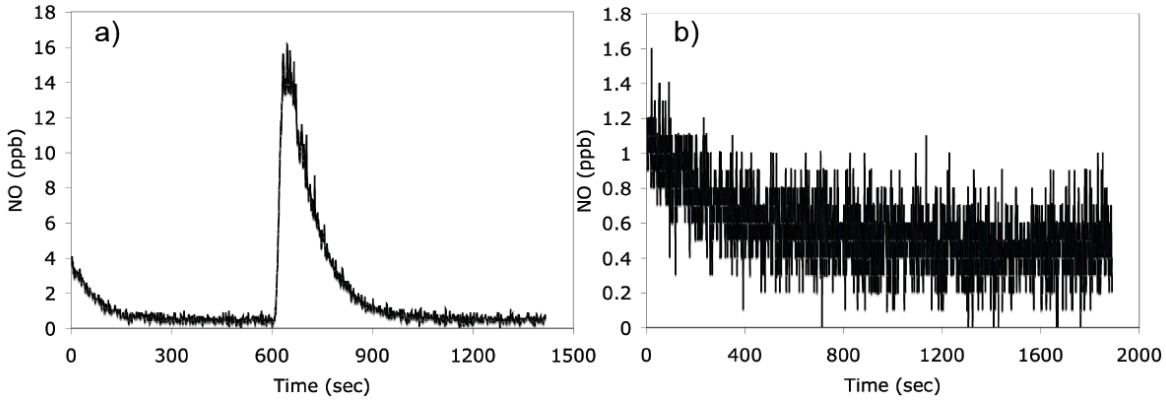

Figure 3.7 Exhaled breath condensate from the same subject analyzed using **a)** 5 mM $CuCl_2$ with 3 mM Cys and **b)** using 5 mM SeCA with 0.5 mM GSH.

To ensure that the collection process and the condenser were not responsible for the lack of RSNOs in the EBC samples, 5 mL of 10 μM GSNO was sprayed into the condenser with the collected solution then analyzed with the new SeCA/GSH assay method. A control of just the solution sprayed into a foil-covered vial showed an 8% loss

of GSNO, while the sample sprayed into the condenser and collected showed a loss of 11%. This indicates that only 3% of the sample was lost due to the collection device and process. With literature values of 0.03-0.94 μM, a 3% loss would not greatly alter these concentrations and they should still be detectable using either the Cu(II)/Cys or the SeCA/GSH assays.

3.3.2 Characterization of Saville-Griess Assay

Using nitrite and GSNO standards, the sensitivity and limit of detection was determined for both the Saville and the Griess assay. Typical calibration curves are shown in Figure 3.8. The background solution for the calibration was water since this is the major component of the EBC matrix and the limit of detection for the Griess assay was determined to be 80 nM (based on S/N ratio = 3). The results for the Saville assay were determined by subtracting out the nitrite signal from the standards. The Griess and Saville reagents could be stored for up to 1 week, with a new calibration curve generated for each fresh batch.

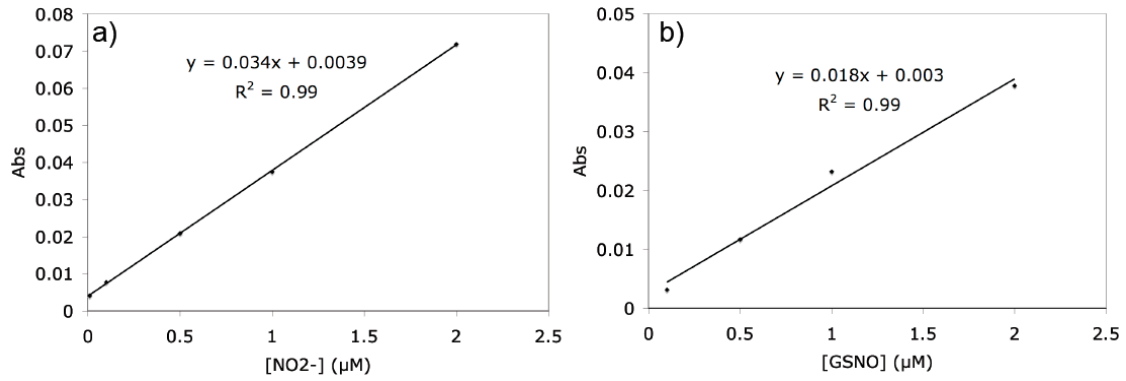

Figure 3.8 A typical calibration curve for **a)** the Griess Assay using nitrite as the standard and **b)** for the Saville Assay using GSNO as the standard.

3.3.3 Saville-Griess Assay Results

The Griess assay was initially used to determine nitrite concentrations in the EBC samples. The average nitrite measured was 0.26 μM ± 0.07 (n = 5), which is similar to both the literature values and the value determined by the Cu(II)/Cys NOA assay (see Table 3.2). Simultaneous testing using the Cu(II)/Cys assay and the Griess assay was not possible due to lack of sample volume. The results from the Saville assay were inconsistent with the results from the SeCA chemiluminescent assay. In three samples there were measurable RSNOs, with an average value of 0.058 μM ± 0.044. This is surprising given that this concentration is readily detectable using the SeCA/GSH assay; however these RSNOs may not be endogenous to the EBC.

Table 3.2 A comparison of the nitrite concentrations determined using the chemiluminescent assay and the Griess assay.

	Cu/Cys NOA Assay	**Griess Assay**
A	0.200 μM	0.260 μM
B	0.110 μM	1.15 μM *
C	0.240 μM	--
D	--	0.209 μM
E	--	0.330 μM
Avg	0.19 μM ± 0.08	0.25 μM ± 0.05

*Q-tested out

There are literature reports stating that artifactual RSNOs can be produced after sample collection due to compounds within the sample reacting.[19] In the lower airways

there is a very high concentration of glutathione, ca. 430 μM, with 96% of it in the reduced state.[20] While the concentration of GSH is much lower in EBC, ca. 7-14 nM, it is possible that some of this GSH is reacting.[21, 22] Under the acidic conditions that the Griess assay operates, it is possible that acidified nitrite could react with the GSH, generating GSNO. In order to ascertain the true RSNO concentration, it would be advantageous to remove or bind all free thiols using SH-alkylating agents, such as *N*-ethylmaleimide.[23]

3.3.4 Explanation of Previous Studies

The report from Corradi et al. concludes that there is an increase in the RSNO concentrations for people with asthma. They report values for healthy patients around 0.1 μM, while those for severe asthmatics around 0.8 μM. They used the Saville-Griess assay method from a commercial kit, with a limit of detection reported at 0.025 μM; however, the manufacturer of the kit reports the limit of detection to be around 0.1 μM. An additional issue with the article is the source of the specimen. Corradi uses EBC, while the Gaston group uses tracheal samples. The tracheal samples are a better option because there is no dilution from the water vapor of breath, which is not addressed in the Corradi paper. There is no mention of standardization for different degrees of dilution in different subjects.

Gaston has recently published a report stating that there is an increase in *S*-nitrosoglutathione reductase in the airways.[24] This finding supports his previous publications reporting a decrease in RSNOs in asthmatics and adds doubt to the report from Corradi et al. claiming an increase in RSNOs. This report continues to say that

there are high levels of protons and nitrite in asthmatic airways, which can lead to increased levels of RSNOs artifactually. Glutathione is naturally present in the airways, so combining that with acidified nitrite will generate GSNO. It is impossible to distinguish between GSNO produced in the lungs and detected in the EBC, and GSNO formed after sample collection.

3.3.5 Potential Downfalls of EBC Collection

There are many factors that influence the reproducibility of an EBC study. Condensation temperature can impact the concentration of analyte present, likely because it can affect the volume of sample collected, with cooler temperatures condensing more droplets.[25] There are several commercial EBC collection devices, but even these have variability. In one study, the RTube system and the EcoScreen condenser were both used to examine the pH of the EBC. Subjects breathed for 15 min and it was found that the pH of the samples collected with EcoScreen were significantly higher than the pH of the RTube samples.[26] Differences in samples from the same patient can also be seen depending on the time of day as well as from day to day.[27]

Since the concentrations of the inflammatory markers are quite low, there is often large variability among assays. There can be large differences between two assays run with the same sample and oftentimes the response is below the limit of detection.[4] While EBC may be a useful technique for some biomarkers, it is not advantageous to use for markers that can be artifactually generated and that can easily undergo thermal or photodecomposition.

3.4 Conclusion

Based on measuring EBC from n=5 subjects using the new selective and sensitive SeCA/GSH chemiluminescence assay scheme developed in Chapter 2, it can be concluded that there are no endogenous RSNOs detected in normal exhaled breath condensate. A signal was seen using the Cu(II)/Cys chemiluminescent assay, but this signal was observed to originate from nitrite, with an average concentration of 0.26 μM present. These results were further confirmed with the Saville-Griess assay; however, this latter assay is fraught with problems and is not reliable in determining RSNO concentrations.

3.5 References

(1) Barnes, P. J. *Exhaled Breath Condensate: A New Approach to Monitoring Lung Inflammation*; CRC Press: Boca Raton, FL, 2005.

(2) Bates, C. A.; Silkoff, P. E. *Exhaled Breath Condensate: Comparisons with Other Methods for Assessing Lung Inflammation*; CRC Press: Boca Raton, FL, 2005.

(3) Cepelak, I.; Dodig, S. *Clinical Chemistry and Laboratory Medicine* **2007**, *45*, 945-952.

(4) Horvath, I.; Hunt, J.; Barnes, P. J. *European Respiratory Journal* **2005**, *26*, 523-548.

(5) Montuschi, P.; Barnes, P. J. *TRENDS in Pharmacological Sciences* **2002**, *23*, 232-237.

(6) Montuschi, P.; Corradi, M.; Ciabattoni, G.; Nightingale, J.; Kharitonov, S. A.; Barnes, P. J. *American Journal of Respiratory and Critical Care Medicine* **1999**, *160*, 216-220.

(7) Biernacki, W. A.; Kharitonov, S. A.; Barnes, P. J. *Thorax* **2003**, *58*, 294-298.

(8) Andreadis, A. A.; Hazen, S. T.; Comhair, S. A. A.; Erzurum, S. C. *Free Radical Biology and Medicine* **2003**, *35*, 213-225.

(9) Rothenberg, M. E.; Hogan, S. P. *Annual Review of Immunology* **2006**, *24*, 147-174.

(10) Barreto, M.; Villa, M. P.; Corradi, M.; Barberi, S.; Monaco, G.; Martella, S.; Bohmerova, Z.; Sabatino, G.; Ronchetti, R. *International Journal of Immunopathology and Pharmacology* **2006**, *19*, 601-608.

(11) Balint, B.; Donnelly, L.; Hanazawa, T.; Kharitonov, S. A.; Barnes, P. J. *Thorax* **2001**, *56*, 456-461.

(12) Kharitonov, S. A.; Donnelly, L.; Montuschi, P.; Corradi, M.; Collins, J. V.; Barnes, P. J. *Thorax* **2002**, *57*, 889-896.

(13) Corradi, M.; Montuschi, P.; Donnelly, L.; Pesci, A.; Kharitonov, S. A.; Barnes, P. J. *American Journal of Respiratory and Critical Care Medicine* **2001**, *163*, 854-858.

(14) Gaston, B.; Sears, S.; Woods, J.; Hunt, J.; Ponaman, M.; McMahon, T.; Stamler, J. S. *Lancet* **1998**, *351*, 1317-1319.

(15) Oh, B. K.; Meyerhoff, M. E. *Biomaterials* **2004**, *25*, 283-293.

(16) Ho, L. P.; Innes, J. A.; Greening, A. P. *Thorax* **1998**, *53*, 680-684.

(17) Chladkova, J.; Krcmova, I.; Chladek, J.; Cap, P.; Micuda, S.; Hanzalkova, Y. *Respiration* **2006**, *73*, 173-179.

(18) Lundberg, J. O.; Weitzberg, E.; Gladwin, M. T. *Nature Reviews Drug Discovery* **2008**, *7*, 156-167.

(19) Tsikas, D.; Gutzki, F. M.; Rossa, S.; Bauer, H.; Neumann, C.; Dockendorff, K.; Sandmann, J.; Frolich, J. C. *Analytical Biochemistry* **1997**, *244*, 208-220.

(20) Cantin, A. M.; North, S. L.; Hubbard, R. C.; Crystal, R. G. *Journal of Applied Physiology* **1987**, *63*, 152-157.

(21) Corradi, M.; Folesani, G.; Andreoli, R. *American Journal of Respiratory and Critical Care Medicine* **2003**, *167*, 395-399.

(22) Yeh, M. Y.; Burnham, E. L.; Moss, M.; Brown, L. A. S. *Respiratory Medicine* **2008**, *102*, 248-255.

(23) Giustarini, D.; Milzani, A.; Dalle-Donne, I.; Rossi, R. *Journal of Chromatography B* **2007**, *851*, 124-139.

(24) Gaston, B. *Biochimica et biophysica acta* **2011**, *1810*, 1017-1024.

(25) Goldoni, M.; Caglieri, A.; Andreoli, R.; Poli, D.; Manini, P.; Vettori, M. V.; Corradi, M.; Mutti, A. *BMC Pulmonary Medicine* **2005**, *5*.

(26) Prieto, L.; Ferrer, A.; Palop, J.; Domenech, J.; Llusar, R.; Rojas, R. *Respiratory Medicine* **2007**, *101*, 1715-1720.

(27) Montuschi, P. *Clinica Chimica Acta* **2005**, *356*, 22-34.

CHAPTER 4

QUANTIFYING EXHALED NASAL NITRIC OXIDE USING OXYHEMOGLOBIN AND NITRATE ION-SELECTIVE ELECTRODES

4.1 Introduction

Nitric oxide is produced throughout the respiratory system, but is in much greater quantity within the nasal passages. While the exact origin of nasal NO is not well defined, it is believed to come primarily from the paranasal sinuses.[1] Of the three nitric oxide synthase (NOS) isoforms, inducible NOS is mainly responsible for the NO production in this location.[2] As stated in Chapter 1, this NO has multiple functions including host defense, acting as an aerocrine messanger molecule, and controlling ciliary motility.[3] Variations in nasal NO concentration have been linked to specific disease states, such as primary ciliary dyskinesia, cystic fibrosis, and chronic sinusitis.[3] All of these conditions exhibit a lower concentration of nasal NO, likely due to blockage from mucus as well as deficiencies in the expression of NOS. With the development of inexpensive and easy to use methods, nasal NO could be used a diagnostic tool.

Chemiluminescence detection is the most commonly used method in exhaled NO studies. It is a sensitive and selective technique, however it is costly and not easily made to be portable. In Chapter 1, hand-held methods were discussed, including a hand-held

chemiluminescence device, as well as an electrochemical device.[4, 5] These are more easily operated in a point-of-care situation, but the chemiluminescence device is still expensive, and the electrochemical device has a limited dynamic range. Mass spectrometry and gas chromatography coupled with mass spectrometry have also been used, but these methods are bulky and can not be readily used in a point-of-care situation.[6, 7]

There have also been several studies reporting an increase in nasal NO with humming. This increase is likely due to the rapid gas exchange occurring between the sinuses and the nose. After repeated humming, nasal NO was measured again and found to be lower than the original value because the sinuses are essentially flushed during the humming maneuvers.[8-10]

Nitric oxide can also be detected using the oxyhemoglobin (oxyHb) assay. Oxyhemoglobin quickly reacts with NO to form methemoglobin (metHb) and nitrate.[11] This reaction is nearly diffusion limited, with a rate constant of 3.7×10^7 $M^{-1}s^{-1}$, about 26 times faster than the reaction between NO and oxygen.[11] The fast reaction rate makes this assay ideal for measuring NO in an oxygenated environment. The affinity of hemoglobin for NO is 3×10^5 higher than that of oxygen; however, during the reaction, the NO does not displace the oxygen, rather it binds directly to the bound oxygen, creating $ONOO^-$, which isomerizes and is released as NO_3^-. The iron center of the heme is oxidized in the process, giving metHb, the production of which can be detected optically.[11]

Most applications of the oxyHb assay monitor the change in the UV-Vis spectrum as oxyHb becomes metHb. The oxyHb has a characteristic Soret band at 415 nm. As the

oxyHb is oxidized to metHb, the band shifts to 406 nm. Sarkar et al. used this assay to show an increase in NO production when certain viruses attack specific plant species.[12] In another study, Berka et al. were able to examine endothelial nitric oxide synthase activity when changes to the redox state of tetrahydrobiopterin, a co-factor for NO production, were made.[13] In all applications reported in the literature, the optical change is detected and this is how the authors correlate the NO production.

Optical detection of the oxyHb assay is well understood and can easily be used, When applying this assay to nasal air analysis, carbon monoxide can be a major interference due to its binding to oxyHb. Carboxyhemoglobin (carboxyHb) also has a distinctive absorbance spectrum, with a Soret band at 419 nm. As a result, various methods have been created in order to differentiate the hemoglobin species. Some utilize absorbances at different wavelengths, while others add additional reagents, such as potassium cyanide, to displace any NO bound, allowing for quantitation to be made.[14, 15] While CO will bind to hemes, oxyHb does have a greater affinity for NO over CO.[16] This will not completely prevent CO from binding, but it will lower the amount of CO binding. This represents the major disadvantage to using the optical detection method for nasal NO analysis.

Detection of nitrate from the oxyHb assay is not commonly reported on in the literature, but provides a method of NO detection without the need for CO correction. Nitrate can be detected using ion-selective electrodes, which measure the change in potential across a polymeric membrane versus a reference electrode. The polymeric membrane consists of a polymer matrix, a plasticizer to control the rigidity and resistance of the membrane, an ionophore to improve binding of the target analyte ion, and an ion

exchanger to maintain charge neutrality within the membrane and to improve the permselectivity.[17] An inner filling solution containing the ion of interest and chloride poises the potential on the back-side of the membrane. A conditioning solution of the ion of interest fills the binding sites from the front side of the membrane. The overall potential across the membrane is determine by three terms, shown in Equation 4.1.

$$E_M = E_D + E_{PB,inner} + E_{PB,outer} \quad (4.1)$$

The diffusion potential, E_D, is negligible because the diffusion of ions within the membrane is low once all sites are bound. Each side of the membrane has a phase boundary term dictated by the activity of ions in the aqueous and organic phases. On the back-side of the membrane there is no change in the aqueous phase or the organic phase making this term a constant. The terms E_D and $E_{PB,inner}$ can therefore be combined into one term, E_{const}, leaving $E_{PB,outer}$. Again, the activity of the ions in the organic phase is not changing, therefore the overall membrane potential is dictated by the activity of ions in the sample (Equation 4.2).

$$E_M = E_{const} + \frac{RT}{zF} \ln \frac{a_{x(aq)}}{a_{x(org)}} \quad (4.2)$$

Nitrate ion-selective electrodes have been used for environmental applications such as soil and water sampling, and in the food industry for meat preservative testing.[18, 19] A few examples of compounds incorporated into nitrate ISEs are bis-thiourea compounds, polypyrrole films, or a tetraoctadecylammonium nitrate ion exchanger.[20-22] Hutchins et al. describe using electropolymerized polypyrrole films as a molecular imprinted matrix, giving increased selectivity for nitrate over perchlorate and iodide.[23] Additionally, tris(1,10-phenanthroline)nickel(II) salts have been used by Ross, however,

the crystal structure of this compound reveals no specific interaction between nitrate and the salt making it likely that the selectivity of these sensors originates from the high lipophilicity of nitrate.[24, 25] There are some commercially available nitrate electrodes, however most of these are more selective for anions more lipophilic than nitrate.[23, 26] Due to the high lipophilicity of nitrate, a sensor containing only an ion-exchanger salt may be suitable for the application presented in this thesis.

In this chapter, a new application of the oxyHb assay is presented. The reaction with NO is examined using UV-Vis as well as ion-selective electrodes. Using the optical detection method, responses to carbon monoxide are also examined, with calculations made to account for the different hemoglobin species. The membrane composition of the ISE is optimized and altered to remove the response to the oxyHb itself. Vanadyl salen, is synthesized and added to the ISE membrane to evaluate its performance as a possible nitrate ionophore. Gas phase proof-of-concept experiments are performed by loading oxyHb into gas permeable silicone rubber tubing and submerging the tubing into a solution containing NO. The NO_3^- formed is then detected with a nitrate ISE. Finally, nasal air is collected and bubbled through an oxyHb solution, and then analyzed using both optical and electrochemical detection methods.

4.2 Experimental

4.2.1 Materials and Instruments

Sodium nitrate was purchased from Mallinckrodt (St. Louis, MO). Sodium nitrite, sodium perchlorate, tetrahydrofuran (THF), methylene chloride, chloroform, 1,1,2,2-tetrachloroethane, vanadium(IV) oxide sulfate hydrate, sodium sulfate, sodium

hydroxide, sulfuric acid, sodium phosphate monobasic, sodium phosphate dibasic, bovine, procine and human hemoglobins, Tris-PO_4, and bis(2-ethylhexyl) sebacate (DOS) were obtained from Sigma (St. Louis, MO). Tridodecylmethylammonium chloride (TDMAC), 2-nitrophenyloctyl ether (NPOE), poly(vinyl chloride) (PVC) were purchased from Fluka (St. Louis, MO). Cellulose triacetate, tributylphosphate, dibutylphthalate, trioctyltrimellitate were gifts from Scientific Polymer Products, Inc. (Ontario, NY). The anti-foaming agent was purchased from GE Analytical (Boulder, CO). Sodium dithionite was from Riedel-de haen (St. Louis, MO). Carbon monoxide gas was purchased from Matheson (Howell, MI). All buffers and solutions were prepared using Milli-Q grade deionized water (18.2 MΩ, Millipore Corp., Billerica, MA).

Polystyrene disposable cuvettes and polyethylene tubing were obtained from Fisher (Pittsburgh, PA). The nasal mask, connector, stop-cock and gas collection bag used in the nasal NO measurement setup were all purchased from Hans Rudolph, Inc. (Shawnee, KS). Hytrel tubing was used to connect the nasal mask to the gas collection bag and was obtained from Vacumed (Ventura, CA). Electrode bodies for mounting ISE membranes were obtained from Oesch Sensor Technology (Sargans, Switzerland). Gas-tight syringes were products of Hamilton Company (Reno, NV). Silicone tubing (1.47 mm i.d.; 1.96 mm o.d.; 0.23 mm wall) samples were provided by Helix Medical (Carpinteria, CA).

For all UV-Vis measurements a PerkinElmer Lambda 35 spectrophotometer (Waltham, MA) was used. All potentiometric measurements were performed using a Lawson Labs high impedance interface, EMF 16 (Malvern, PA) connected to a Dell laptop computer (Round Rock, TX).

4.2.2 Oxyhemoglobin Preparation

Approximately 60 mg of hemoglobin, either bovine, human or porcine, was dissolved in 2.5 mL of 10 mM phosphate buffer (pH 7.4). Solid sodium dithionite, in 2-3 fold molar excess of the heme, was added, causing the hemoglobin solution to change from dark brown red to dark red. Compressed house air was blown over the surface for 1.2 h, with small amounts of buffer added to account for the solution lost to evaporation. A PD-10 column packed with Sephadex G-25 was conditioned with 25 mL buffer and then the hemoglobin solution was loaded on the top of the column. To elute the protein, 3.5 mL buffer was added with the eluent collected in four fractions and then analyzed using UV-Vis to determine oxyhemoglobin concentration.[11]

4.2.3 Carbon Monoxide and Nitric Oxide Solutions

A sealed vial containing 10 mL water was first purged with Ar for 30 min. The vial was then placed into an ice bath and bubbled with pure CO for 30 min with a needle outlet. The [CO] in the solution should be ca. 0.9 mM, based on a Henry's constant.[27]

Nitric oxide solutions were prepared by generating NO from deoxygenated acidified nitrite. First, a round bottom flask is filled with 20 mL of a 10.9 M solution of sodium nitrite and the whole setup is deoxygenated with N_2. Twenty milliliters of 4 M sulfuric acid is added dropwise to the stirred nitrite solution and the generated gas is bubbled through a 20% NaOH solution before being collected in a vial with 10 mL water in an ice bath. The exact NO concentration in the solution was determined by NOA measurements.

4.2.4 Nitric Oxide and Carbon Monoxide Calibrations with oxyHb

Buffer along with oxyHb were added to a cuvette and an initial UV-Vis absorption scan was taken. Into the same cuvette, without removing it from the spectrophotometer, a gas-tight syringe was used to deliver an aliquot of a NO or a CO solution. Another spectrum was taken and the procedure was repeated for each concentration of the gas solutions. A difference spectrum was generated by subtracting the oxyHb spectrum from the metHb or carboxyHb spectrum. Calibration curves were plotted as the maximum difference absorbance versus concentration.

4.2.5 Synthesis of Vanadyl Salen Ionophore

The synthetic route for preparation of vanadyl (R,R)-(-)-N,N'-bis(3,5-di-tert-butylsalicylidene)-1,2-cyclohexanediamie was previously published and is described here.[28] Dimeric salen ligand was dissolved in ethanol/CH_2Cl_2 with an aqueous solution of vanadyl sulfate hydrate added dropwise under nitrogen. The solution was then refluxed for 4 h, then cooled to room temperature and stirred for 2 h. The side arm of the flask was open during this time. The solvent was allowed to completely evaporate, with the remaining solid dissolved in 10 mL CH_2Cl_2, washed three times in 5 mL water and once with brine. Anhydrous Na_2SO_4 was used to dry the organic layer, which was then filtered and evaporated to give the vanadyl salen complex (VO salen). The reaction product was characterized using mass spectrometry and UV-Vis, with a m/z value of 611 and the expected change in the optical spectrum observed.

4.2.6 Nitrate Ion-Selective Electrode Preparation

Plasticized PVC membranes were made by dissolving TDMAC in distilled THF. In a separate vial, a 1:2 PVC:NPOE mixture was weighed out and dissolved in THF, with TDMAC added. For membranes containing the VO salen ionophore, 2 wt% of the ionophore was added, along with 50, 25, or 10 mol% TDMAC (relative to ionophore). In all preparations, 140 mg total was used. After shaking for 1 h, the dissolved cocktail was poured into a glass ring fixed to a glass plate with a rubber band. Another glass slide was placed on top, followed by a heavy book to slow the rate of solvent evaporation. After drying in the hood overnight, disks of the films were punched out and mounted in electrode bodies using 1 mM $NaNO_3$ and 1 mM NaCl as the internal filling solution. The sensors were conditioned overnight in 1 mM $NaNO_3$.

4.2.7 Asymmetrical Cellulose Triacetate Ion-Selective Membrane Preparation

To prepare asymmetrical cellulose triacetate ISE membranes for nitrate sensors, a procedure similar to that reported by Cha et al. was employed.[29] Cellulose triacetate (100 mg) was added to 1.5 mL methylene chloride, 0.5 mL chloroform and 0.5 mL 1,1,2,2-tetrachloroethane and shaken for 2 h or until fully dissolved. The solution was then poured into a 36-mm glass ring fixed to a glass plate with a rubber band. The film was allowed to dry in the hood for 2 d. Water was used to remove the thin film from the glass plate. To hydrolyze the acetyl groups on the bottom of the film, the membrane was floated on a solution of 1 M NaOH for 4.5 h, then rinsed with water and left to air dry. The ion-selective membrane (ISM) cocktail was prepared by dissolving 35 mg cellulose triacetate in 0.8 mL chloroform and 0.8 mL methylene chloride with 88.9 μL NPOE and

50 mol% TDMAC. A 22-mm glass ring was placed on top of the cellulose membrane with 1.2 mL methylene chloride added to pretreat the membrane for 30 min in a desiccator prior to the addition of the ISM cocktail. A large glass plate covered the desiccator with only a small crack open to the ambient air to allow for slow solvent evaporation overnight. The sensors were assembled and conditioned in the same manner as the plasticized PVC membranes.

4.2.8 Determining Potentiometric Response of Nitrate Sensing Membrane Electrodes

In order to generate a calibration curve for the various nitrate ISEs, the electrodes were placed into a cell containing 10 mM PB, along with a Ag/AgCl reference electrode containing 1 mM KCl as the internal filling solution to prevent excess Cl^- leaching into the bulk. Nitrate stock solutions of 1 M and 1 mM were made in the buffer, with aliquots added to the sensors to make final nitrate concentrations ranging from 1×10^{-6} M to 1.7×10^{-2} M. The voltage reading at each concentration was then plotted versus log of the activity, with the sensitivity and LOD determined from this plot.

4.2.9 Nitric Oxide Detection Through Gas Permeable Tubing

Using a syringe, ca. 100 μL of a 200 μM oxyHb solution was pulled into silicone rubber tubing. The tubing was 1.47 mm i.d., 1.96 mm o.d. and had a wall thickness of 0.23 mm. It was formed into a loop and tied closed with a small length of fishing line. The loop was then placed into a vial containing 10 mL of N_2 purged buffer and 100 μM of NO was added. The vial was sealed with a stir bar and left to incubate for 5, 10 or 15 min. After the incubation, the fishing line was cut away and a pipet was used to force the

oxyHb solution into a cell containing 1900 μL buffer and the nitrate ISE prepared with an asymmetric cellulose triacetate membrane. After recording the drop in voltage, 1 mL of the solution was transferred to a cuvette and an optical UV-Vis spectrum was taken.

4.2.10 Nasal Nitric Oxide Analysis

Nasal air was collected into a 2 L gas collection bag (made out of polyethylene, a polymer with low gas permeability).[30] The collected gas was then pulled through a fine fritted sparger into a solution of oxyHb with anti-foaming agent via vacuum (Figure 4.1). The air was bubbled out at a rate of ca. 20 mL/min. The oxyHb solution was then added to a cell containing 10 mM PB with the nitrate ISEs and a Ag/AgCl reference electrode, and the EMF response of the ISE was recorded (Figure 4.1). After the mV response reached a steady-state (5.5 min), 1 mL of solution was removed and a UV-Vis spectrum was obtained. As a control, the nasal air was also bubbled through a solution of buffer only with the anti-foaming agent, and the potentiometric response of the nitrate sensor was recorded, with the mV value after 5 min used for calculations. In order to account for the control response, a nitrate concentration was calculated from a nitrate calibration curve using the mV value. The mV response from the oxyHb trial was then used to to determine the level of nitrate produced from the NO in the nasal air reacting with oxyHb, and the control concentration was subtracted. Once the final nitrate value was obtained, further calculations were performed to determine the NO concentration in ppb.

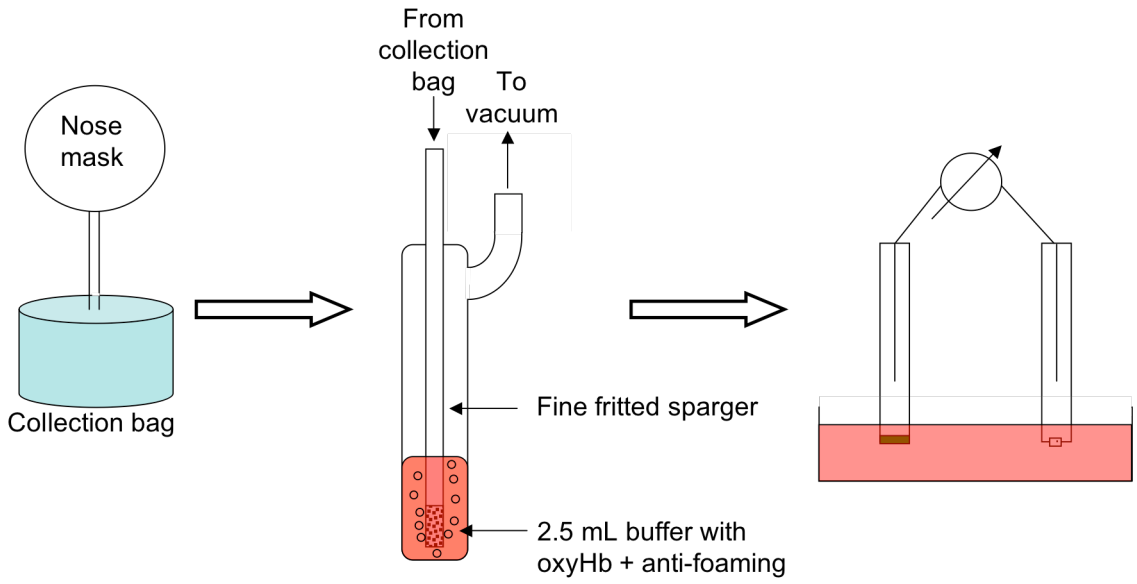

Figure 4.1 Schematic diagram illustrating the collection and testing of exhaled nasal air.

4.3 Results and Discussion

4.3.1 Characterization of oxyHb with Nitric Oxide and Carbon Monoxide

Oxyhemoglobin was successfully prepared from all three protein sources. The UV-Vis spectra clearly show the Soret band with a maximum absorbance at 413-415 nm, depending on the source, with two smaller bands between 500 and 600 nm (Figure 4.2). The concentration of oxyHb was determined using Equation 4.3.[11]

$$[oxyHb] = \left(A_{542nm} - A_{510nm}\right)\frac{300}{\Delta\varepsilon_{542nm-510nm}} \qquad (4.3)$$

When the oxyHb is converted to metHb upon addition of NO, the Soret band shifts to 406 nm and the absorption bands between 500 and 600 nm disappear (Figure 4.3).

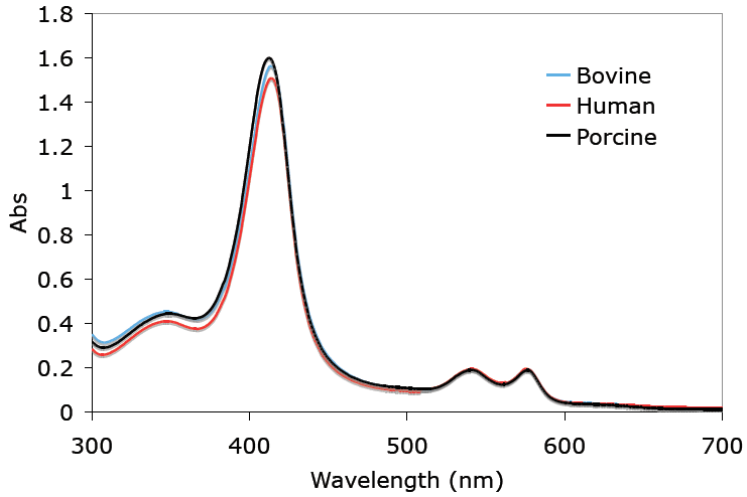

Figure 4.2 Spectra of the three oxyHb species showing the Soret band at 415 nm.

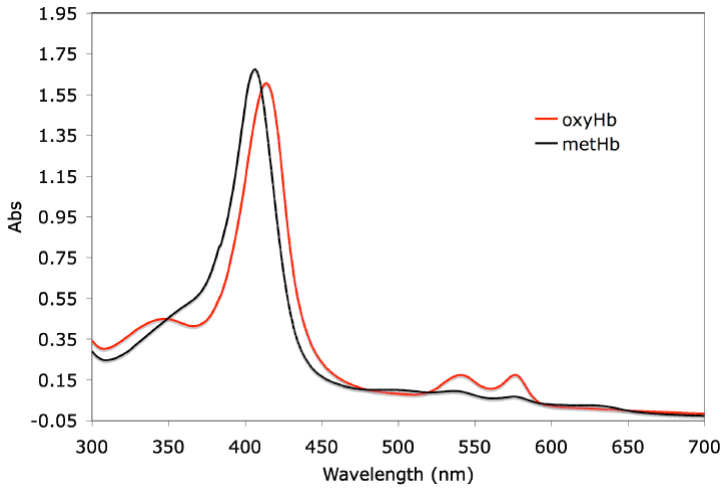

Figure 4.3 Spectra of bovine oxyHb and metHb with the Soret band shifting from 413 nm to 406 nm, and the two smaller bands between 500 and 600 nm diminishing.

In order to calibrate the change in the oxyHb spectrum with the addition of NO (Figure 4.4a), the oxyHb spectrum was subtracted from the spectrum taken after each NO addition, generating a difference plot (Figure 4.4b). The maximum absorbance at 401 nm plotted versus concentration yields a linear curve for both 5 μM and 10 μM bovine oxyHb when aliquots of an NO stock solution are added to the same cuvette. The calibration curve (Figure 4.5) is linear up to 4 times the concentration of the oxyHb,

indicating a 1:1 stoichiometry between NO and the number of heme sites, which is consistent with the literature.[31] These curves were reproducible with each type of Hb.

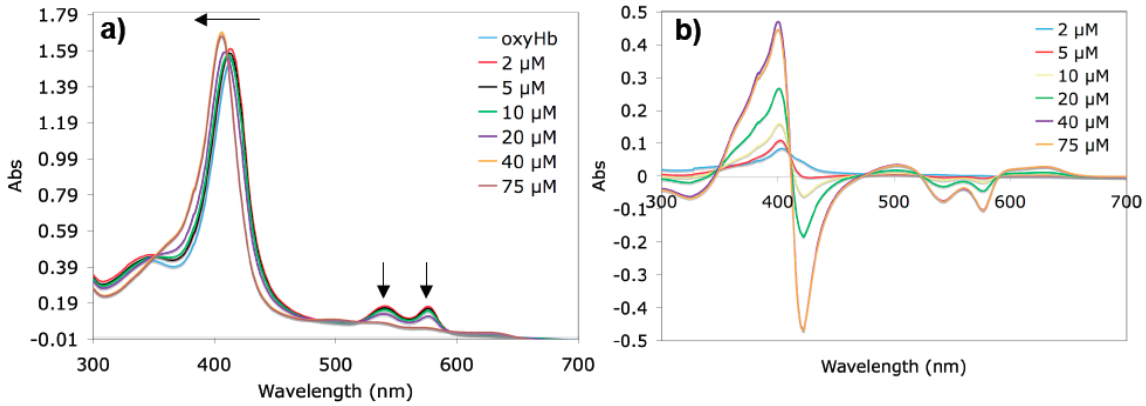

Figure 4.4 As NO is added to the oxyHb solution, **a)** the Soret band shifts and the secondary bands decrease. **b)** The difference spectrum shows the band at 401 nm increasing with each NO addition.

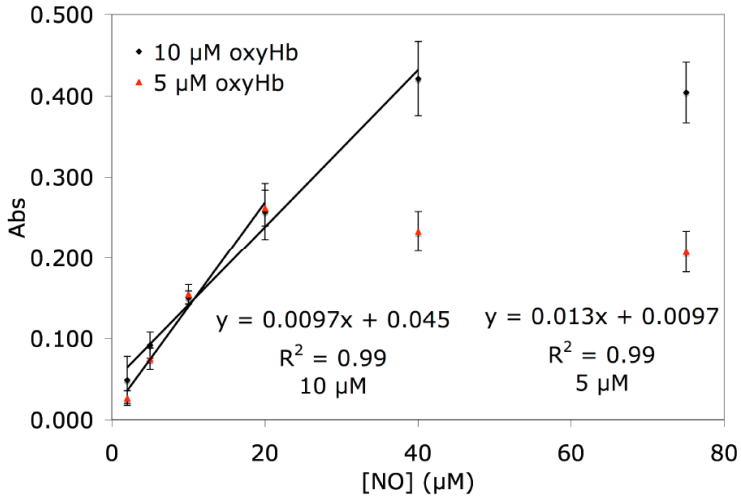

Figure 4.5 Calibration curves toward NO for 5 μM and 10 μM bovine oxyHb.

Upon addition of CO, the Soret band shifts to 419 nm and the two smaller peaks shift ca. 6 nm (Figure 4.6a). The difference plots show a maximum at 422 nm (Figure 4.6b), which when plotted versus concentration gives a calibration curve (Figure 4.7). For 10 μM bovine oxyHb, the curve is linear up to 10 μM CO, indicating a 1:1 CO:oxyHb stoichiometry. This is contrary to literature reports, that state a 1:1 CO:heme

stoichiometry, so using the difference plot for quantitation of carboxyHb may not be accurate.[31]

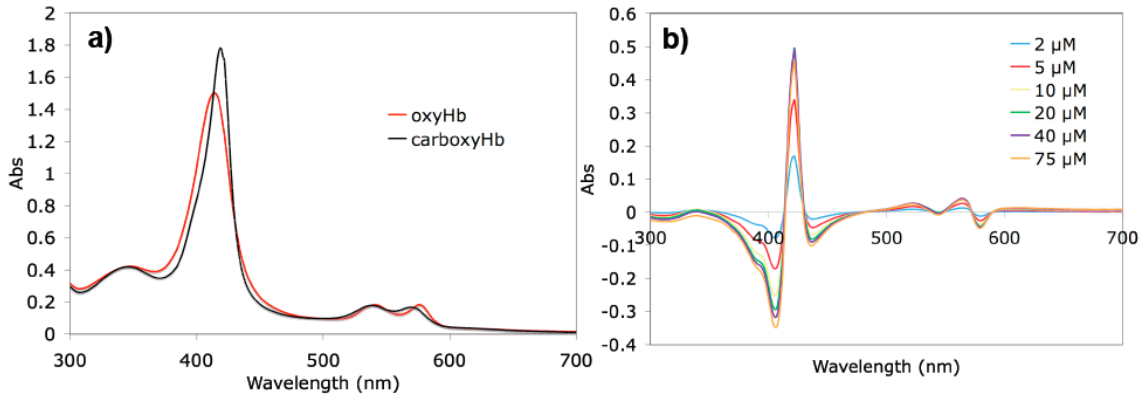

Figure 4.6 a) Oxyhemoglobin binding to CO to form carboxyHb. **b)** As CO is added, a difference plot can be generated, with a maximum at 420 nm.

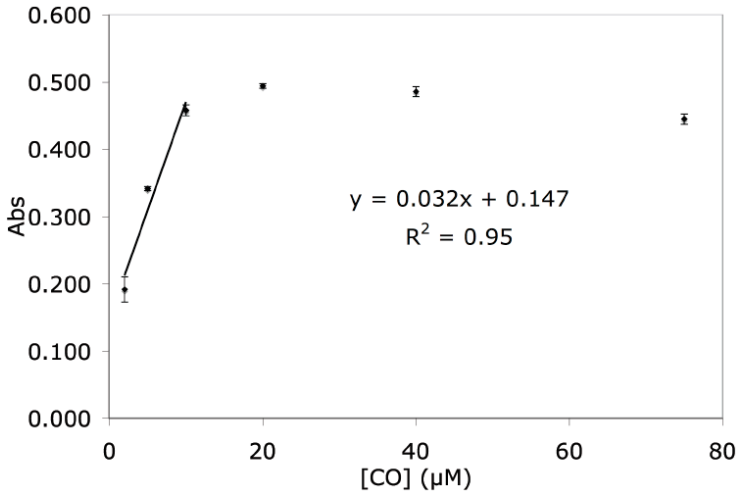

Figure 4.7 Typical calibration curve for CO using 10 μM bovine oxyHb. Data points are average ± s.d. for n = 3 measurements.

4.3.2 Determining oxyHb Affinity for CO and NO

Carbon monoxide is produced in the nasal cavity along with NO, but in much greater quantity.[32] In order to determine if the CO is a major interference in terms of occupying heme sites, NO and CO were added to solutions containing oxyHb. With 10 μM oxyHb present, 200 μM CO was added first, causing the peak at 413 nm shift to 419 nm; however, upon addition of 20 μM NO, the peak shifted back, with the maximum at

406 nm and a shoulder at 417 nm (Figure 4.8). Reversing the addition of the gases first causes the peak at 413 nm to shift to 406 nm. With the further addition of CO, the peak did not shift, but the absorbance at 406 nm decreased (Figure 4.9). When the gases were added at the same time, the peak shifted to 406 nm, indicating metHb formation over carboxyHb formation (Figure 4.10). Even with 20-fold more CO than NO, the NO still binds preferentially. This data supports the prior literature and suggests that a large concentration of oxyHb will not be needed in order to efficiently trap all of the NO in exhaled nasal air.[16, 33]

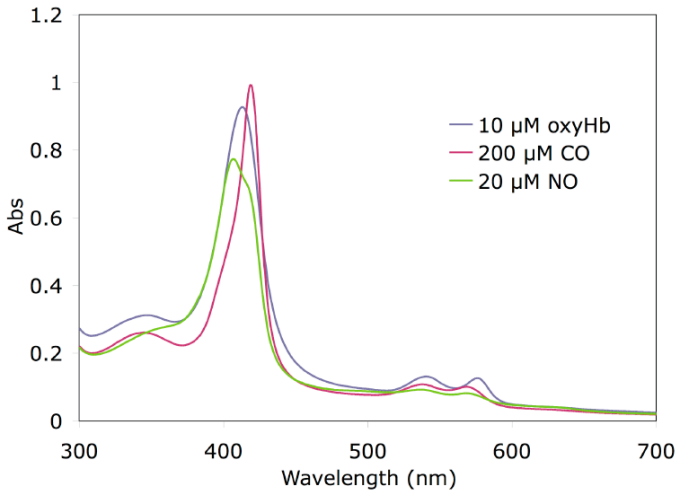

Figure 4.8 Spectra of oxyHb with CO added followed by NO.

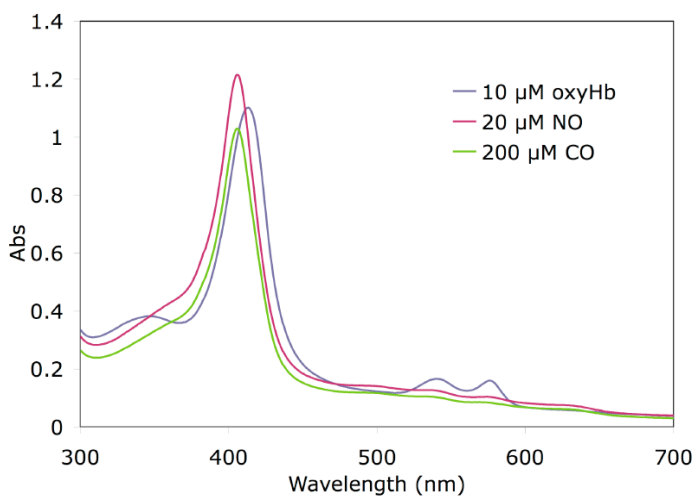

Figure 4.9 Spectra of oxyHb with NO added followed by CO.

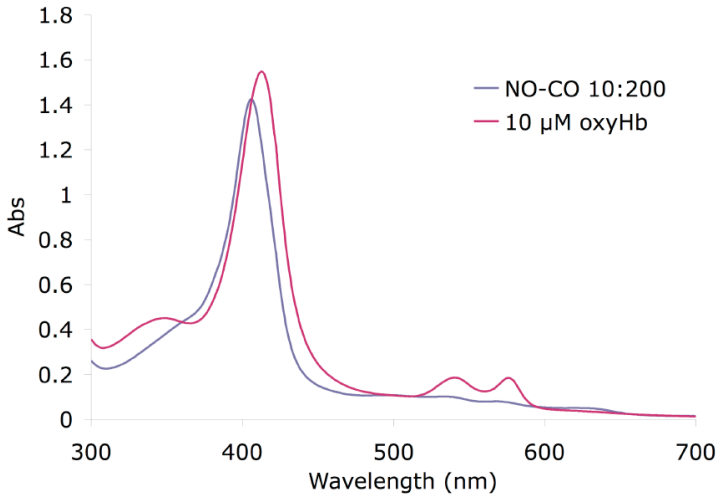

Figure 4.10 Spectra of oxyHb and oxyHb with NO and CO added at the same time.

4.3.3 Synthesis of Vanadyl Salen Ionophore

The synthesis of the vanadyl salen ionophore (Figure 4.11) resulted in a dark green solid that was characterized using TOF MS with electrospray ionization in the positive ion mode. Figure 4.12 shows only one major peak is present at 611.0 m/z, which is the expect m/z value for the VO salen complex. Two separate lots of the ionophore were synthesized, with both having this result. The first lot, synthesized by Dr. Kebede Gemene, was also characterized using UV-Vis. The spectrum of the salen ligand was compared against the spectrum of the VO salen complex, with a clear difference seen in the spectra, indicating complexation (Figure 4.13).

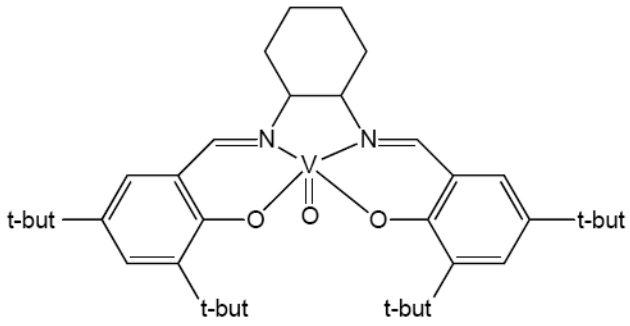

Figure 4.11 Structure of the synthesized vanadyl salen ionophore.

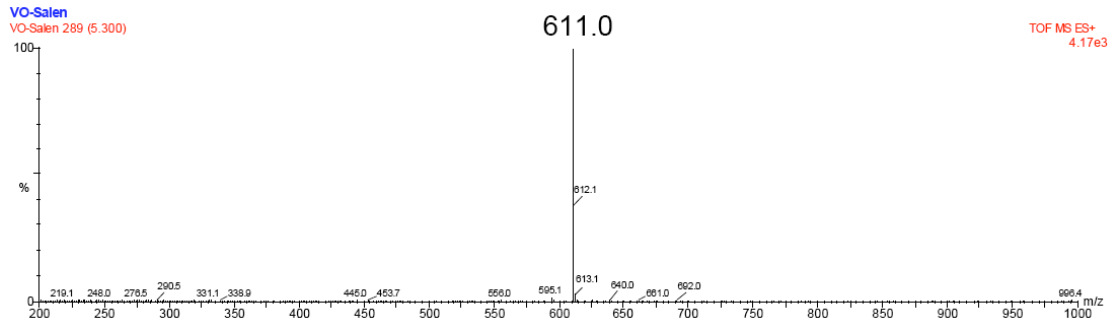

Figure 4.12 Mass spectrum of the synthesized vanadyl salen ionophore with the expected m/z value of 611.0.

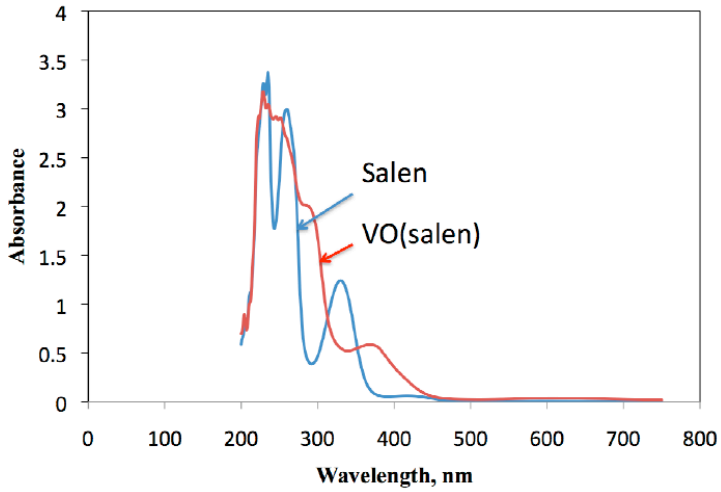

Figure 4.13 UV-Vis spectra of the salen ligand and the vanadyl salen complex. Data provided by Dr. Kebede Gemene.

4.3.4 Nitrate Ion-Selective Electrode Membrane Optimization

Membrane electrodes with and without the VO salen ionophore (TDMAC only) along with a commercially available (from Oesch Sensor Technology) nitrate ISE (membrane composition unknown), were tested with varying buffer compositions in order to determine the best background electrolyte solution for nitrate detection. Achieving the lowest LOD was important since the final nitrate concentration detected from a nasal air sample was expected to be in the micromolar range. Figure 4.14a illustrates a typical potentiometric nitrate response curve with each nitrate addition

causing a drop in the voltage. The limit of detection was determined using the IUPAC method, demonstrated in Figure 4.14b.[34] Results from the buffer trials are shown in Table 4.1, with the best LOD found using 10 mM phosphate buffer (PB) with the vanadium ionophore present. It should be noted that all buffers used were at pH 7.4 and for the rest of the chapter, a 10 mM PB was used for all experiments.

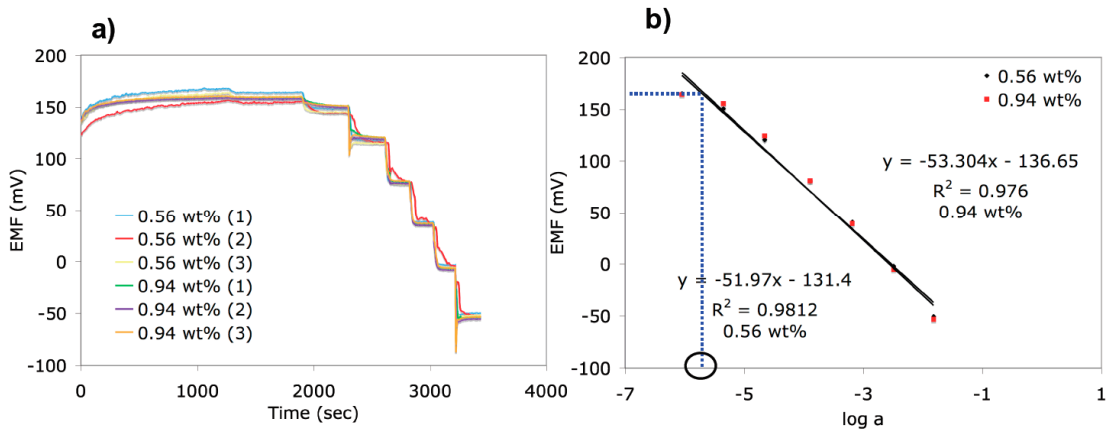

Figure 4.14 a) Typical nitrate response for sensors containing 0.56 wt% and 0.94 wt% TDMAC, 0 wt% ionophore and 1:2 PVC:NPOE. **b)** Calibration curve with the dotted line indicating how LOD is calculated.

Table 4.1 Summary of results from different buffer compositions used.

	2 wt% Ionophore		**TDMAC Only**		**Oesch (Commercially available NO_3^- ISE)**	
	Sens. (mV/decade)	**LOD (M)**	**Sens. (mV/decade)**	**LOD (M)**	**Sens. (mV/decade)**	**LOD (M)**
10 mM Tris-PO_4 + 1 mM NaCl	-54.3	$10^{-5.75}$	-56.1	$10^{-5.5}$	-56.8	$10^{-5.5}$
10 mM Tris-PO_4	-55.9	10^{-5}	-58.3	10^{-5}	-62.0	10^{-5}
10 mM PB	-51.9	$10^{-5.8}$	-59.2	$10^{-5.4}$	-54.4	$10^{-5.6}$
50 mM PB	-54.4	$10^{-5.2}$	-60.7	$10^{-4.8}$	-57.7	$10^{-5.2}$
50 mM Tris-SO_4	-54.2	$10^{-5.3}$	-63.6	$10^{-4.7}$	-59.4	$10^{-5.1}$

The membrane composition was also varied using different wt% of the ion exchanger, TDMAC, with and without the ionophore, as well as different plasticizers to realize the best nitrate response (Figure 4.14). Table 4.2 tabulates the results for all of the combinations that were examined. A lower wt% of TDMAC was not as effective as higher ones, with a slight difference between 25 wt% and 50 wt%. As the dielectric constant of the plasticizer increased, the LOD and selectivity over nitrite were better, which is why NPOE was used as the plasticizer in all further experiments. Additionally, lowering the nitrate concentration in the inner filling solution did not improve the LOD.

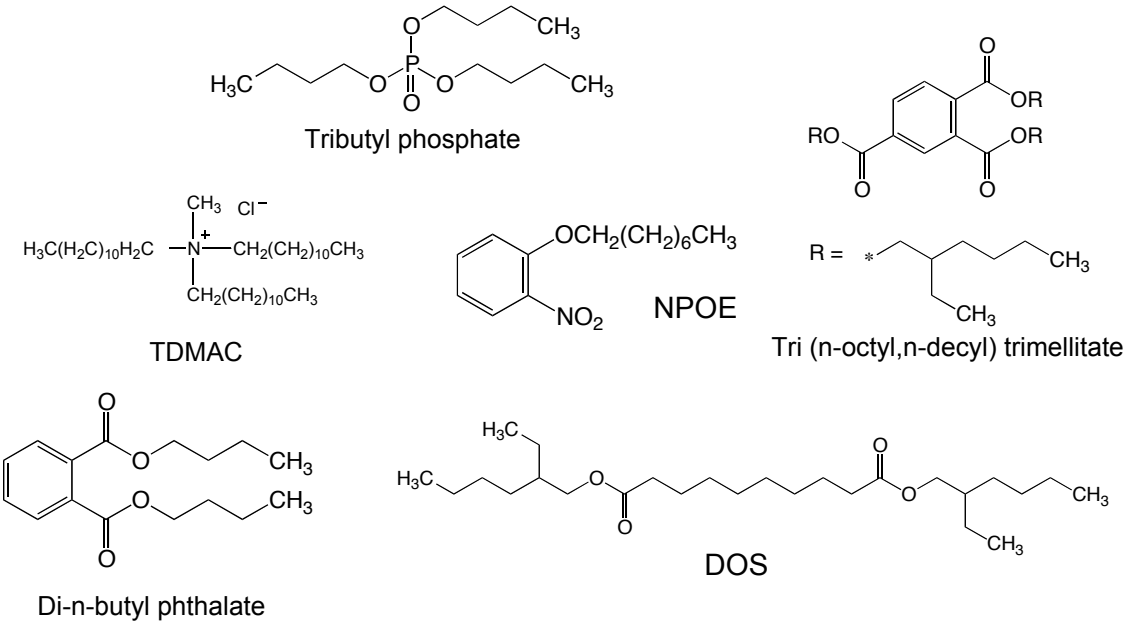

Figure 4.15 Structures of TDMAC and the various plasticizers used to prepare nitrate responsive membrane electrodes.

Table 4.2 Different membrane compositions made for nitrate detection.

Membrane	Sensitivity (mV/decade)	LOD (M)	$\log k^{pot}_{NO_3^-/NO_2^-}$
2 wt% ionophore 50 mol% TDMAC 1:2 PVC:**DOS**	-43.2	-4.2	-
2 wt% ionophore 50 mol% TDMAC 1:2 PVC: **Tri (n-octyl,n-decyl) trimellitate**	-28.1	-2.9	-
2 wt% ionophore 50 mol% TDMAC 1:2 PVC: **Di-n-butyl phthalate**	-63.6	-4.7	-1.61
2 wt% ionophore 50 mol% TDMAC 1:2 PVC: **Tributyl phosphate**	-59.1	-4.9	-1.29
2 wt% ionophore **50 mol%** TDMAC 1:2 PVC: NPOE	-59.7	-6.0	-1.83
2 wt% ionophore **50 mol%** TDMAC 1:1 PVC: NPOE	-64.5	-4.8	-1.97
0 wt% ionophore **50 mol%** TDMAC 1:2 PVC : NPOE	-68.6	-5.8	-1.89
2 wt% ionophore **25 mol%** TDMAC 1:2 PVC : NPOE	-57.5	-5.9	-1.94 ± 0.05
0 wt% ionophore **25 mol%** TDMAC 1:2 PVC : NPOE	-55.1	-5.8	-1.90 ± 0.07
2 wt% ionophore **10 mol%** TDMAC 1:2 PVC : NPOE	-50.8	-4.9	-1.1 ± 0.1
0 wt% ionophore **10 mol%** TDMAC 1:2 PVC : NPOE	-47.6	-4.5	-1.01 ± 0.05
0 wt% ionophore 25 mol% TDMAC 1:2 PVC : NPOE **10% of normal IFS**	-60.7	-5.6	-1.96

Note: Ionophore = VO Salen

Membranes with and without the VO salen ionophore were tested for selectivity over nitrite to see if the ionophore was beneficial. The NO stock solution used for calibration with the oxyHb has a background nitrite level of 0.6 mM, thus the importance of determining the selectivity for nitrate over nitrite. Log *K* values for all sensors were calculated using Equation 4.4.

$$\log k^{NO_3^-,NO_2^-} = \frac{\left(E_{NO_2^-} - E_{NO_3^-}\right)}{0.059/z_{NO_3^-}} \tag{4.4}$$

where the E terms are cell potentials extrapolated on the calibration curves to 1 M. In theory, the ionophore should make the membrane more selective for the analyte of interest, but in this case, the selectivity for nitrate is not that much greater, if at all, than the control membranes (Table 4.2). There was an effect on the LOD, but the reason for this is not exactly clear.

To better determine if the ionophore was binding to nitrate at all, a membrane with just 2 wt% ionophore, no TDMAC and 1:2 PVC:NPOE and a membrane with 2 wt% ionophore, no TDMAC and 1:2 polyurethane:NPOE were both calibrated for the response toward nitrate. Poly(vinyl chloride) contains negatively charged impurities[17] and polyurethane contains positively charged impurities[35], both of which can act as an ion-exchanger to maintain charge neutrality within the membrane. If the ionophore is interacting with nitrate, a response should be seen with the polyurethane membrane, but this is not the case, as shown in Figure 4.16. There is no response with either membrane until 10^{-2} M nitrate is added, indicating that the vanadium compound is likely not interacting or binding to the nitrate and that the response observed for membranes

containing the VO salen and the anion exchanger (TDMAC) was caused by the TDMAC species in the membrane.

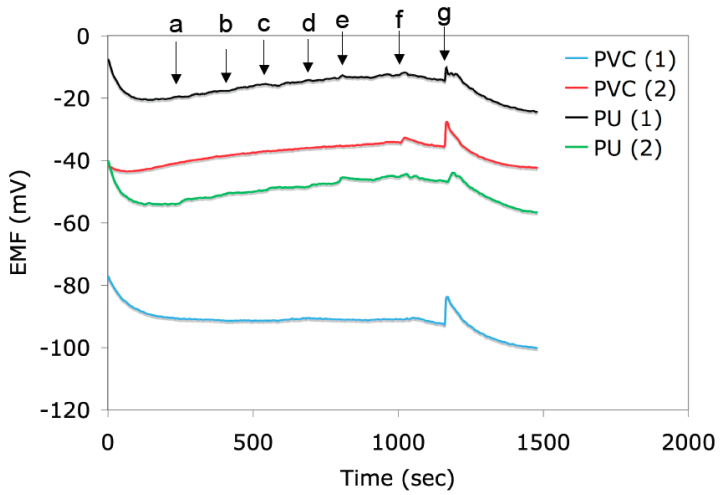

Figure 4.16 Nitrate response with membranes containing 2 wt% ionophore and 1:2 polymer:NPOE ratio, with the polymer being either PVC or polyurethane (PU). The nitrate concentrations used are a) 1 x 10^{-6} M, b) 5 x 10^{-6} M, c) 2.5 x 10^{-5} M, d) 1.25 x 10^{-4} M, e) 6.25 x 10^{-4} M, f) 3.12 x 10^{-3} M and g) 1.56 x 10^{-2} M.

4.3.5 Potentiometric Response to oxyHb

With the designed nasal NO detection setup, a solution of oxyHb will be added to a cell containing buffer, the ISE and a Ag/AgCl reference electrode. Thus, it is critically important that the ISE not have any response to the oxyHb itself. Preliminary experiments with plasticized PVC membranes with only TDMAC showed a ca. 30 mV drop in voltage with the addition of 10 μM bovine oxyHb (Figure 4.17). Additional experiments indicated that it was the oxy-form of the hemoglobin that was generating the voltage drop. In an effort to minimize this response, different buffers and pHs were examined. The pI of hemoglobin ranges from 6.9-7.2,[31, 36] so MES buffer at pH 6.0 and 5.5 were examined, along with phosphate buffer and Tris-SO_4 buffer at pHs 6.8, 7.0, and 7.4, to see if the charge on the protein was the issue. Despite these changes, the response remained the same, likely due to the development of a protein asymmetry potential.[37]

The protein can interact with the membrane surface and with multiple charges on a protein itself, a charge separation between the front and back sides of the membrane is generated (Figure 4.18). As a result, the potential decreases in response to the protein, not only the ion of interest.

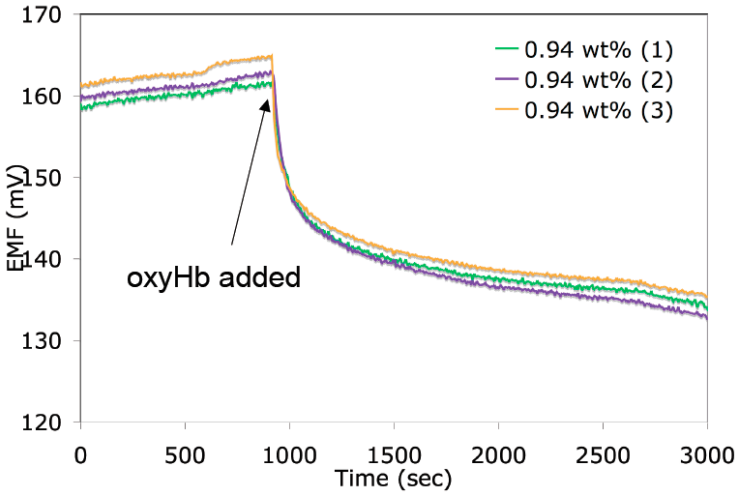

Figure 4.17 Response to oxyHb added to solution in which plasticized PVC sensors with 0.94 wt% TDMAC were placed.

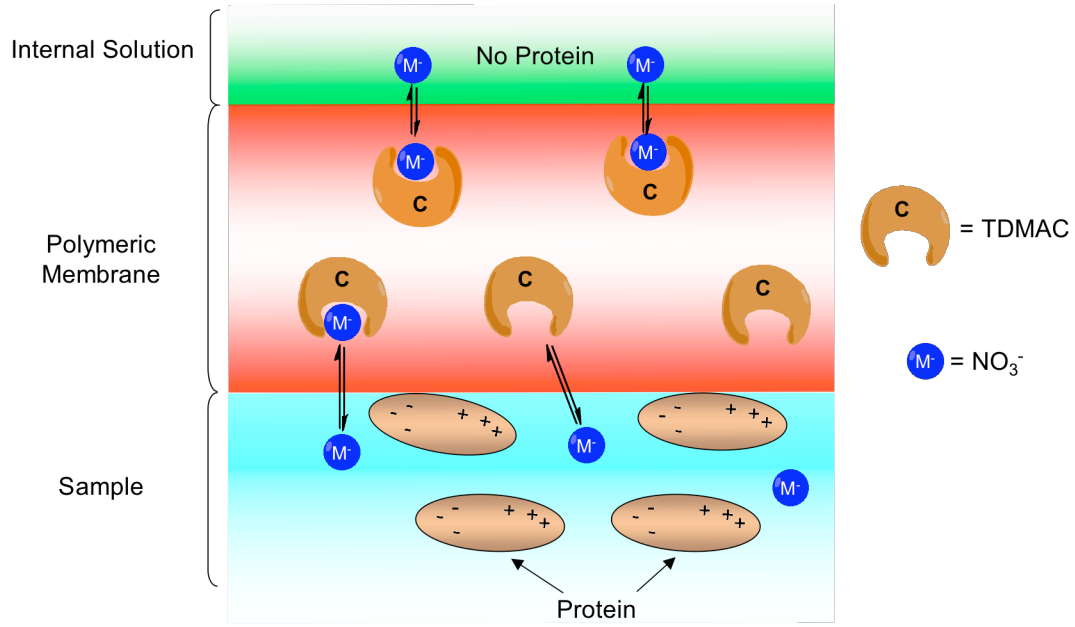

Figure 4.18 Asymmetry potential caused by oxyHb interacting at the membrane/sample interface.

To eliminate this response, an asymmetrical cellulose triacetate membrane was made. Cha et al. initially used these membranes to further immobilize enzymes to the surface, but later also used them to eliminate the response from salicylate on a chloride-selective electrode.[29, 38] The cellulose triacetate (CTA) film was cast and then hydrolyzed to create a more hydrophilic surface and to make the film more porous (Figure 4.19). The ion-selective membrane cocktail was similar to the PVC membrane cocktail, but used CTA as the polymer and was deposited on the nonhydrolyzed side of the CTA film. Slow solvent evaporation ensured the two membranes fused together to form one asymmetric film. Asymmetric membranes (ASM) made with TDMAC only were first tested for nitrate response and compared to plasticized PVC membranes (Figure 4.20). Little difference was found between the two types. The response to oxyHb was then examined (Figure 4.21) and while the same 30 mV drop was observed for a PVC membrane, there was no change in the signal for either of the ASMs.

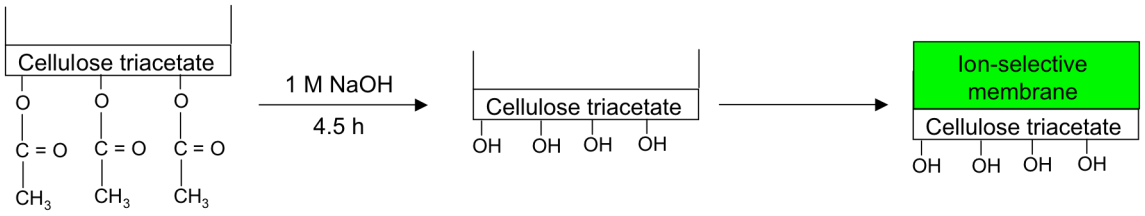

Figure 4.19 Schematic diagram demonstrating the preparation of the new asymmetric cellulose triacetate nitrate ISE.

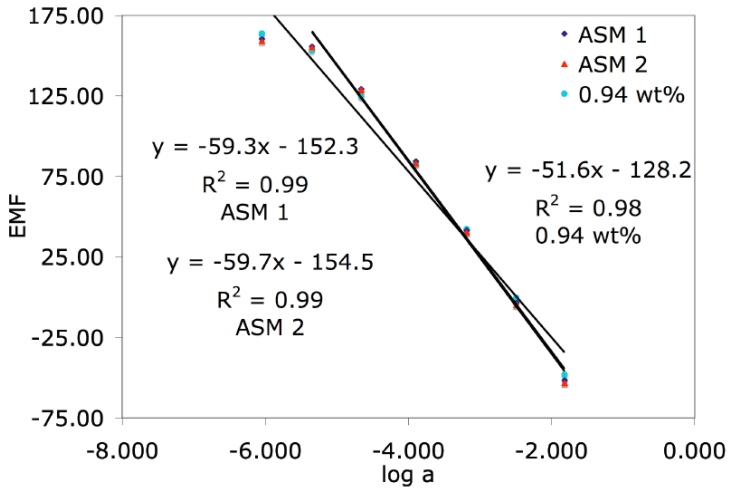

Figure 4.20 Comparison of nitrate response for ASMs and PVC membranes

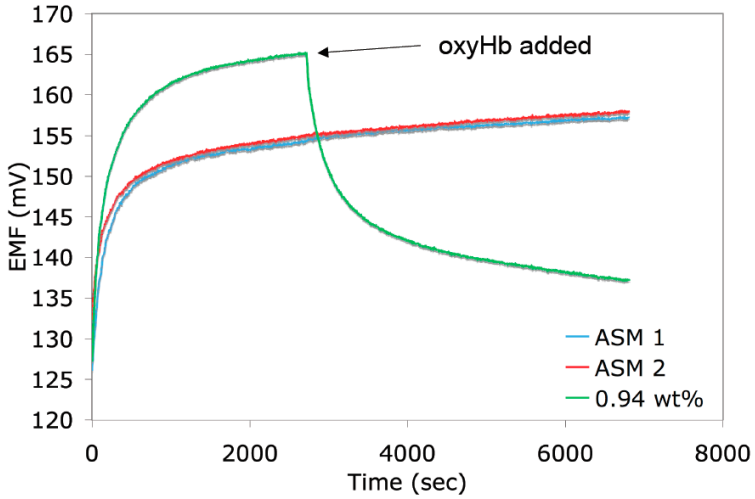

Figure 4.21 Response toward oxyHb added for both ASMs and PVC membranes.

Additional membranes were made incorporating the vanadyl ionophore and the selectivity over nitrite was determined for all sensor types (Table 4.3). Again, the ionophore did not improve selectivity over nitrite, so TDMAC only films were primarily used for all further studies.

Table 4.3 Selectivity over nitrite for both asymmetric membranes and plasticized PVC membranes.[a]

	log k				
	Trial 1		Trial 2		PVC
	ASM 1	ASM 2	ASM 1	ASM 2	
2 wt% Ionophore (1)	-1.64	-1.75	-1.78	-1.91	-1.95
2 wt% Ionophore (2)	N/A		-1.86	-1.86	
TDMAC (1)	-2.29	-2.36	-2.01	-2.29	-2.07
TDMAC (2)	-2.10	-1.98	-2.06	-1.73	

[a] $k = k^{pot}_{NO_3^-/NO_2^-}$

4.3.6 Nitric Oxide Calibration with Asymmetric Cellulose Triacetate Membrane

Nitric oxide calibrations were performed using these membranes with two concentrations of oxyHb added, 10 μM and 50 μM. In each case, a control of just the NO stock solution was run because of the background nitrite in the solution. In each of the calibrations, shown in Figures 4.22 and 4.23, this background nitrite signal is first calculated in terms of nitrate concentration based on a nitrate calibration curve, and is then subtracted from the nitrate concentration determined in the presence of oxyHb. With 50 μM oxyHb present, the response was linear to 50 μM NO. This result suggests a 1:1 stoichiometry between the NO and the hemoglobin, which is different from the UV-Vis calibrations that suggested a 1:1 NO:heme stoichiometry, a result supported by the literature. Looking at the trials containing 10 μM oxyHb, the response is linear up to 25 μM NO, although this response is less linear than that at 50 μM oxyHb. The discrepancy between the electrochemical and optical results has been suggested to be because of a difference in sensitivity, with the optical method being superior.[11] At 50 μM oxyHb, a response should be detected up to 200 μM NO, a concentration easily observed with

these sensors, but this is not the case. Additionally, it is possible that the background correction is higher than necessary because while most of the signal is likely from the background nitrite, some of it is also likely to be from the NO reacting with oxygen in the solution to produce more nitrite; however, the exact cause for this inconsistency is not yet known.

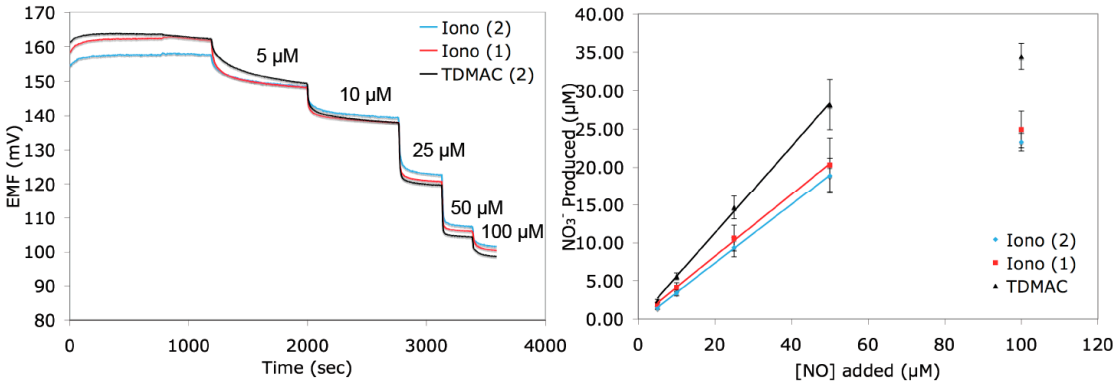

Figure 4.22 Calibration of nitrate produced from 50 µM oxyHb reacting with NO. Error bars are ± s.d. for n = 3 measurements.

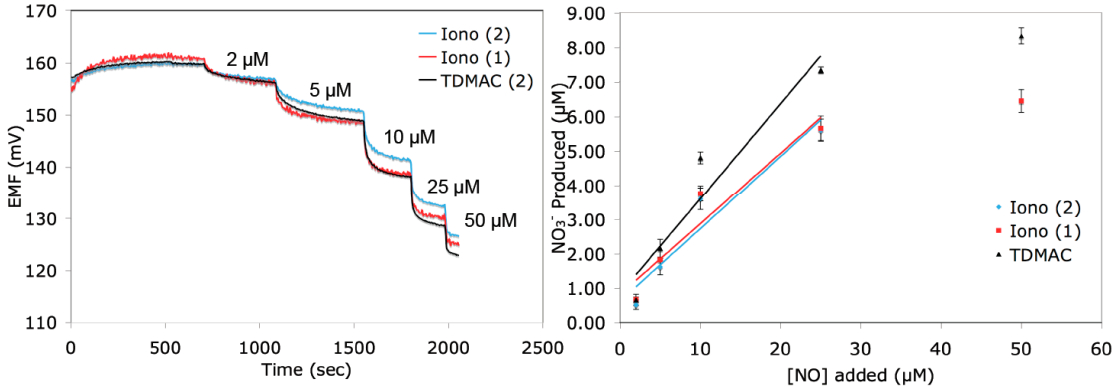

Figure 4.23 Calibration of nitrate produced from 10 µM oxyHb reacting with NO. Error bars are ± s.d. for n = 3 measurements.

4.3.7 Gas Phase Testing

As a way to test the oxyHb assay using gas phase NO, the oxyHb solution was put into a thin walled silicone rubber tubing. The tubing was then submerged in a sealed vial containing deoxygenated buffer and NO stock solution was added to the bulk. After

letting the tubing incubate at 5, 10, and 15 min, the oxyHb solution was removed and added to the sensor setup. Once the sensor response stabilized, 1 mL was removed and a UV-Vis spectrum was obtained. Table 4.4 summarizes the results, with the longer incubation times resulting in more NO being trapped by the oxyHb and converted to nitrate and metHb. In addition to providing a method of testing gas phase NO, the tubing blocks nitrite so the response seen is directly from the NO. Controls were also run with only buffer in the tubing, and with oxyHb in the tubing, but no NO added. There was still a 1-2 mV decrease in signal when buffer was used due to NO reacting with oxygen to produce nitrite. Kinetically, this reaction is slower than the reaction with oxyHb, so nitrite production should not be an issue in the presence of the protein. With the oxyHb only and no NO added, the ISEs did have a response. In previous experiments it was determined that the sensors can drop a maximum of ~1 mV with the additional of oxyHb, which accounts for some of this response. Additionally, a Teflon coated stir bar was used so it is possible that some NO had dissolved into it from previous trials, then diffused into the bulk solution during experiments without NO present. A larger standard deviation (see Table 4.4) is observed during the 15 min incubation because the tubing had been exposed to NO prior to the one of the trials. Some NO was likely still in the tubing and diffused out during the incubation time without additional NO present. There was little change in the UV-Vis spectrum, indicating the oxyHb was not being autooxidized to metHb while under low oxygen conditions.

Table 4.4 Varying incubation time of oxyHb in silicone rubber tubing with and without NO.

Conditions	Incubation Time	ISE (ΔmV)	UV (μM)
oxyHb + NO	5 min	-8.7 ± 1.4 $\approx 10^{-5.2}$ M	14.5 ± 2.2
	10 min	-13.4 ± 2.2 $\approx 10^{-5.1}$ M	22.4 ± 5.8
	15 min	-13.4 ± 1.0 $\approx 10^{-5.1}$ M	34.2 ± 2.4
oxyHb only	5 min	-1.7 ± 0.8	0
	10 min	-1.8 ± 1.6	0
	15 min	-1.0 ± 3.1	0
Buffer + NO	5 min	-1.2	--
	10 min	-1.1	--
	15 min	-2.0	--

4.3.8 Nasal Nitric Oxide Testing

Exhaled nasal air was collected in a 2 L non-gas permeable collection bag. After purging the air into a solution containing 20 μM oxyHb with the anti-foaming agent, the pH of the resulting solution dropped from 7.4 to 6.7, likely due to carbon dioxide dissolving into the solution to form bicarbonate. In all nasal NO experiments, three ASMs containing 0.94 wt% TDMAC were used. The logarithm of the selectivity coefficient for the nitrate electrode over bicarbonate was determined to be -3.1, but there is still a response once the concentration reaches 10^{-2} M. Upon addition of the oxyHb solution to the sensors, the signal dropped, indicating the presence of nitrate and bicarbonate. Control experiments were performed with only buffer and the anti-foaming agent present. The pH still dropped from 7.4 to 6.7 and the sensors still responded, but

the response was less than with oxyHb present. The nitrate concentration corresponding to the sensor response was calculated from a nitrate calibration curve and subtracted from the nitrate concentration observed in the presence of oxyHb to determine the nitrate produced from the NO reacting with the oxyHb. This value was then used to calculate an NO concentration of 140 ppb ± 38 (Figure 4.24) as shown in the sample calculation below for the response of one sensor.

$$2.98 \times 10^{-6} M \times 0.0055\ L = 1.64 \times 10^{-8}\ mol\left(\frac{22.4\ L}{1\ mol}\right) = 3.67 \times 10^{-7} L$$

$$\frac{3.67 \times 10^{-7} L}{2\ L} = 1.84 \times 10^{-7}\ L/L = 184\ ppb$$

Some oxyHb was lost due to foaming of the solution during the bubbling, so another trial was run with 50 μM oxyHb present. In this case, a NO concentration of 320 ppb ± 85 was detected, which was due to either more NO in the sample or more NO being trapped by the oxyHb (Figure 4.25). The control (buffer only) response is also shown in Figure 4.25, with the gradual positive drift likely caused from CO_2 coming out of the solution. Upon repeating the trial, it was determined that the higher concentration of oxyHb may not be the factor, with 170 ± 120 ppb detected (Figure 4.26). In all trials, the optical spectra showed a shift of the Soret band from 413 nm to 408 nm, supporting the conclusion that NO was being trapped (Data not shown).

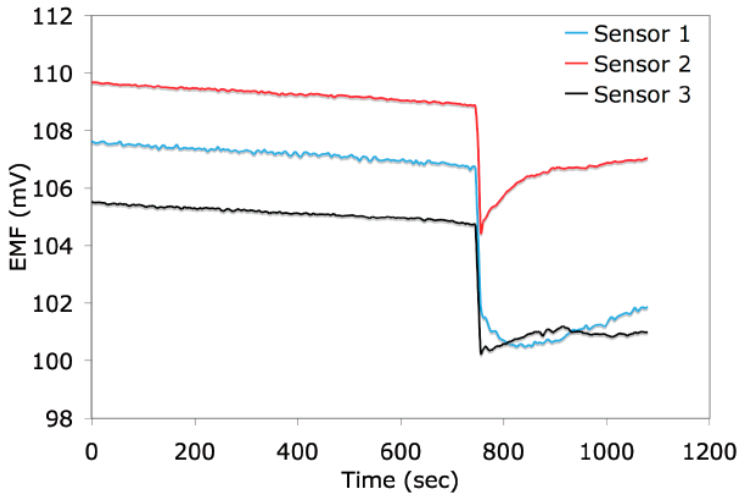

Figure 4.24 Potentiometric response to a nasal air sample bubbled into 25 μM oxyHb.

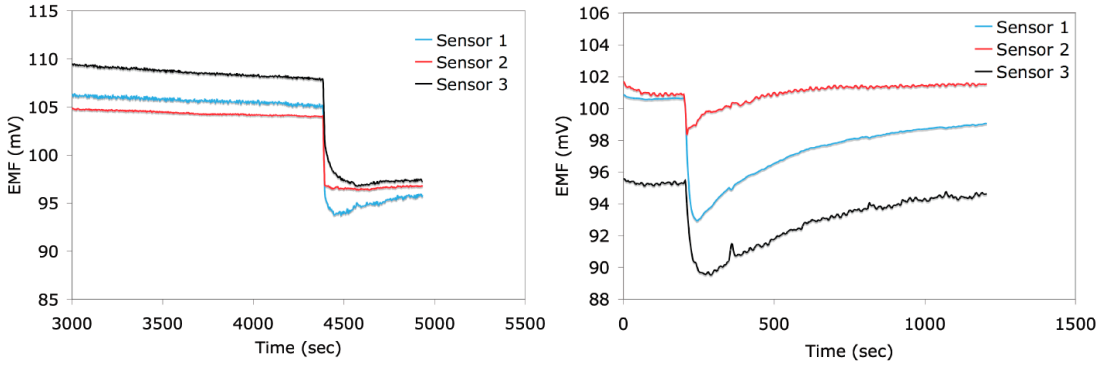

Figure 4.25 (Left) Potentiometric response to a nasal air sample bubbled into a solution containing 50 μM oxyHb. **(Right)** The control response for the air bubbled through buffer only.

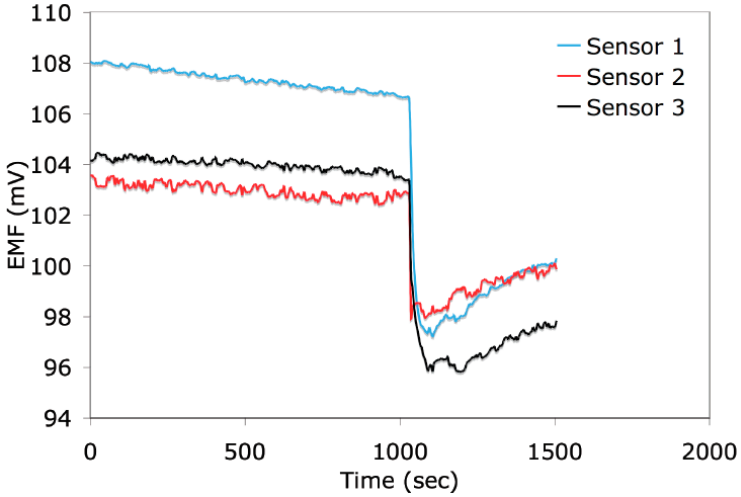

Figure 4.26 The potentiometric response for another nasal air sample bubbled through a solution containing 50 μM oxyHb.

The collection bag was also filled with nitrogen gas, which was then bubbled first through buffer, and then another trial was bubbled through oxyHb (Figure 4.27a and 4.27b). In both trials, the pH of the solution did not change and there was little sensor response with the buffer. The oxyHb did show some response, but this is not likely NO_3^- produced from the presence of NO because the optical spectrum remained the same, with the Soret band maximum at 413 nm. This response was more likely from contaminating gas species dissolving into the solution as anions, since the N_2 source was house supplied, with an uncertain purity.

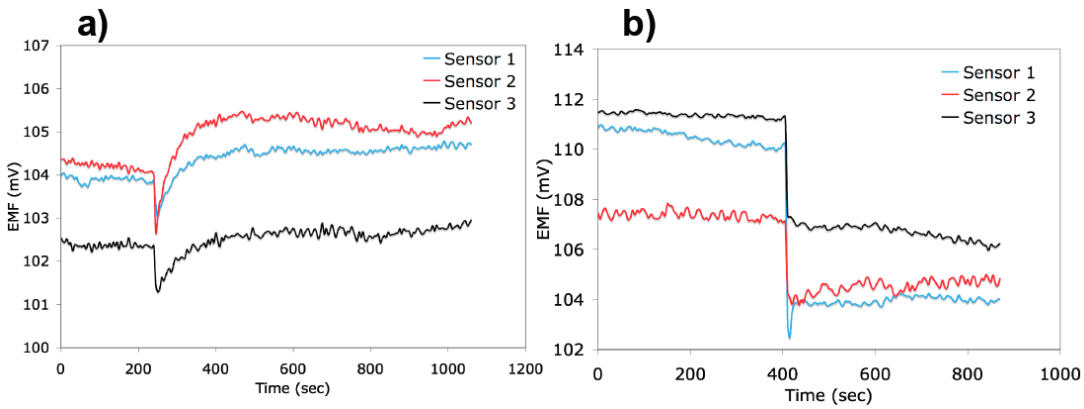

Figure 4.27 a) A sample of nitrogen gas bubbled through buffer, as well as **b)** through 50 μM oxyHb.

In a separate experiment, a solution of 50 μM oxyHb with anti-foaming agent was added directly to the sensors and a response was observed (Figure 4.28). This solution was more concentrated since no protein was lost due to foaming, but the response was still relatively small. Sensor 1 had the largest response, of ca. 6 mV, but this sensor was 3 months old and was beginning to fail. As seen by the other sensors, as well as in Figure 4.22, this concentration of oxyHb does not typically cause a sensor response of more than 1 mV.

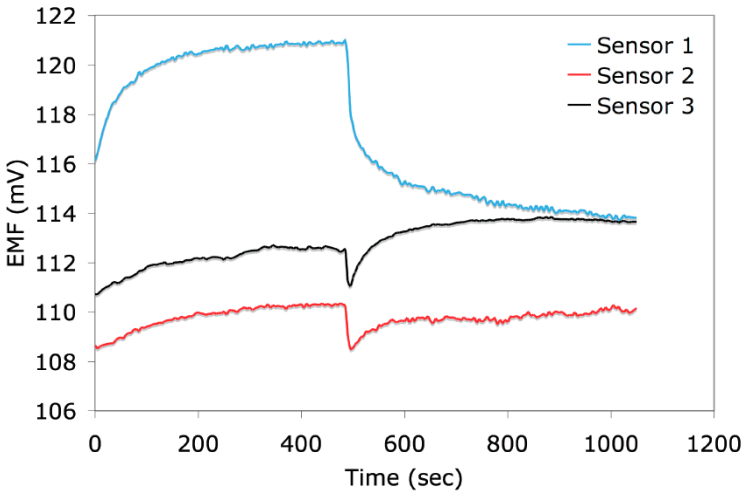

Figure 4.28 A control experiment with the addition of a sample containing only 50 μM oxyHb.

An additional control was performed by filling the gas collection bag with compressed room air and bubbling this through solutions with and without oxyHb present (Figure 4.29a and 4.29b). In this case, the pH dropped only to 7.27 with oxyHb present and did not change at all without it. These results are consistent with the fact that there is ca. 0.40 ppt of CO_2 in the ambient air, while exhaled breath is 4.5% CO_2, equivalent to 45 ppt. Potentiometrically, the response dropped 2 mV, after subtracting out the control response, which is likely due to a low amount of NO present in the atmosphere.[39]

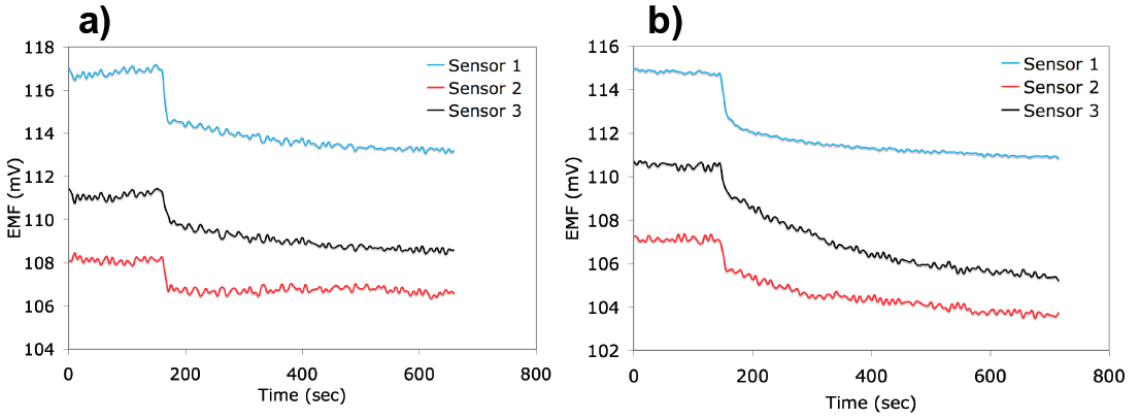

Figure 4.29 a) A sample of compressed air bubbled through buffer and **b)** through 25 μM oxyHb.

4.4 Conclusions

A method to potentially detect nasal NO has been developed using the oxyHb assay and nitrate ISEs. Optical detection was first used to characterize and calibrate the oxyHb reaction with NO and CO, generating linear calibration curves for both gases. Plasticized PVC membranes for nitrate ISEs were made and evaluated for nitrate sensing and oxyHb response, but needed to be altered due to an asymmetry potential caused by the protein interacting at the sample/membrane interface. Asymmetric cellulose triacetate membranes were then used to obtain a linear calibration curve for nitrate produced from the oxyHb and NO reaction, without significant response to the oxyHb reagent. Gas phase NO testing was completed using gas-permeable silicone rubber tubing, proving the trapping efficiency of oxyHb. Finally, nasal NO was detected in the exhaled nasal air at an average concentration of 210 ppb.

4.5 References

(1) Serrano, C.; Valero, A.; Picado, C. *Archivos de Bronconeumologia* **2004**, *40*, 222-230.

(2) Maniscalco, M.; Lundberg, J. O. *European Respiratory Monograph* **2010**, *49*, 71-81.

(3) Jorissen, M.; Lefevere, L.; Willems, T. *Allergy* **2001**, *56*, 1026-1033.

(4) Hemmingsson, T.; Linnarsson, D.; Gambert, R. *Journal of Clinical Monitoring and Computing* **2004**, *18*, 379-387.

(5) Maniscalco, M.; de Laurentiis, D.; Weitzberg, E.; Lundberg, J. O.; Sofia, M. *European Journal of Clinical Investigation* **2008**, *38*, 197-200.

(6) Gustafsson, L. E.; Leone, A. M.; Persson, M. G.; Wiklund, N. P.; Moncada, S. *Biochemical and Biophysical Research Communications* **1991**, *181*, 852-857.

(7) Leone, A. M.; Gustafsson, L. E.; Francis, P. L.; Persson, M. G.; Wiklund, N. P.; Moncada, S. *Biochemical and Biophysical Research Communications* **1994**, *201*, 883-887.

(8) Maniscalco, M.; Sofia, M.; Weitzberg, E.; Carratu, L.; Lundberg, J. O. *European Journal of Clinical Investigation* **2003**, *33*, 1090-1094.

(9) Weitzberg, E.; Lundberg, J. O. *American Journal of Respiratory and Critical Care Medicine* **2002**, *166*, 144-145.

(10) de Winter-de Groot, K. M.; van der Ent, C. T. *European Journal of Clinical Investigation* **2009**, *39*, 72-77.

(11) Feelisch, M.; Kubitzek, D.; Werringloer, J. In *Methods in Nitric Oxide Research*; Feelisch, M., Stamler, J. S., Eds.; John Wiley & Sons, Ltd.: New York, NY, 1996, pp 455-478.

(12) Sarkar, T. S.; Majumdar, U.; Roy, A.; Maiti, D.; Goswamy, A. M.; Bhattacharjess, A.; Ghosh, S. K.; Ghosh, S. *Plant Signaling & Behavior* **2010**, *5*, 668-676.

(13) Berka, V.; Yeh, H.-C.; Gao, D.; Kiran, F.; Tsai, A.-L. *Biochemistry* **2004**, *43*, 13137-13148.

(14) Bjerre, S. *Clinical Biochemistry* **1968**, *1*, 299-310.

(15) Siek, T., J.; Rieders, F. *Journal of Forensic Sciences* **1984**, *29*, 39-54.

(16) Hartsfield, C. *Antioxidants & Redox Signaling* **2002**, *4*, 301-307.

(17) Bakker, E.; Buhlmann, P.; Pretsch, E. *Chemical Reviews* **1997**, *97*, 3083-3132.

(18) Milham, P. J.; Awad, A. S.; Paull, R. E.; Bull, J. H. *Analyst* **1970**, *95*, 751-757.

(19) Choi, K. K.; Fung, K. W. *Analyst* **1980**, *105*, 241-245.

(20) Rawat, A.; Chandra, S.; Sarkar, A. *Sensor Letters* **2009**, *7*, 1100-1105.

(21) Bendikov, T. A.; Harmon, T. C. *Journal of Chemical Education* **2005**, *82*, 439-441.

(22) Hara, H.; Ohkubo, H.; Sawai, K. *Analyst* **1993**, *118*, 549-552.

(23) Hutchins, R. S.; Bachas, L. G. *Analytical Chemistry* **1995**, *67*, 1654-1660.

(24) Ross, J. W. *Chemical Abstracts* **1970**, *72*, 38268t.

(25) Buhlmann, P.; Pretsch, E.; Bakker, E. *Chemical Reviews* **1998**, *98*, 1593-1687.

(26) Davies, J. E. W.; Moody, G. J.; Thomas, J. D. R. *Analyst* **1972**, *97*, 87-94.

(27) Lide, D. R.; Frederikse, H. P. R., Eds. *CRC Handbook of Chemistry and Physics*, 76 ed.; CRC Press, Inc.: Boca Raton, FL, 1995.

(28) Khan, N.-u. H.; Agrawal, S.; Kureshy, R. I.; Abdi, S. H. R.; Mayani, V. J.; Jasra, R. V. *European Journal of Organic Chemistry* **2006**, *2006*, 3175-3180.

(29) Cha, G. S.; Meyerhoff, M. E. *Talanta* **1989**, *36*, 271-278.

(30) Fried, J. R. In *Polymer Science and Technology*; Prentice-Hall, Inc.: Englewood Cliffs, NJ, 1995, pp 433.

(31) Antonini, E.; Brunori, M., Eds. *Hemoglobin and Myoglobin in their Reactions with Ligands*; North-Holland Publishing Company: Amsterdam, 1971.

(32) Andersson, J. A.; Uddman, R.; Cardell, L.-O. *Journal of Allergy and Clinical Immunology* **2000**, *105*.

(33) Gibson, Q. H. *Biochemical Society Transactions* **1990**, *18*, 1-6.

(34) Guilbault, G. G.; Durst, R. A.; Frant, M. S.; Freiser, H.; Hansen, E. H.; Light, T. S.; Pungor, E.; Rechnitz, G.; Rice, N. M.; Rohm, T. J.; Simon, W.; Thomas, J. D. R. *Pure and Applied Chemistry* **1976**, *48*, 127-132.

(35) Nagele, M.; Pretsch, E. *Mikrochimica Acta* **1995**, *121*, 269-279.

(36) Voet, D.; Voet, J. G.; Pratt, C. W. *Fundamentals of Biochemistry: Life at the Molecular Level*, 2 ed.; John Wiley & Sons: Hoboken, NJ, 2006.

(37) Durselen, L. F. J.; Wegmann, D.; May, K.; Oesch, U.; Simon, W. *Analytical Chemistry* **1988**, *60*, 1455-1458.

(38) Cha, M. J.; Shin, J. H.; Oh, B. K.; Kim, C. Y.; Cha, G. S.; Shin, D. S.; Kim, B. *Analytica Chimica Acta* **1995**, *315*, 311-319.

(39) Corradi, M.; Pelizzoni, A.; Majori, M.; Cuomo, A.; de'Munari, E.; Pesci, A. *Thorax* **1998**, *53*, 673-676.

CHAPTER 5

CONCLUSIONS

5.1 Summary of Results and Contributions

S-Nitrosothiols (RSNOs) and nitric oxide (NO) are important biomolecules with complex chemistry. Their role in disease states has been well established, making the detection of these molecules all the more important. As discussed in Chapter 1, numerous methods of RSNO and NO detection have previously been proposed and applied to different biological samples with mixed results. For example, the RSNO concentration reported in plasma varies from undetectable up to 22 μM.[1] Many methodological errors have been present, including not protecting samples from light, which may account for some of the variation seen in the RSNO results. Indeed, for many of the RSNO assays there are numerous steps involved and several reagents required, adding time, cost, and potential for errors to occur in the analysis. Furthermore, many of the methods, including mass spectrometry, chemiluminescence, and EPR, require expensive and complex instrumentation, which is not practical for a point-of-care situation. The work presented in this thesis addresses many of these issues, by developing a new RSNO assay that does not require any additional sample preparation, and by utilizing a well known NO assay in a different way to detect NO in nasal air.

In Chapter 2, a new chemiluminescence assay using a homogeneous organoselenium catalyst with a free thiol reducing agent was developed for *S*-nitrosothiol detection. Linear calibration curves were generated for all three low molecular weight RSNOs, with a LOD below 20 nM. Compared to the well known copper(II)-based RSNO assay, the SeCA assay is slightly more sensitive. The most important advantage of this assay system is the improved selectivity over nitrite. The sensitivity for the high molecular weight RSNO, AlbSNO, was also examined. It was further determined that the thiols on the protein can act as the reducing agent for the catalyst. The assay was then used to analyze transnitrosation reactions and to look at RSNO decomposition in plasma. Finally, the new SeCA assay was evaluated as a new detection method for quantitating HbSNO from animal blood samples.

In Chapter 3, the SeCA assay developed in Chapter 2 was used to prove the absence of measurable RSNOs in exhaled breath condensate (EBC). Exhaled breath condensate was collected from five volunteers and analyzed using both the Cu(II) and SeCA chemiluminescence assays, as well as the optical Griess and Saville assays. When using the Cu(II) assay in unbuffered conditions, a signal was seen from the EBC due to slightly acidic conditions reducing nitrite to NO. Retesting the EBC with the buffered Cu(II) assay gave no signal. Testing EBC using the SeCA assay also gave no change in the baseline, indicating the presence of nitrite, but not RSNOs. Nitrite was further confirmed using the Griess assay, and while the Saville assay did indicate the presence of RSNOs, this signal was shown to be due to artifactual RSNOs. Previous literature reported the presence of RSNOs in EBC, but these groups utilized the Griess and Saville assays.

In Chapter 4, exhaled nasal NO was detected using the oxyhemoglobin assay combined with a nitrate ion-selective electrodes. The oxyhemoglobin assay was first characterized optically by monitoring the change in the spectrum as methemoglobin was produced. Using the optical detection, the reaction with CO was also observed and it was determined that oxyhemoglobin has a stronger affinity for NO over CO. Nitrate ISEs were developed using an asymmetric cellulose triacetate membrane in order to prevent the oxyHb from causing an asymmetry potential across the sensing membrane. Calibration curves for the nitrate produced from the oxyHb reaction with NO were generated. Gas phase NO was detected using a gas-permeable silicone rubber tubing loaded with oxyHb. Finally, NO from exhaled nasal air was detected, with an average concentration of 210 ppb seen.

5.2 Future Work

Use of ion-selective electrodes for the detection of nitrate produced from the oxyhemoglobin reaction with NO has not previously been reported. In this work, a simple ISE was employed, but this sensor could be further optimized, perhaps with a new ionophore. Indeed, work is currently being performed in this lab to develop a cobalt-corrole ionophore for nitrite (Figure 5.1a). During the membrane optimization, performed by Si Yang, it was discovered that using tributylphosphate as the plasticizer with PVC and TDMAC, the sensor had excellent response and selectivity for nitrate over nitrite, with a log K value of -1.2 and a LOD of $10^{-5.4}$ M (Figure 5.1b). This sensor operates the best at pH 4.5, so in order for this to be used with oxyHb, the pH of the oxyHb solution would need to be altered immediately prior to testing with the membrane

electrode; however, to eliminate bicarbonate from a nasal NO sample bubbled through the oxyHb solution, this change in pH needs to be made anyway.

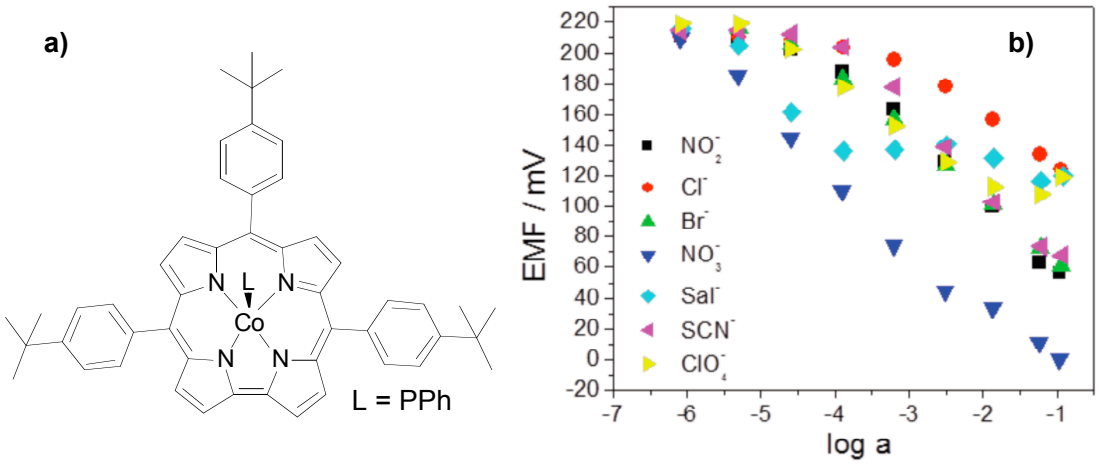

Figure 5.1a) The structure of the cobalt-corrole ionophore. **b)** Preliminary data showing the sensor response to 7 anions, with the highest selectivity shown for nitrate.

Another immediate application of the oxyHb assay with potentiometric nitrate detection is to detect NO release from polymeric materials made in this lab. These materials include implantable sensors, vascular grafts, and wraps, all with NO release coatings. Currently, the chemiluminescence Nitric Oxide Analyzer is used to quantify NO release because it is the "gold standard" for NO detection, but it operates under a nitrogen environment, and the NO release is tested using buffers as the aqueous medium. All of the studied polymer materials that release NO would be in contact with blood, so the use of the ISEs would enable more realistic testing conditions, i.e. in the presence of oxygen and hemoglobin.

Preliminary experiments tested a NO release film that can be wrapped around the sites where a vascular graft is sown to a blood vessel to help improve biocompatibility. The wrap, fabricated and tested by Elizabeth Brisbois, consists of an NO donor,

diazeniumdiolated dibutylhexanediamine (DBHD/N_2O_2), in a matrix with poly(lactic-co-glycolic) acid (PLGA) and polyurethane, specifically SG80A (Figure 5.2). The copolymer of lactic and glycolic acids slowly hydrolyzes creating an acidic environment in the process. Nitric oxide is released from the DBHB/N_2O_2 under acidic conditions (Figure 5.2), making PLGA an ideal polymeric additive.[2, 3] Tested in the NOA over 10 days, with soaking in PBS at 37 °C, the NO release starts around 20 units of flux, defined as 1 x 10^{-10} molcm^{-2}min^{-1}, and gradually dropping to around 7 units of flux (Figure 5.3). A 1 cm by 1 cm square of this same type of wrap was soaked in 10 mM phosphate buffer with 25 μM oxyHb for 30 min at 37 °C. This solution was then added to a setup with 3 nitrate ISEs. This experiment was repeated two more times, with the results shown in Figure 5.4. An average of 24 units of flux was observed using the oxyHb assay, similar to the 20 units of flux detected using the NOA. As a control, a solution of 25 μM oxyHb was incubated for 30 min at 37 °C, without the wrap. This solution was then added to the sensor setup and a small response of ca. 1 mV was observed, likely from the oxyHb itself. From this preliminary experiment, the oxyHb assay seems like an excellent method to use to detect NO release from implantable polymeric materials being developed in this laboratory[2, 4, 5] and elsewhere[6-8].

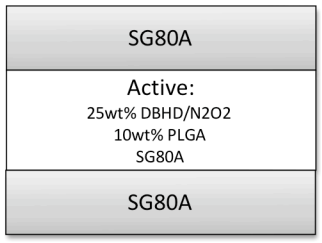

Thin wrap ~ 0.3 mm

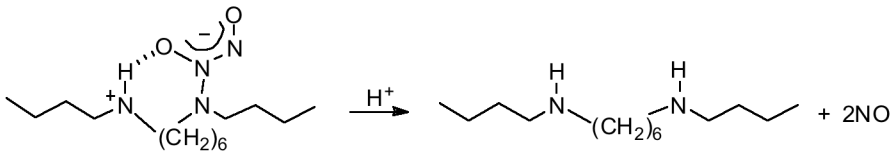

diazeniuamdiolated dibutylhexanediame
($DBHD/N_2O_2$)

Figure 5.2 Schematic diagram showing the composition of the NO releasing film, along with the mechanism of NO release from $DBHD/N_2O_2$.

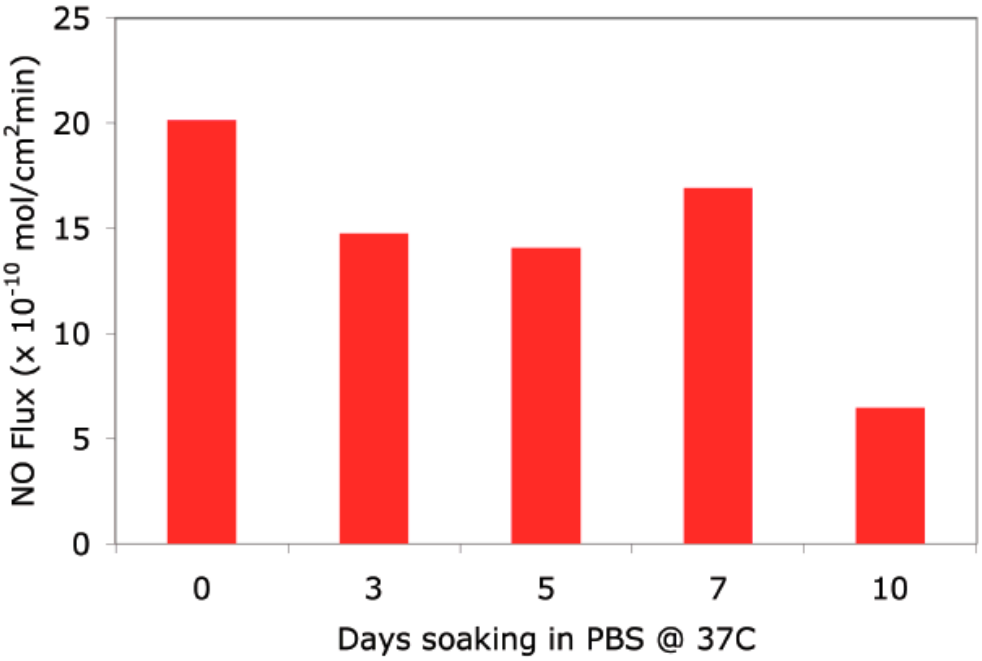

Figure 5.3 Nitric oxide flux from the NO releasing film over the course of 10 d. Data was collected using the chemiluminescence analyzer.

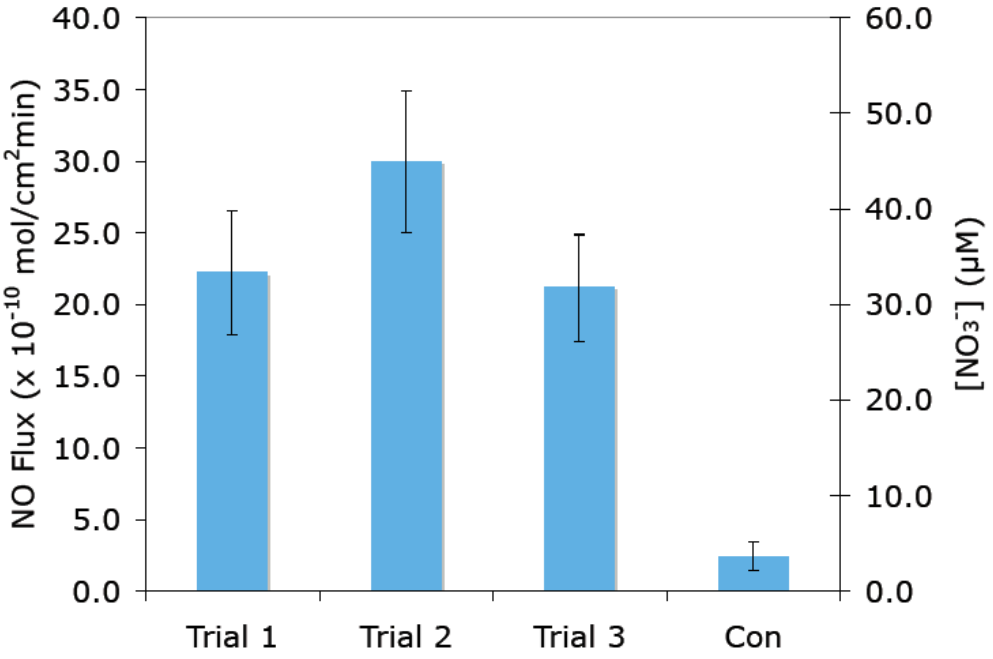

Figure 5.4 Nitric oxide released from the wrap that reacted with oxyHb to produce nitrate. The nitrate was then detected potentiometrically with the error bars representing ± s.d. for n = 3 measurements.

Overall, the research presented in this thesis provides an important new RSNO assay system, along with a new approach to NO detection. With further improvements in the performance of the nitrate ISE, the oxyHb assay could be used for a variety of new applications, including the nasal NO one presented here, and may provide more realistic testing conditions for new NO releasing blood contacting devices.

5.3 References

(1) Giustarini, D.; Milzani, A.; Dalle-Donne, I.; Rossi, R. *Journal of Chromatography B* **2007**, *851*, 124-139.

(2) Batchelor, M. M.; Reoma, S. L.; Fleser, P. S.; Nuthakki, V. K.; Callahan, R. E.; Shanley, C. J.; Politis, J. K.; Elmore, J.; Merz, S. I.; Meyerhoff, M. E. *Journal of Medicinal Chemistry* **2003**, *46*, 5153-5161.

(3) Zhou, Z.; Meyerhoff, M. E. *Biomacromolecules* **2005**, *6*, 780-789.

(4) Major, T. C.; Brant, D. O.; Reynolds, M. M.; Bartlett, R. H.; Meyerhoff, M. E.; Handa, H.; Annich, G. M. *Biomaterials* **2010**, *31*, 2736-2745.

(5) Frost, M. C.; Meyerhoff, M. E. *Journal of the American Chemical Society* **2004**, *126*, 1348-1349.

(6) Peter, N.; Coneski, P. N.; Schoenfisch, M. H. *Polymer Chemistry* **2011**, *2*, 906-913.

(7) Riccio, D. A.; Dobmeier, K. P.; Hetrick, E. M.; Privette, B. J.; Paul, H. S.; Schoenfisch, M. H. *Biomaterials* **2009**, *30*, 4494-4502.

(8) Shishido, S. M.; Seabra, A. B.; Loh, W.; de Oliveira, M. G. *Biomaterials* **2003**, *24*, 3543-3553.